ADVANCED ENERGY MATERIALS
www.advenergymat.de

Spin Matters: A Multidisciplinary Roadmap to Understanding Spin Effects in Oxygen Evolution Reaction During Water Electrolysis

Emma van der Minne, Priscila Vensaus,* Vadim Ratovskii, Seenivasan Hariharan, Jan Behrends, Cesare Franchini, Jonas Fransson, Sarnjeet S. Dhesi, Felix Gunkel, Florian Gossing, Georgios Katsoukis, Ulrike I. Kramm, Magalí Lingenfelder, Qianqian Lan, Yury V. Kolen'ko, Yang Li, Ramsundar Rani Mohan, Jeffrey McCord, Lingmei Ni, Eva Pavarini, Rossitza Pentcheva, David H. Waldeck, Michael Verhage, Anke Yu, Zhichuan J. Xu, Piero Torelli, Silvia Mauri, Narcis Avarvari, Anja Bieberle-Hütter, and Christoph Baeumer**

A central challenge in water electrolysis lies with the oxygen evolution reaction (OER) where the formation of molecular oxygen (O_2) is hindered by the constraint of angular momentum conservation. While the reactants OH^- or H_2O are diamagnetic (DM), the O_2 product has a paramagnetic (PM) triplet ground state, requiring a change in spin configuration when being formed. This constraint has prompted interest in spin-selective catalysts as a means to facilitate OER. In this context, the roles of magnetism and chirality-induced spin selectivity (CISS) in promoting the OER reaction have recently been investigated through both theoretical and experimental studies. However, pinpointing the key principles and their relative contribution in mediating spin-enhancement remains a significant challenge. This roadmap offers a forward-looking perspective on current experimental trends and theoretical developments in spin-enhanced OER electrocatalysis and outlines strategic directions for integrating incisive experiments and operando approaches with computational modeling to disentangle key mechanisms. By providing a conceptual framework and identifying critical knowledge gaps, this perspective aims to guide researchers toward dedicated experimental and computational studies that will deepen the understanding of spin-induced OER enhancement and accelerate the development of next-generation catalysts.

1. Introduction

Shifting away from fossil fuels to renewable energy sources is essential to reduce carbon emissions and mitigate climate change. The intermittent nature of renewable electricity and the industrial and agricultural need for carbon-neutral feedstocks necessitate production of green energy carriers, such as hydrogen.[1,2] The "power-to-hydrogen" strategy therefore aims at splitting water into O_2 and H_2 via the oxygen and hydrogen evolution reactions. However, this remains an energy-inefficient process because of the complex reaction pathway and resulting high overpotentials of the OER.[3]

One important factor contributing to these high overpotential and sluggish kinetics of the OER is the spin-state mismatch between reactants and products; while the reactants (OH^- or H_2O, depending on the electrolyte pH) are DM,

E. van der Minne, V. Ratovskii, F. Gunkel, G. Katsoukis, C. Baeumer
MESA+ Institute for Nanotechnology, Faculty of Science and Technology
University of Twente
Enschede 7500AE, The Netherlands
E-mail: e.vanderminne@utwente.nl; c.baeumer@utwente.nl

The ORCID identification number(s) for the author(s) of this article can be found under https://doi.org/10.1002/aenm.202503556

DOI: 10.1002/aenm.202503556

P. Vensaus, M. Lingenfelder
Max Planck-EPFL Laboratory for Molecular Nanoscience
École Polytechnique Fédérale de Lausanne (EPFL)
Lausanne 1015, Switzerland
E-mail: priscila.vensaus@epfl.ch

P. Vensaus
Instituto de Nanosistemas, Escuela de Bio y Nanotecnologías
Universidad Nacional de San Martín
San Martín, Buenos Aires B1650, Argentina

P. Vensaus
Laboratory of Nanoscience for Energy Technologies (LNET)
École Polytechnique Fédérale de Lausanne (EPFL)
Lausanne 1015, Switzerland

the final product, molecular oxygen (O_2), is a PM species in its triplet ground state, see **Figure 1**.[4–6] Spin is thus not conserved between reactants and products, and this process would, in principle, be forbidden by the spin selection rule. To be more specific, we can assume that, although the reaction is complex and involves at least four steps of electron transfer (typically considered as proton coupled electron transfer steps), there will be a step in the mechanism that involves the transition from a singlet intermediate to a triplet one. Because each of these electronic steps involves a non-radiative transition, they must be isoenergetic and comply with the relevant selection rules. In particular, total angular momentum must be conserved during the transition, which gives rise to the spin selection rule for chemical reactions.

Additional energy may be required to access a reaction pathway that follows the angular momentum conservation rules. This could involve the initial formation of singlet $^1O_2$, a diamagnetic excited state without unpaired electrons, which can subsequently relax to the triplet ground state via secondary processes. However, because the singlet state energy is ≈1 eV higher than the triplet state, this pathway is extremely unlikely at usual OER overpotentials. Alternatively, the reaction may fail to proceed altogether if there is spin misalignment between key intermediates which

S. Hariharan
Institute for Theoretical Physics
University of Amsterdam
Amsterdam 1098 XH, The Netherlands

S. Hariharan
QuSoft
CWI
Amsterdam 1098 XG, The Netherlands

S. Hariharan
Quantum Application Lab
Science Park, Startup Village, Amsterdam 1098 XH, The Netherlands

J. Behrends
Department of Physics
Freie Universität Berlin
14195 Berlin, Germany

C. Franchini
Faculty of Physics and Center for Computational Materials Science
University of Vienna
Vienna A-1090, Austria

C. Franchini
Department of Physics and Astronomy
University of Bologna
Bologna 40129, Italy

J. Fransson
Department of Physics and Astronomy
Uppsala University
Uppsala 752 37, Sweden

S. S. Dhesi
Diamond Light Source Ltd.
Science and Technology Facilities Council UK
Didcot, Oxfordshire OX11 0DE, UK

F. Gunkel, C. Baeumer
Peter Grünberg Institute (PGI-7)
Forschungszentrum Jülich GmbH
52425 Jülich, Germany

F. Gossing, J. McCord
Nanoscale Magnetic Materials–Magnetic Domains
Department of Materials Science
Kiel University
24143 Kiel, Germany

U. I. Kramm, L. Ni
Catalysts and Electrocatalysts Group
Department of Chemistry
Technische Universität Darmstadt
64287 Darmstadt, Germany

M. Lingenfelder
Helvetia Institute for Science and Innovation
Wollerau 8832, Switzerland

M. Lingenfelder
Institute of Physics (IPHYS)
École Polytechnique Fédérale de Lausanne (EPFL)
Lausanne 1015, Switzerland

Q. Lan
Ernst Ruska-Centrum für Mikroskopie und Spektroskopie mit Elektronen (ER-C-1)
Forschungszentrum Jülich GmbH
52425 Jülich, Germany

Y. V. Kolen'ko, R. R. Mohan
International Iberian Nanotechnology Laboratory (INL)
Braga 4715-330, Portugal

Y. Li
Department of Materials Science and Metallurgy
University of Cambridge
Cambridge CB3 0FS, UK

Y. Li
Cambridge Graphene Centre
University of Cambridge
Cambridge CB3 0FA, UK

E. Pavarini
Peter Grünberg Institute (PGI)
Forschungszentrum Jülich GmbH
52425 Jülich, Germany

R. Pentcheva
Department of Physics, Theoretical Physics and Center for Nanointegration (CENIDE)
University of Duisburg-Essen
47057 Duisburg, Germany

D. H. Waldeck
Department of Chemistry
University of Pittsburgh
Pittsburgh, PA 15260, USA

M. Verhage
Molecular Materials and Nanosystems (M2N), Applied Physics and Science Education
Eindhoven University of Technology
Eindhoven 5600 MB, The Netherlands

A. Yu, Z. J. Xu
School of Materials Science and Engineering
Nanyang Technological University
Singapore 639798, Singapore

P. Torelli, S. Mauri
Istituto Officina dei Materiali (CNR-IOM)
Area Science Park, S.S. 14 km 163,5, Basovizza, TS I-34149, Italy

S. Mauri
MAX IV Laboratory, Science division
Lund University
Lund 22484, Sweden

N. Avarvari
Univ Angers
CNRS
MOLTECH-Anjou, SFR MATRIX, F-49000 Angers, France

A. Bieberle-Hütter
Electrochemical Materials and Interfaces
Dutch Institute for Fundamental Energy Research (DIFFER)
Eindhoven 5600 HH, The Netherlands

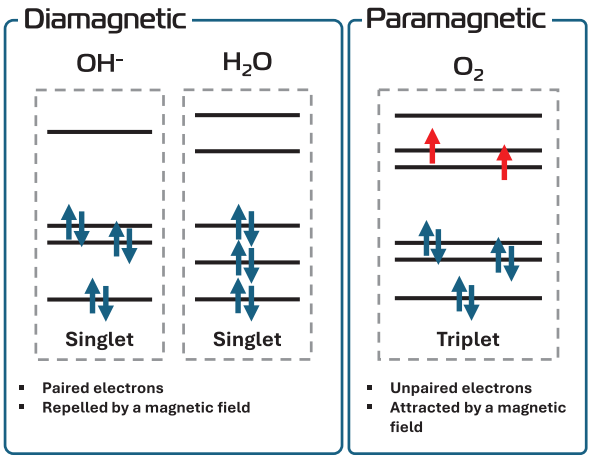

Figure 1. Schematic orbital filling of the reactants OH^-, H_2O and the triplet ground state of O_2 and their respective magnetic states.

prevents the formation of triplet O_2 due to the spin-forbidden nature of the transition. In such cases, the intermediates must either undergo a spin flip to access a spin-allowed pathway or revert to their original states, causing the reaction to restart repeatedly until spin-aligned intermediates are formed. This decreases the efficiency and effective turnover of the catalytic cycle. Both of these effects lead to an increase in the overpotential to reach a certain current density.

Spin-selective electron removal or parallel spin alignment between reaction intermediates can facilitate the direct formation of triplet O_2 and satisfy spin conservation during O–O bond formation by ensuring spin alignment in the intermediates.[4–6] This avoids the need for higher energy barriers, spin-flip transitions or non-productive reaction cycles, thereby lowering the activation energy and ultimately reducing the overpotential of the OER. This spin-dependent catalytic process is similar to the way nature fuels life in photosynthesis, where spin-order in oxygen-evolving centers plays a key role.[7]

Furthermore, OER involves multiple proton-coupled electron transfer steps and formation of intermediate species that are highly sensitive to the local electronic structure, spin states, and interfacial environment of the catalyst.[8,9] Given these caveats, recent quantum theory and experiments have revealed that OER electrocatalysts should exhibit favorable spin alignment to minimize the energy cost of each individual step and to facilitate the formation of triplet O_2.[8–11]

To achieve spin-selectivity and thereby enhance OER activity, magnetic[12] and chiral catalyst materials,[5] or a combination of both can be employed. An overview of the different material classes and observed enhancements is shown in **Figure 2**. Magnetic materials possess magnetic moments arising from unpaired electron spins which in turn can couple through long-range exchange interactions. When these interactions favor parallel alignment, they can give rise to remanent magnetization. In contrast, if the interactions favor antiparallel alignment, antiferromagnetic order emerges with vanishing net magnetization. Moreover, external magnetic field align the moments, with the field strength required to achieve alignment depending on the strength of the exchange interactions. As a result, magnetic materials have been proposed to alter adsorption energies, to induce spin-polarization in adsorbed intermediates and to create spin-selective channels based on their long-range spin exchange interactions both with and without externally applied magnetic fields.[8,9,11,13] Chiral materials are materials that lack mirror symmetry and can generate spin-polarized currents via the CISS effect which, in turn, can induce spin-selective electron removal.[10]

The emerging field of spin-enhanced catalysis seeks to uncover how magnetic order and the CISS effect influence catalytic activity and selectivity - and how these effects can be harnessed to improve catalyst performance.[14] Moreover, due to the different origins of spin-induced effects in magnetic and chiral materials, the specific spin-related phenomena that they exhibit can vary significantly. For instance, magnetic materials show strong spin-spin exchange interactions, spin-polarized conductivity, and the formation of magnetic domains. In contrast, both magnetic and chiral materials can induce spin-polarized currents, albeit through different mechanisms. Given these distinctions, it is promising to compare the extent of spin-related effects on the OER in these materials to identify which mechanisms play a key role in enhancing catalytic performance.

Although spin-enhanced catalysis - both in general and specifically for the OER – has attracted growing interest in recent years,[10,13,15,16] its underlying mechanisms remain elusive. As Yu et al. have recently noted, improvements in OER performance likely result from a combination of spin-related effects in the catalyst and other influences introduced by external magnetic fields.[11] Disentangling these contributions, including spin polarization of the active site, intrinsic catalyst magnetism, field-induced spin ordering and magnetic effects on the electrolyte is a significant challenge.[11,13,16] This complexity and the existence of different or even contradictory results and conclusions in various studies of similar materials and experimental systems require carefully controlled experiments to isolate the role of each factor.[11,15,16] Furthermore, the experimental exploration of intrinsic long-range ordering and spin polarization is limited, compared to external field-induced effects. Moreover, the accurate theoretical description of strong correlation effects, polaron formation, spin dynamics, and solvent interactions, requires theoretical tools that go beyond traditional computational frameworks. Addressing the aforementioned challenges and achieving a comprehensive understanding of the spin-enhanced OER mechanism requires not only systematic and collaborative efforts across theoretical and experimental domains, but also the development of innovative approaches and methodologies tailored to this emerging field.

In this perspective, we present emerging trends, new/novel observations, and recent theoretical developments in spin-enhanced OER electrocatalysis, and propose strategic directions to advance both experimental and computational approaches. We begin with a critical overview of the current state of the field, highlighting major findings and the methodologies that enabled them. By examining techniques used across different subfields, we identify opportunities for cross-disciplinary learning and propose methodological improvements to enhance reproducibility and deepen mechanistic insight. Building on this foundation, we outline key principles that may drive spin-enhanced OER activity. Disentangling these contributions and quantifying their individual roles remains essential for establishing a robust mechanistic

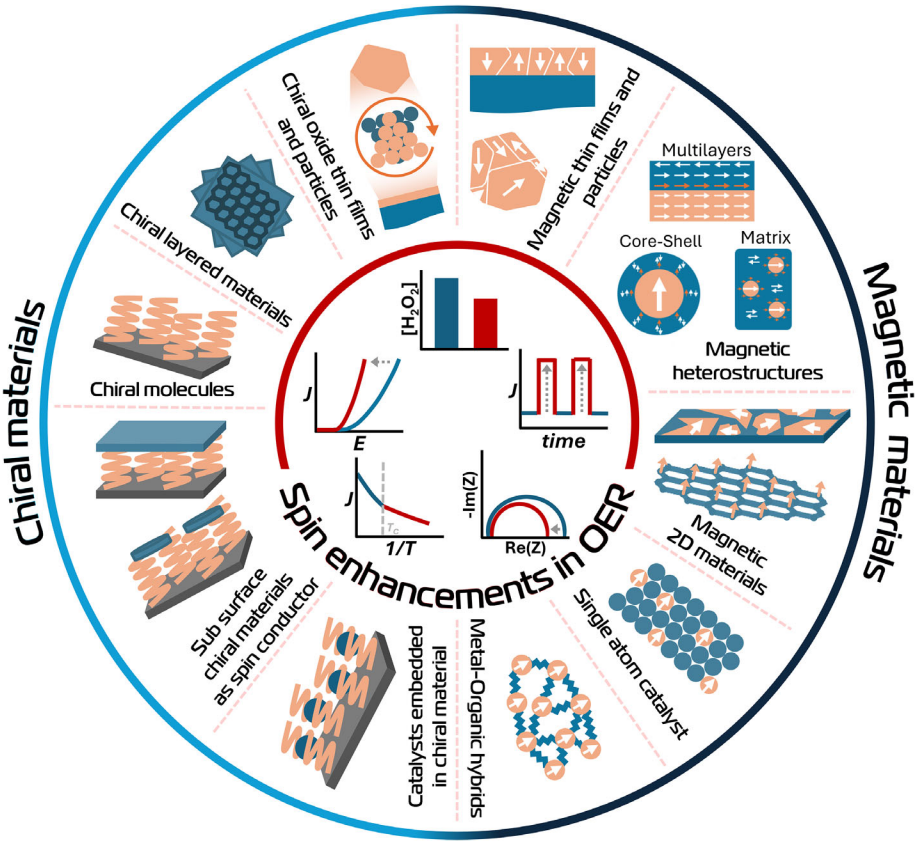

Figure 2. Schematic representation of material classes and electrochemical methodologies used in spin-dependent OER research to date. The two materials classes, chiral materials and magnetic materials, are shown in the outer circle with focus on specific structures and states of each. In the center, commonly used electrochemical techniques that have been used to demonstrate spin-enhancement effects are summarized, including current density enhancements observed in cyclic voltammetry (CV), reduced H_2O_2 generation, increased current density in chronoamperometry (CA), lowered resistances in electrochemical impedance spectroscopy, and changes in activation energy derived from Arrhenius plots.

framework and design principles for improved catalysts. We then articulate the key open questions and challenges that must be addressed. Looking ahead, we explore how existing tools can be refined and highlight underutilized experimental and theoretical approaches with the potential to yield new insights. Lastly, we outline pathways that can bridge the gap between theoretical frameworks and practical experimentation, as well as in unifying the understanding of chiral and magnetic order-enhanced OER. We aim to provide the community, as well as those seeking to enter it, with guidance and inspiration for designing new studies spanning the entire field. Our goal is to support the next steps into this emerging collaborative research landscape and to advance our understanding of the origin of spin-enhanced OER.

2. Existing Results and Methodology

This section reviews recent advancements in spin-enhanced OER and is structured into three parts: theoretical studies on magnetically and CISS-enhanced OER, experimental investigations within the same domains, and analyses of magnetohydrodynamic (MHD) effects. We will examine the approaches taken so far and the insights these have provided. Finally, we will summarize the key principles that may contribute to spin-enhancement in the OER.

2.1. Theoretical Exploration of Spin-Enhanced OER

A theoretical understanding of spin-enhanced OER has gradually taken shape, informed in part by early contributions from Gracia and colleagues.[6,17–19] We review key methodologies and findings, in i) magnetically enchanced OER and ii) CISS enhanced OER. In studies of spin order in magnetically enhanced OER, strong correlation effects in transition metal oxides are central. Density functional theory (DFT), both with and without Hubbard *U* corrections, is commonly used to study spin-resolved energetics and magnetic configurations, offering valuable insights into catalytic behavior. We also note the growing focus into the investigation of polarons (quasiparticles formed by charge carriers coupled with lattice distortions), which can significantly impact surface electronic and magnetic properties. Finally, we discuss computational models of the CISS effect, which have deepened understanding of spin polarization in chiral catalysts and its link to enhancement of activity in OER.

2.1.1. Magnetically Enhanced OER

Modeling Strongly Correlated OER Catalysts with DFT: DFT is the most widely used method for predicting electronic and

magnetic properties from first principles. DFT yields the ground-state energy of an interacting electron system; the latter is expressed as a functional, $E[n]$, of the electron density, which in turn is minimized by the actual ground state electron density, $n(r)$. In practical DFT implementations, $n(r)$ is obtained by mapping the interacting system on a fictitious non-interacting problem, the so-called Kohn–Sham (KS) problem, with the constraint that the latter has the same ground-state density of the original interacting Hamiltonian. KS eigenstates have in principle no physical meaning; however, in practice, they turn out to be an excellent approximation of quasi-particle dispersions for entire classes of materials, underpinning the success of ab initio band structure methods in weakly correlated systems.

In DFT, all many body interactions are captured in the Hartree term and the exchange-correlation functional, but the exact form of the latter is not known. For practical purposes, DFT calculations thus rely on approximate forms of this exchange-correlation functional. The choice of functional is therefore crucial in DFT studies of spin-dependent OER. It directly affects how accurately the model captures key phenomena, such as electron localization, spin polarization at active sites and reaction intermediates, the interaction between the active site and the intermediates and energies of adsorption and desorption processes. The open-source library LibXC includes over 600 different functionals, offering a wide range of options.[20] The most commonly used functionals in the field of catalysis are PBE96, PBEsol and RPBE within the generalized gradient approximation (GGA), which considers not only the dependence on the density but also on its gradient. A detailed discussion of available functionals and their respective advantages and limitations can be found elsewhere.[21,22]

Materials with localized *d* electrons, such as transition metal oxides, exhibit strong Coulomb interactions that lead to phenomena like Mott insulating behavior, local magnetic moments, and orbital or spin ordering, which lie beyond the reach of the single-electron approximation. This class of systems includes several OER-active oxides, such as manganites, cobaltites, and nickelates that similarly combine strong electron correlations, mixed valency, and complex magnetic or orbital order. Describing the electronic and magnetic properties of these strongly-correlated systems requires methods that explicitly incorporate the effects of the strong local Coulomb repulsion U. For such systems, the DFT+U approximation provides a pragmatic extension to DFT by adding a static, site-dependent correction that penalizes double occupancy, thus capturing key correlation effects with minimal computational overhead.

In the context of OER, where spin degrees of freedom and local electron correlations play a central role in determining catalyst-reactant interactions, spin-polarized DFT+U is thus one of the most widely used approaches. It corrects self-interaction errors and improves the treatment of open-shell configurations by accounting for on-site Coulomb interactions, thereby enabling more accurate treatment of unpaired electrons, magnetic ordering, and spin-state changes during catalysis within the strongly correlated transition metal cations, which are often the active sites used in catalysis.

Predicting OER Activity Using Free Energy of Reaction Intermediates: The electronic structure methods discussed above can provide accurate energies of intermediates (ΔE) at 0 K on catalyst surfaces. This is achieved by placing the adsorbate-catalyst complex in a periodic or cluster-based DFT framework. To connect these results to experimental electrochemistry, it is more appropriate to determine free energies (ΔG), which contain entropy and zero point energy corrections. Two decades ago, Rossmeisl and coworkers established a DFT-based approach to determine free energies of electrochemical intermediates, particularly for OER and ORR.[23,24] This approach has been widely used in the field to find the potential limiting steps and determine the theoretical overpotential.[25,26] Starting from total energies at 0 K of adsorbed species (*OH, *O, *OOH) at surfaces, zero-point and entropy corrections are taken into account to obtain finite-temperature free energies. The computational hydrogen electrode (CHE) model then accounts for applied potentials by shifting proton-electron pair energies by $-eU$, linking theory to experiment. Plotting the reaction free energy profile reveals the potential-determining step and theoretical overpotential, and can be used to derive the widely-used volcano plots.[27] This method has enabled high-throughput screening across diverse catalyst families and remains a cornerstone of computational electrochemistry.[28,29]

Key Results and Methodological Limitations: Spin-polarized DFT+U calculations of free energies of intermediates have established a strong connection between magnetism, spin state and catalytic performance in systems such as RuO_2,[30] doped Fe_2O_3,[31,32] Co_3O_4,[33,34] $Co_{1-x}Ni_xFe_2O_4(001)$[35] CoOOH [36] and $LaCo_xFe_{1-x}O_3$.[37] These studies demonstrate that factors such as doping, surface termination, facet orientation, and the presence of adsorbates can significantly influence the charge and spin states of catalytic reaction sites, thereby affecting the overpotential. Moreover, multiple studies consistently report substantial variations in the magnetic moments of the active site and surrounding atoms along the reaction pathway[31–33,35,37] which can further be influenced by the applied potential,[38] indicating changes in valence and spin states. These changes, in turn, have been associated with differences in the overpotential.

Other investigations provide a link between spin state or magnetic order and catalytic performance. In RuO_2, antiferromagnetic (antiFM) configurations can lower OER overpotentials by 20–240 mV compared to nonmagnetic RuO_2 surfaces, depending on OH coverage.[30] In CoOOH, the high-spin (HS) state significantly lowers the transition state barrier for O-O coupling compared to the low-spin (LS) state (1.21 eV vs 2.91 eV), such that OER on LS CoOOH follows an alternative OER pathway that circumvents O-O coupling. This leads to a much lower overpotential for HS CoOOH (0.32 V) compared to LS CoOOH (0.66 V), demonstrating a strong spin-dependent enhancement of OER kinetics.[36] For $Co_3O_4(001)$ surfaces, which show a superior OER performance compared to (111),[34] the octahedral Co active site that is LS in the bulk acquires a finite magnetic moment that varies between 0.5-2.1μ_B during OER.[33] Moreover, the transformed NiOO(H) layer on $LaNiO_3(111)$ exhibits a regular pattern of LS Ni^{4+} and HS Ni^{3+} stripes that favorably impacts the binding of intermediates, thus lowering the overpotential.[26] These system-specific observations confirm the significant influence of spin states and spin ordering on OER overpotentials. Complementary studies using schematic models suggest that ferromagnetic (FM) ordering can generally lead to milder adsorption energies and lower activation barriers, including reduced transition state energies.[8,9,39]

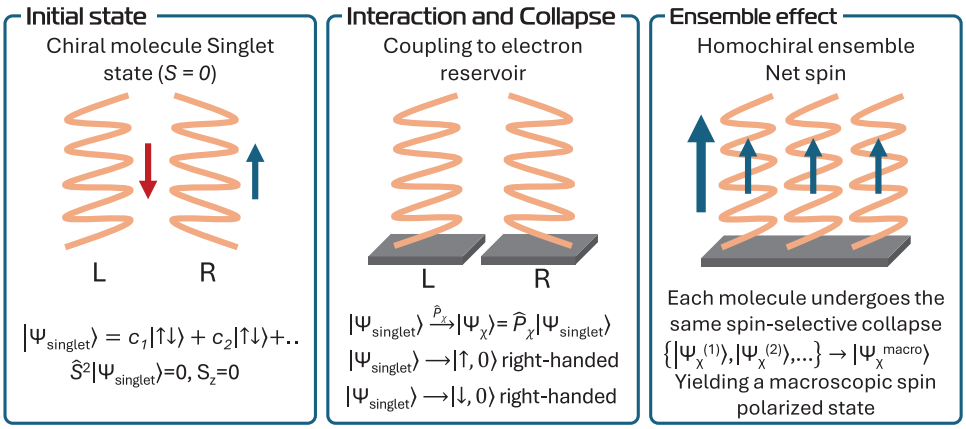

Figure 3. Proposed spin-selective symmetry breaking mechanism in chiral molecules: a) *Initial state*: The isolated singlet state of a molecule is an entangled superposition of spin-correlated configurations denoted as $|\Psi_{singlet}\rangle$. b) *Interaction and collapse*: Upon coupling to an electron reservoir (e.g., a metal electrode), the singlet state is hypothesized to collapse into a specific spin configuration, $|\Psi_\chi\rangle = \hat{P}_\chi|\Psi_{singlet}\rangle$, where $\hat{P}_\chi$ is a projection operator reflecting the interaction-induced symmetry breaking. c) *Ensemble effect*: In chiral systems, this collapse is not random but biased by the molecular chirality, leading to homochiral assemblies with aligned spin configurations. The resulting ensemble of states ($|\Psi_\chi^{(1)}\rangle, |\Psi_\chi^{(2)}\rangle, \ldots$) gives rise to a macroscopic spin-polarized state $|\Psi_\chi^{macro}\rangle$, generating an emergent spin anisotropy. This provides a theoretical foundation for spin-polarized charge transport in chiral molecules–a hallmark of the CISS effect.[62]

As an alternative route to address spin excitations and dynamic spin effects in electrocatalysis, which cannot be described with spin polarized DFT+*U*, Gracia and co-workers pointed out the role of quantum spin exchange interactions (QSEI)[40,41] and quantum excitation interactions (QEXI)[8] in spin-dependent electrocatalysis. These approaches aim to incorporate spin-dependent quantum correlations into the evaluation of intermediate free energies and transition state barriers, starting from spin-polarized DFT+*U* calculations. QSEI describes how spin alignment lowers Coulomb repulsion and stabilizes open-shell orbitals, while QEXI explains spin excitations and spin-selective charge transport through schematic diagrams. Together, they highlight the role of spin alignment and orbital symmetry in driving activity in OER. The framework introduced by Gracia and co-workers, while being qualitative, is thus an important step toward the development of quantitatively predictive methods to fully capture spin effects in OER catalysis.[9]

Another emerging focus in OER catalysis is the role of polarons, quasiparticles formed when charge carriers (electrons or holes) locally distort and couple to the lattice. Excess charge carriers on transition metal oxide surfaces introduced by defects, light exposure or adsorbates during the OER cycle can localize through electron-phonon interactions to form polarons that act as local spin centers.[42] The critical role of polarons has been revealed for the photoelectrochemical OER on TiO_2(110), where the presence of light-induced polarons modifies the adsorbate binding energies and enhances the charge transfer between the catalyst surface and adsorbed species.[43] Including these quasiparticles at different sites in free energy calculations has been shown to alter the predicted overpotentials.[44]

In addition to shaping the free energy landscape, spin effects on dynamic processes–such as reaction kinetics and electron transfer to and within the catalyst–must also be taken into account. Spin configurations, exchange interactions, and long-range magnetic order have been identified as critical factors that directly impact electron transport and reaction kinetics in transition metal oxide catalysts,[7,18,39,45] and FM order has even been hypothesized to contribute to the conservation of angular momentum.[18] Based on schematic models, recent studies propose that quantum correlations and electron delocalization in FM bonds and spin-polarized electronic channels can enhance electron transport by spin-selective charge transfer and improve predicted OER performance. Similarly, layered antiferromagnetic (antiFM) structures can also be beneficial due to the formation of spin-sensitive transport channels;[40] but usually, strong spin-charge confinement and electron localization in antiFM bonds tend to restrict charge transfer.[9,13,18] Conducting PM materials may also exhibit high activity, particularly when featuring localized spins, spin-polarized states, or embedded FM channels.[46] In such systems, dynamic orbital occupancies and fluctuating exchange interactions introduce flexibility that may be intrinsically advantageous under OER conditions. Ultimately, magnetic interactions that enable efficient spin-dependent electron transfer appear to be a critical factor to enhance OER catalysis.

2.1.2. CISS Enhanced OER

The CISS effect describes how molecular chirality induces spin-polarization in electron- related processes.[47] To elucidate the influence of the CISS effect on the OER theoretical models that describe the role of chirality in inducing spin-polarization of electron transport are critical. Such models can provide insights into the underlying mechanisms of the effects which are vital for understanding the spin-dependent catalysis in chiral materials.

Experimentally, spin selectivity is often studied by placing a chiral molecule between a non-magnetic and a magnetizable FM electrode. Reversing the magnetization of the FM electrode yields two different current measurements; any resulting asymmetry indicates spin-polarized transport. While FM contacts are

commonly used to probe this effect, it is important to note that this is not a prerequisite for the CISS effect to occur, but rather a convenient means of probing the spin-polarization. Theoretical efforts have mainly focused on explaining the origin of these asymmetric current responses.

For about a decade, the theoretical progress about the CISS effect was centered around constructing effective models that account for the spin-orbit coupling (SOC) in chiral molecules, using, e.g., scattering theory,[48,49] calculating the transmission matrix using wave functions for chiral potentials,[50,51] and through semi-analytical models.[52] In these models, SOC connects the molecular structure with the electronic spin. However, the SOC is known to be small (less than 5 meV) in organic molecules and cannot give rise to the experimentally observed anisotropies in the spin structure on its own.

Moreover, these single-electron models discuss a non-interacting electron gas and assume that there are no particle-particle interactions. This simplification makes the model easier to solve (linear matrix equation) and has proven useful for studying charge flow through molecules connected to metal electrodes. The main drawback, however, is that without electron correlations, the electronic structure in such models is built up by independent electrons from which no coherent spin structure can be obtained. These approaches thus cannot describe a delocalized chiral state which is needed to understand the CISS effect in the absence of magnetic fields.

Despite these shortcomings, single-electron models have demonstrated that multi-orbital structures can give rise to a minor CISS effect.[53–55] This CISS effect can arise if nuclear sites possess multiple valence states that are mixed via spin-orbit coupling, which in turn has to connect to the molecular geometry. This requirement stems from the fact that chirality is a global property and, therefore, can only exert a significant influence on delocalized or conjugated electronic states.

Theoretical models that account for electron correlations, on the other hand, offer deeper insight into the mechanisms for induced, or emergent, spin-polarization. Such models of chiral molecules can be categorized into those that include direct Coulomb electron-electron interactions,[56–58] and those for which the correlations are indirectly mediated by molecular vibrations.[59–61]

In such models, the electron correlations provide a singlet-type electronic structure in the chiral molecule, and can be obtained by many-body calculations. The singlet state of a molecule is an entangled mixture of correlated states, each of which describes a coherent spin structure (**Figure 3a**). Upon attachment of the chiral molecule to an electron reservoir, e.g., a metal, it is hypothesized that the superposition of states that form the singlet state collapses into one of the spin configurations due to interaction-induced symmetry breaking (Figure 3b). For a chiral molecule this collapse is not arbitrary but is defined by its chirality,[62] hence the molecules in a homochiral assembly all collapse into the same spin configuration and, thereby, constructs a collection of molecules with identical spin configurations (Figure 3c). The collapse of the singlet state into a specific spin configuration, which thereby would be regarded as a result of symmetry breaking, is thus determined by the chirality, and can be viewed as a spin anisotropy which has a spin-polarizing effect on electron flow through the molecule, explaining the spin-polarization within chiral materials. This emergent spin-polarization in chiral molecules connected to electrodes is, from a theoretical perspective, one of the most viable causes for the CISS effect.

Besides the study of these fundamental aspects, the role of CISS in electrochemical applications has been investigated. While the OER has not yet been explicitly addressed in computational models, some progress has been made for its reverse reaction, the oxygen reduction reaction (ORR). Chiral molecules have been shown to efficiently catalyze ORR and it has been suggested that a cathode modified with chiral molecules provides a steady stream of spin-polarized electrons to the reactant O_2.[63] While the reason why spin-polarized electrons better facilitate the reactions remain elusive, a few reports in the theoretical literature predict both spin-polarized currents and spin-polarized molecular density of electron states under non-equilibrium conditions.[64–66] These results are based-respectively-on spin polarized DFT calculations employing an local-density approximation (LDA) functional in combination with non-equilibrium Green functions for simulations of the transport properties,[64] and on model Hamiltonians capturing the molecular correlated electronic structure combined with non-equilibrium Green function calculations.[63,65,66]

Although theoretical models within the CISS field for spin-enhanced OER are not yet sufficiently developed to allow for quantitative predictions, they can still aid in phenomenological interpretation. Theoretical insights suggest that the relevance of chirality in chemical reactions that involve electron transfer likely stems from the CISS effect, which ensures that electrons with a specific spin projection are preferentially supplied or extracted with high probability. Chemical reactions that involve compounds with different spin angular momentum, such as OER and ORR, benefit from being supported by electron transfer of a specific spin-projection, because it conserves angular momentum without the necessity of spin-flip processes.[67]

2.2. Experimental Exploration of Spin Enhanced OER

To verify, explore and possibly exploit the theoretical propositions given above, numerous experimental studies have been performed using both magnetic and chiral materials. A non-exhaustive overview with selected examples of the current state-of-the-art, including utilized catalyst material classes, spin order engineering techniques, and measurement approaches is given in **Tables 1** and **2** for magnetically and CISS enhanced OER, respectively. Moreover, **Figure 4** shows an example of spin-induced enhancements in OER that arise from specific underlying mechanisms.

A key observation from the tables is that all of these studies across different systems show that increasing chirality or magnetic order through external stimuli or intrinsic material properties decreases the OER overpotentials. Other measurables and the size of their increment vary noticeably across different studies, indicating that experimental design can greatly influence the results. Thus, it is essential to look closely at the electrochemical methodology, material selection and synthesis, as well as engineering strategies used to modify spin-polarization and magnetic and chiral properties of the active site, along with the techniques employed to characterize these properties. In this subsection, we

Table 1. Non-exhaustive summary of selected works showing the enhancement of OER via magnetic interactions.

Material choice	Magnetic field/material engineering	Measurables studied	Size of increment	Spin order measurement	Electro-chemical methods	Electrochemical environment	Proposed origin of OER enhancement	Spin order manipulation method	Refs.
$CoFe_2O_4$ particles	External field	Current density; Overpotential; Tafel slope	Tafel slope reduction from 106 to 82.8 mV/dec @ 10000 Oe	SQUID	LSV; CA; CV	1 M KOH	Increased spin-polarization under magnetic field	Magnetic field	[103]
$CoFe_2O_4$ nanoparticles on $CoFeMo_3O_6$ nanosheets	External field (113.06 Oe) and materials engineering	Current density; Overpotential; Tafel slope; Charge transfer resistance; TOF	~30 mV overpotential decrease @ 10 mA/cm^2; Tafel slope reduction from 35.30 to 26.06 mV/dec @ 113.06 Oe	VSM	LSV; EIS; CA	1 M KOH	Spin alignment via magnetic proximity effect	Interface effects in heterostructures	[121]
$CoFe_2O_4$	External field	Current density; Overpotential; Charge transfer resistance	39 mV overpotential decrease @ 10 mA/cm^2; Tafel slope reduction from 92 to 83 mV/dec@ 4000 Oe	XES	LSV; EIS	1 M KOH	Increased spin-polarization under magnetic field	Magnetic field	[70]
$CoFe_2O_4$ nanocrystals	External field and materials engineering	Current density; Overpotential; Tafel slope; Charge transfer resistance	68 mV overpotential decrease @ 10 mA/cm^2 @14000 Oe; Tafel slope reduction by 61.8 mV/dec @ 14000 Oe	VSM	LSV; CV; EIS; CA	1 M KOH	Domain removal and negative MR	Change in amount of domains by particle size	[69]
$CoFe_2O_4$ nanowires	External field (500 mT)	Current density; Overpotential; Tafel slope;	26 mV overpotential decrease @ 10 mA/cm^2, 95 mV overpotential decrease @ 100 mA/cm^2;; Tafel slope reduction from 50 to 43 mV/dec @ 500mT	SQUID, TEM	LSV; CA	1 M KOH	Increased spin- polarization under magnetic field	Magnetic field	[385]
$CoFe_2O_4$ particles	External field and materials engineering	Current density; Charge transfer resistance	~320% current density increase @ pH 14 @ 1.64 V @ field larger than coercivity H	Squid	CV; EIS	0.01, 0.1 and 1 M KOH	Transition from multi-domain to single-domain particles	Change in amount of domains by particle size	[68]

(*Continued*)

Table 1. (Continued)

Material choice	Magnetic field/material engineering	Measurables studied	Size of increment	Spin order measurement	Electro-chemical methods	Electrochemical environment	Proposed origin of OER enhancement	Spin order manipulation method	Refs.
$Co_xNi_{1-x}Fe_2O_4$ nanosheets on Ni foam	External field and materials engineering	Current density; Overpotential; Tafel slope; Charge transfer resistance	21 mV overpotential decrease @ 10 mA/cm^2 @100 mT; Tafel slope from 52.82 to 46.59 mV/dec @ 100 mT	VSM	LSV; EIS; CA	1 M KOH	Increase in saturation magnetization through enhanced spin exchange interactions	Tuning of Ni:Co ratio in nanosheets	[116]
Ba doped Co_3O_4	External field and materials engineering	Current density; Overpotential	1.5–3% current density enhancement @ ~100-140 mA/cm^2 @ 8000 Oe	SQUID	LSV; CA	1 M KOH	MR effects, increased magnetization	Ba doping; Magnetic field; Change of field direction relative to cell geometry	[101]
Cr_2Te_3/CrOOH 2D heterostructure	External field and materials engineering	Current density; Overpotential; Tafel slope; Charge transfer resistance	~70 mV overpotential decrease @ 10 mA/cm^2; Tafel slope reduction from 120 to 87 mV/dec @ 7000 Oe	VSM	LSV; EIS	1 M KOH	Proximity-induced FM order in Cr_2Te_3 after magnetization	Magnetic proximity effect; temperature	[80]
Cu-Ni_6Fe_2-layered double hydroxides	External field and materials engineering	Current density; Overpotential; Tafel slope; Charge transfer resistance	~60 mV overpotential reduction @ 10 mA/cm^2 via doping; Tafel slope reduction from 101 to 33.8 mV/dec via doping; ~30 mV overpotential reduction @ 10 mA/cm^2 @ 8000 Oe	VSM	LSV; ECSA; EIS; FT-IR	1 M KOH	Low spin state to high spin state transition of Fe3+	Alteration of Jahn-Teller effect by Cu doping	[138]
$Fe_{0.5}Co_{0.5}$ metal-organic framework	External field and materials engineering	Current density; Tafel slope; Charge transfer resistance	5.9 times current density increase @1.56V; Tafel slope reduction from 84 to 59 mV/dec	SQUID; Mössbauer	LSV; EIS;CP	1 M KOH	Induced FM coupling between metals	Magnetic exchange with magnetic particles in electrolyte under AC magnetic field	[110]
Fe_xGeTe_2 based van der Waals heterostructure	External field and materials engineering	Current density; Tafel slope; charge transfer, Overpotential	200% current density increase @ 1.7V vs RHE @0.36T; Tafel slope reduction from 66.8 to 57.6mV/dec for graphene/Fe_xGeTe_2 @ 5000 Oe	XMCD; Hall measure-ment	LSV	1 M KOH	Quantum spin exchange interaction	Magnetic field combined with tuning thickness of 2D layered material and their electronic properties	[94]
$YFe_{0.6}Mn_{0.4}O_3$ core / YFeOOH shell particles	Materials engineering	Current density; Tafel slope; Charge transfer resistance; Activation energy	Tafel slope reduction from ~267 to 247 mV/dec; ~50% decrease in activation energy	SQUID; VSM	LSV; EIS; OCP	1 M KOH	Transition from antiFM to weak FM to PM	Temperature combined with spin pinning through magnetic coupling	[85]

(*Continued*)

Table 1. (Continued)

Material choice	Magnetic field/material engineering	Measurables studied	Size of increment	Spin order measurement	Electro-chemical methods	Electrochemical environment	Proposed origin of OER enhancement	Spin order manipulation method	Refs.
Fe_2O_3 particles	External field and materials engineering	Current density; Overpotential; Tafel slope	~9mV overpotential decrease @100 mA/cm^2; Tafel slope reduction from 68.9-61.7mV/dec @ 2000 Oe	VSM; Mössbauer	LSV; EIS	1 M KOH	Transition from PM to FM	Transformation of α-Fe_2O_3 into γ-Fe_2O_3 by Co doping	[117]
Fe_3O_4@Ni(OH)$_2$ core–shell particles	External field and materials engineering	Current density; Overpotential; TOF; Tafel slope	Maximal 43.8% current density increase @ 1.55 V @ 3000 Oe; Tafel slope reduction from 78,4 to 64.3 mV/dec @ 3000 Oe; 5-fold boost of current density (monodomain core–shell particle vs bulk Fe_3O_4)	VSM	CV	1 M KOH	Increased spin polarization and transition to single magnetic domain by interfacial spin coupling	Tuning of FM-antiFM coupling via nanoparticle shell thickness	[104]
Fe_7Se_8 nanosheets	External field	Current density; Overpotential; Tafel slope; Intermediates	87 mV overpotential decrease @ 10 mA/cm^2 @ 2000 Oe	in situ MFM; VSM	LSV;CA; operando Raman	1 M KOH	Domain removal	Magnetic field	[81]
Single Fe atoms incorporated in nitrogen-doped carbon nanofibers	Materials engineering	Current density; Overpotential; TOF; Tafel slope; Charge transfer resistance	~120 mV overpotential decrease @ 10 mA/cm^2; ~190 mV overpotential decrease @ 30 mA/cm^2; Tafel slope reduction from 114 mV/dec to 51.7 mV/dec	EPR	LSV; EIS; CA	1 M KOH	High spin to low spin state transition of Fe	Mg doping	[97]
Single Fe atoms incorporated in nitrogen-doped carbon nanofibers	External field and materials engineering	Current density; Overpotential; Tafel slope	~50 mV overpotential decrease @ 10 mA/cm^2; Tafel slope reduction from 101 to 68.6 mV/dec	Mössbauer; XAFS	LSV; Raman; FTIR; Galvanostatic charge/discharge curves	1 M KOH	Low spin to high spin state transition of Fe	Cu substitution	[71]
$LaCoO_3$ epitaxial thin films	Materials engineering	Current density; Overpotential; Tafel slope; Charge transfer resistance	~430% current density increase @ 1.8 V vs RHE; Tafel slope reduction from 315 to 180 mV/dec	VSM	LSV; EIS; CA	1 M KOH	Low spin to intermediate spin state transition	Tuning of the exposed facet and strain	[112]
$LaCoO_3$ particles	Materials engineering	Current density; Overpotential; Tafel slope; Charge transfer resistance	~130 mV overpotential decrease @ 10 mA/cm^2; Tafel slope reduction from 102 mV/dec to 69 mV/dec	SQUID	LSV; EIS	0.1 M KOH	Optimization of low spin:high spin state ratio	Particle size variation	[113]

(*Continued*)

Table 1. (Continued)

Material choice	Magnetic field/material engineering	Measurables studied	Size of increment	Spin order measurement	Electro-chemical methods	Electrochemical environment	Proposed origin of OER enhancement	Spin order manipulation method	Refs.
$LaCoO_3$ particles	Materials engineering	Current density; Overpotential; Tafel slope; Charge transfer resistance	~20 mV overpotential decrease @ 10 mA/cm^2 when comparing facets; ~30 mV overpotential decrease @ 10 mA/cm^2 upon doping; Tafel slope increase from 121 to 125 mV/dec when comparing facets; Tafel slope reduction from 125 to 87 mV/dec upon doping	EPR	CV; EIS	1 M KOH	Low spin to high spin state transition of Co	Tuning of the exposed facet and Sr doping	[111]
$LaCoO_3$ particles	Materials engineering	Current density; Overpotential; Tafel slope; Charge transfer resistance	250% increase in current density @ 1.65 V vs RHE; Tafel slope reduction from 71 mV/dec to 62 mV/dec	EPR; SQUID	LSV; EIS	1 M KOH	Low spin to high spin state transition of Co	Mn doping	[96]
$La_{0.7}Sr_{0.2}Ca_{0.1}MnO_3$ thin film	External field and materials engineering	Current density; Overpotential; Tafel slope, charge transfer resistance	~90% current density increase at 300K (close to T_c) @ 5000 Oe	SQUID	LSV; EIS; CA	1 M KOH	Transition from FM to PM; Domain alignment	Temperature and magnetic field	[78]
$La_{0.67}Sr_{0.33}MnO_3$ thin film	External field and materials engineering	Current density; Tafel slope; Charge transfer resistance; Activation energy	35% current density increase at 1.8V vs RHE (PM to FM transition); 0.4% current density increase at 1.8V vs RHE @ 350 Oe	VSM; Scanning SQUID microscopy; resonan X-ray reflectivity	CV; CA; EIS	0.1 M KOH	Transition from PM to FM; Domain alignment	Temperature and magnetic field	[72]
Sr doped $LaMnO_3$ on glassy carbon	External field and materials engineering	Current density; Overpotential; Charge transfer resistance; Double layer capacitance	120 mV overpotential decrease @ 10 mA/cm^2 @ hl10000 Oe	MR measure-ments; VSM	LSV; EIS	1 M KOH	Negative MR	Sr doping changes magnetic coupling	[100]
Ni, NiO, $NiOH_2$	External field	Current density; Overpotential; Charge transfer resistance	~20 mV overpotential decrease @ 10 mA/cm^2 @ 14000 Oe	VSM	LSV; EIS	1 M KOH	Negative MR	Oxidation state change	[99]
Ni Foam, Ni sheet, Pt sheet	External field	Current density; Overpotential	+3.6 to 2.5% alterations of current density @ ~120–140 mA/cm^2 @ 8000 Oe in different directions	SQUID	LSV; CA	1 M KOH	MR effects; MHD	Magnetic field; Change of field direction relative to cell geometry	[101]

(*Continued*)

Table 1. (Continued)

Material choice	Magnetic field/material engineering	Measurables studied	Size of increment	Spin order measurement	Electro-chemical methods	Electrochemical environment	Proposed origin of OER enhancement	Spin order manipulation method	Refs.
Layered double hydroxides: NiCoFe, NiFe and CoFe	External field and materials engineering	Current density; Overpotential; Tafel slope; Charge transfer resistance	overpotential decrease of ~24 mV @ 10 mA/cm^2 and of ~26 mV @ 100 mA/cm^2 @ 7000 Oe for NiCoFe which showed the biggest effect.	VSM	LSV; EIS; CA; operando Raman	1 M KOH	Increase in magnetization	Doping with different transition metals	[115]
NiFe thin films	External field	Current density; Overpotential; Charge transfer resistance	16 mV overpotential decrease @ 10 mA/cm^2 @ 2000 Oe	MFM; SQUID	CV; EIS	1 M KOH	Domain wall removal under magnetic field	Domain size alteration through film thickness	[93]
(Ru-Ni)O_x nanosheet	External field and materials engineering	Current density; Overpotential; Tafel slope; Charge transfer resistance; TOF	67 mV overpotential decrease @ 1000 mA/cm^2; Tafel slope reduction from 70 to 30 mV/dec @ 3982 Oe	VSM	CV; LSV; EIS; operando Raman	1 M KOH	Improved spin polarization and spin-selective electron transfer through stronger exchange coupling	Tuning of FM-antiFM coupling by doping	[105]
Mn doped RuO_2 nanoflakes	External field and materials engineering	Current density; Overpotential; Tafel slope; TOF	~57 mV overpotential decrease @ 10 mA/cm^2; Tafel slope reduction from 52.8 to 40 mV/dec @ 3309 Oe	XMCD; SQUID	LSV; Chronopo-tentiometry	0.5 M H_2SO_4	Increased spin polarization	Mn doping	[95]
$SrCoO_3$ particles	Materials engineering	Current density; Overpotential; Tafel slope; Charge transfer resistance	~70 mV overpotential decrease @ 150 mA/cm^2; Tafel slope reduction from 117 to 86 mV/dec	VSM	LSV; EIS	1 M KOH	Improved spin-polarized electron transfer via high conductivity spin channel	Trigonal to cubic structural transformation through fluorine doping	[119]
$ZnCo_2O_4$ and $LiCoVO_4$ particles	Materials engineering	Current density	800% current density increase @ 1.8 V	VSM	CV	1 M KOH	Improved spin-polarized electron transfer via high conductivity spin channel; Covalancy engineering	Change of composition	[118]
$ZnCo_2O_4$ particles	Materials engineering	Current density; Overpotential; TOF; Charge transfer resistence	~40 mV overpotential decrease @ 25 μA/cm^2	XAFS; SQUID	CV: EIS	1 M KOH	Low spin to high spin state transition of Co	Increase in calcination temperature	[114]
$ZnCo_xMn_{2-x}O_4$ powder	Materials engineering	Current density; Overpotential; Tafel slope; Charge transfer resistance	~250 mV overpotential decrease @ 25 μA/cm^2; Tafel slope reduction from 126 to 50 mV/dec	DFT calculation of DOS, none experi-mental	LSV	0.1 M KOH	Increased spin-polarization	Increase of the Co:Mn ratio	[386]

Table 2. Summary of selected works showing the enhancement of OER via the CISS effect.

Material choice	Element of chirality	Measurables studied	Size of increment	Measurement of chirality or spin-polarization	Electrochemical methods	Electrochemical environment	Refs.
Au-Ni bilayer coated with L-cysteine	Surface modification with L-cysteine	Current density, H_2, H_2O_2 and O_2 production, Tafel slope	5-fold increase in current density for OER	CD spectroscopy	LSV	0.1 M KOH (pH 13)	[250]
Chiral additives in catalyst binder of IrO_2, RuO_2 and $Fe_{0.7}Co_{2.3}O_4$	Chiral molecular additives (S- or rac-camphor sulfonic acid) in conductive binder	Current density	≈25 mV at $J_{ECSA} = 0.5$ mA/cm^2, 23% increase in mass activity	CD spectroscopy	LSV; EIS; RRDE	1 M NaOH (pH 14), 0.1 M sodium carbonate/bicarbonate buffer (pH 10), 0.02 M phosphate buffer (pH 8), 0.5 M H_2SO_4 (pH<1)	[126]
Chiral Au NPs	Use of D- or L-cysteine as templating agents during synthesis	Current density, H_2O_2 production	Reduction of overpotential of 90 mV at 10 mA/cm^2	mc-AFM, CD spectroscopy	LSV	0.1 M KOH (pH 13)	[129]
Chiral Fe_3O_4 film	Use of L-tartaric acid as templating agent during synthesis	Overpotential, Tafel slope, H_2 and H_2O_2 production	150 mV lower overpotential at 10 mA/cm^2	CD spectroscopy	LSV; EIS; CA	0.1 M KOH (pH 13)	[135]
Chiral $Co_{3-x}Fe_xO_4$ nanoparticles	Use of L- or rac-cysteine as templating agents during synthesis	Overpotential, Tafel slope	28 mV reduction in overpotential of the chiral vs achiral at 10 mA	CD spectroscopy	LSV; RRDE	1 M NaOH (pH 14), 0.1 M Na_2CO_3 (pH 10), 0.02 M potassium phosphate buffer (pH 8)	[73]
Chiral cobalt-doped nickel oxide (Co-NiO)	Use of D- or L-proline as templating agents during synthesis	Current density, Tafel slope, H_2O_2 production	46 mV lower overpotential at 10 mA/cm^2	mc-AFM, CD spectroscopy	LSV; EIS	0.2 M KOH (pH 13.3)	[128]
Chiral cobalt oxide thin film	L-, D-, or meso-tartaric acid as templating agents during synthesis	Current density, Tafel slope, O_2, H_2 and H_2O_2 production	65 mV reduction in overpotential at 10 mA/cm^2, oxygen yield increased by 1.4-fold	CD spectroscopy	LSV	0.1 M KOH (pH 13)	[86]
Chiral CuO	L-, D-, or meso-tartaric acid as templating agents during synthesis	Current density, H_2 and H_2O_2 production	50 mV reduction in onset potential	Mott polarimetry, CD spectroscopy	LSV (EC and PEC)	0.1 M Na_2SO_4 solution (pH 6.5) and 0.2 M borate buffer solution (pH 9)	[387]

(*Continued*)

Table 2. (Continued)

Material choice	Element of chirality	Measurables studied	Size of increment	Measurement of chirality or spin-polarization	Electrochemical methods	Electrochemical environment	Refs.
Chiral molecules below NiFeOx	Enantiopure thiadiazole-helicenes below the catalyst layer	Current density, H_2O_2 production	ca. 130% increase in current density @ 1.65 V vs RHE	N/A	LSV	0.1 M O_2-saturated KOH (pH 13)	[74]
Chiral NiFe oxides	Use of D- or L-proline as templating agents during synthesis	Overpotential, current density, Tafel slope	~100 mV reduction in overpotential	mc-AFM, CD spectroscopy	LSV; CP	1 M KOH (pH 14)	[133]
CdSe quantum dots embedded within a chiral polymer	Chiral polymer	Photocurrent density, H_2 production	Doubling of current density	mc-AFM	LSV (PEC)	0.1 M Na_2SO_4 (pH = 6.5)	[127]
Fe_3O_4 nanoparticles coated with chiral molecules	Surface modification with chiral molecules	(Photo)current density, H_2O_2 production	3.5 times higher current	CD spectroscopy	LSV; CA (EC and PEC)	0.1 M KOH solution (pH 13)	[136]
Hybrid chiral MoS_2 Layers	R-, S- and rac- methylbenzylamine embedded within the structure	Current density, Tafel slope, H_2O_2 production	22% decrease in Tafel slope	CD spectroscopy, mc-AFM	LSV	0.1 M KOH (pH 13)	[388]
Iridium nanoparticles functionalized with chiral molecules	Surface modification with various chiral molecules	Current density, Tafel slope, H_2O_2 production	85% enhancement in activity	CD spectroscopy	LSV	0.1 M KOH (pH 13)	[389]
Ni-based electrodes coated with a chiral Ni-Au film	Use of enantiopure tartaric acid or amino acids as templating agents during synthesis	Current density	60% increase in current density	CD spectroscopy	CV; CP	N/A	[390]
Tartaric acid-FeNi coordination polymer	D-, L-, and rac- tartaric acid within the structure	Current density, H_2O_2 production	35% increase of OER current	CD spectroscopy, mc-AFM	LSV	1 M KOH (pH 14)	[391]
TiO_2 - helicene - Au	Surface modification with enantiopure bis(thiadiazole)-[8]helicene	Current density, H_2O_2 production	33% reduction in H_2O_2 production	N/A	CA	0.25 M CO_2 saturated K_2CO_3 (pH 6.8)	[88]
TiO_2 - molecule - CdSe NP	Surface modification with various chiral molecules	Photocurrent density, H_2 production	Reduced overpotential for H_2 production	mc-AFM	LSV (PEC)	mixture of 0.35 M Na_2SO_3 and 0.25 M Na_2S (pH 9.5)	[5]
TiO_2 modified with triphenylamine-based dye	Surface modification with chiral molecules	Current density, H_2O_2 production	Nearly 50% reduction in H_2O_2 per mA/cm^2, 28% increase in photocurrent	CD spectroscopy	CA (PEC)	0.1 M Na_2SO_4 (pH=6.56)	[87]
TiO_2 modified with Zn porphyrins and TPyA molecules	Helical supramolecular assembly	Photocurrent density, H_2O_2 production	ca. 2 times higher photocurrent	CD spectroscopy, mc-AFM	LSV; CA (PEC)	0.1 M Na_2SO_4 (pH=6.56)	[392]
Topological chiral semimetals (RhSi, RhSn and RhBiS)	Intrinsically chiral crystal structure	Current density, overpotential, H_2O_2 production	Specific activity increase by about 200-fold	single-crystal XRD, TEM	LSV; CA	1 M KOH (pH 14), 0.1 M KOH (pH 13), 1x PBS solution (pH 7.4) and 0.5 M H_2SO_4 (pH 0.2)	[367]

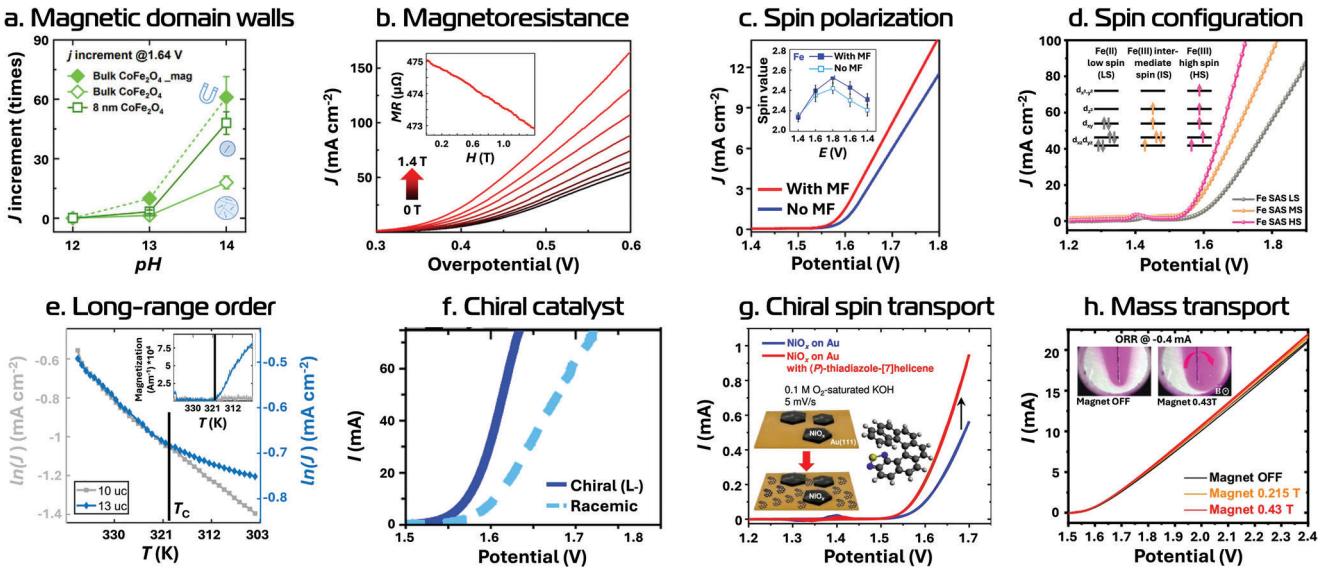

Figure 4. Examples of spin-induced enhancements in OER current densities arising from different underlying mechanisms. a) OER performance of $CoFe_2O_4$ particles under various pH conditions. The enhancements are linked to the transition from magnetic multidomain to single-domain states removal through size reduction or external magnetic field application. Adapted with permission.[68] Copyright 2023, Wiley-VCH GmbH. b) OER performance of $CoFe_2O_4$ nanocrystals under various magnetic fields. The enhancements are linked to the negative magnetoresistance (MR) effect, shown in the inset. Adapted with permission.[69] Copyright 2022, American Chemical Society. c) OER performance of $CoFe_2O_4$ particles with and without a magnetic field. The enhancement is linked to increased spin-polarization on both the Fe and Co as indicated by XES measurements shown in the inset. Reproduced from ref. [70] by Chih-Ying Huang et al. licensed under CC BY 4.0. d) OER performance of single iron atom catalysts coordinated with nitrogen in carbon (Fe-N-C). The enhancements are linked to a transition from a low to intermediate to high spin state as indicated in the inset. Adapted with permission.[71] Copyright 2023, Wiley-VCH GmbH. e) OER performance of $La_{0.67}Sr_{0.33}MnO_3$ thin films as a function of temperature. The enhancements are linked to a transition from PM to FM order as indicated in the inset. Reproduced from ref. [72] by Emma van der Minne et al. licensed under CC BY 4.0.f) OER performance of chiral and achiral $Co_{3-x}Fe_xO_4$ particles. The enhancement is linked to the chirality of the catalyst. Reproduced from ref. [73] by Aravind Vadakkayil et al. licensed under CC BY 4.0. g) OER performance of 2D NiO_x catalysts on Au with and without absorbed thiadiazole-[7]helicene enantiomers. The enhancement is linked to the chiral induced spin-polarization of electron transport. Reproduced from ref. [74] by Yunchang Liang et al. licensed under CC BY 4.0. h) OER performance of a Pt foil under different magnetic fields. The very small enhancements are linked to changes in mass transport as indicated by a change in the OH^- concentration profile. The influence of the magnetic field on the ion movement during ORR is shown in the inset by the change of color of an acid-base indicator that turns pink in high OH^- concentrations. When the magnetic field is off, the generation and migration of OH^- is homogeneous, while with the magnetic field there is a preferential direction of movement. Reproduced from ref. [75] by Priscila Vensaus et al. licensed under CC BY 4.0.

provide an overview of the key studies in the fields of magnetically and CISS enhanced OER, with particular emphasis on the experimental methods used.

2.2.1. Electrochemical Methodology

Various electrochemical methods have been utilized to show spin induced OER enhancements (Figure 2 *center*). Linear sweep voltammetry (LSV) and CV are the most commonly used techniques for investigating OER activity as a function of external stimuli, like magnetic fields and temperature variations, and of engineered variations in long-range magnetic order or chirality. These measurements yield key parameters, such as current densities, overpotentials, Tafel slopes, and turnover frequency, which help to quantify O_2 generation and provide insights into the rate-determining step (RDS) and how it might change.

Electrochemical impedance spectroscopy (EIS) is a widely employed technique for probing interfacial and bulk properties in electrocatalysis and can provide insight into the steady state of electrochemical processes and their kinetics.[76,77] Different features in EIS data represent different processes with characteristic relaxation times. Hence, it enables the determination of uncompensated resistance and charge transfer at the electrode/electrolyte interface, thereby facilitating the study of magneto-resistance effects within bulk of the catalyst and the role of spin ordering in modulating electron transfer into the catalyst.[72,78,79] In addition, EIS allows for the evaluation of surface capacitance, offering insights into processes, such as bubble formation, charge separation in the double layer, mass transport within the electrolyte, the accumulation of ionic or molecular species at the catalytic interface, and the evolution of surface-bound intermediates during the OER.[79–82]

CA is often employed to examine external field-induced OER enhancements over time. This method enables real-time tracking of magnetic field effects, which makes it easier to distinguish fast magnetic field induced changes in the electrode[83] from slower processes in the electrochemical system (e.g., electrode degradation, electrolyte composition changes, gas bubble dynamics, local heating, or double-layer restructuring), which tend to be convoluted over the longer timescales involved in a full CV cycle. In addition, by tracking the system's time evolution with and without a magnetic field, the influence of the magnetic field on these slower processes can be assessed.[84] Moreover, CA is used

to investigate the temperature dependence of OER to derive activation energies.[72,85] Finally, in the context of CISS-enhanced OER, gas chromatography for O_2 and H_2 product detection and chemical probes for H_2O_2 (as side product) identification have been utilized to examine the impact of spin effects on faradaic efficiency.[86–88]

A general limitation of the electrochemical methodology discussed above is the lack of standardized measurable parameters. Additionally, the normalization of current density with active area and resistance corrections can significantly affect the results and thus give rise to discrepancies in the reported findings. Moreover, these methods cannot directly probe the intermediates of the reaction. Lastly, exact determination of the RDS using Tafel slopes remains difficult.[89] Although these limitations pose challenges for the broader OER field, they are even more pronounced for the spin-dependent OER domain, where mechanistic insights are critical and additional effects arising from spin interactions make the system even more complex.

2.2.2. Magnetically Enhanced OER

The work of Garcés-Pineda and co-workers, which demonstrated enhanced OER activity on FM catalysts under an external magnetic field, has sparked significant interest in magnetically driven catalytic effects.[12] This discovery prompted a surge of experimental efforts to explore the link between long-range magnetic order and OER performance, often via catalysts engineered with tunable magnetic properties responsive to external stimuli. A selection of these studies is summarized in Table 1. In the following, we first summarize the key methodologies used to characterize and quantify magnetic properties in these studies, followed by an overview of representative experimental investigations into magnetically enhanced OER, with a focus on proposed mechanisms underlying the observed activity enhancements. For a more comprehensive treatment of magnetic field-enhanced OER systems, readers are referred to several detailed reviews.[15,16,90–92]

Magnetic Characterization: The ex situ vibrating sample (VSM) and superconducting quantum interference device (SQUID) magnetometries are the most commonly used methods to study the magnetic properties of catalysts. Both techniques enable the detection of subtle features in the sample's magnetic moment response to an external magnetic fields as well as precise determination of the Neel and Curie temperatures.[72,78] Moreover, scanning probe microscopy techniques, like magnetic force microscopy (MFM) and scanning SQUID microscopy, have been utilized in the field to visualize magnetic domains.[68,82,93] With modification, these techniques also have been used to probe domain structure evolution under different external magnetic fields to link these structures to the OER activity increments under similar fields.[81]

Less utilized techniques in magnetic OER research are X-ray magnetic circular dichroism (XMCD), electron paramagnetic/ferromagnetic resonance (EPR/FMR) and Mössbauer spectroscopy, although all of these are widely employed in other fields to probe element-specific magnetic properties and electronic spin states. For example, they have revealed the element-specific contribution to the magnetic order,[94,95] the unpaired spins,[96,97] and atomic site occupation,[98] respectively. Therefore, these techniques can provide valuable insights into the relationship between catalytic activity and magnetic structure, both at the active site and throughout the catalyst bulk.

External Magnetic Field Enhanced OER: Using the experimental methods mentioned above, numerous studies have demonstrated that external magnetic fields can significantly enhance the catalytic activity of FM and ferrimagnetic (FiM) catalysts, or those containing FM/FiM interfaces (Figure 4a–d). This is typically inferred from increased current densities in CA, LSV or CV measurements in the presence of external magnetic fields (Figure 2 *center*). Interestingly, such an enhancement is smaller in PM materials. The external field enhancement has been observed across a wide range of materials, including metal oxides such as spinels and perovskites, hydroxides, and alloys, and in morphologies such as bulk crystals, nanostructures, gels, nanosheets, thin films, and core–shell particles (Figure 2). Below, we summarize the potential origins of this enhancement, with a focus on magnetic field-induced changes in the properties of the catalyst. The electrolyte induced effects will be discussed later in this perspective.

To minimize total magnetostatic energy, magnetic materials form domains separated by domain walls. Domain walls are widely reported to hinder activity, and their removal is regarded as a key factor in magnetically enhanced OER. This effect becomes evident when comparing superparamagnetic (sPM) particles, which lack domain walls and behave like single-domain ferromagnets in an applied field, to larger particles that contain multiple domains. Notably, only the latter show OER enhancement under a magnetic field, linking the observed improvement to domain wall removal.[68] This observation has been connected to two possible origins. First, the fact that the magnitude of OER enhancement correlates with the total area of domain walls[93] and in situ MFM and micro-Raman experiments show that domain wall regions have higher onset potentials compared to the interior of the domain,[81] suggest the walls themselves hinder activity. Second, changes in catalyst resistance due to negative MR effects have been proposed as a contributing factor. The MR effect arises from a reduction in electron-spin scattering due to the alignment of the magnetic domains under the applied magnetic field. If the catalyst's bulk resistance limits the OER, this MR-induced reduction in resistance can increase the achievable current density, with the increase scaling linearly to the resistance change. Experimental results indeed have shown that OER activity and charge transfer resistance closely follow the MR trends with respect to field strength and saturation magnetization (Figure 4b), supporting the idea that negative MR plays substantial role in the observed enhancement.[69,99–101]

Additionally, increased spin-polarization at active sites under an external magnetic field has been proposed as a contributing mechanism to magnetically enhanced OER.[70,101–103] This idea is supported with in situ X-ray emission spectroscopy (XES) measurements, which show an increased spin-polarization at active sites under OER conditions in a magnetic field, thus correlating it with improved activity (Figure 4c).[70] Similarly, the observed increase in catalytic activity of magnetic heterostructures upon application of an external magnetic field[104,105] and correlation between coercivity and OER enhancement[69] indicate that an increase in the strength of exchange interactions between spins in different domains or across magnetic interfaces (e.g.,

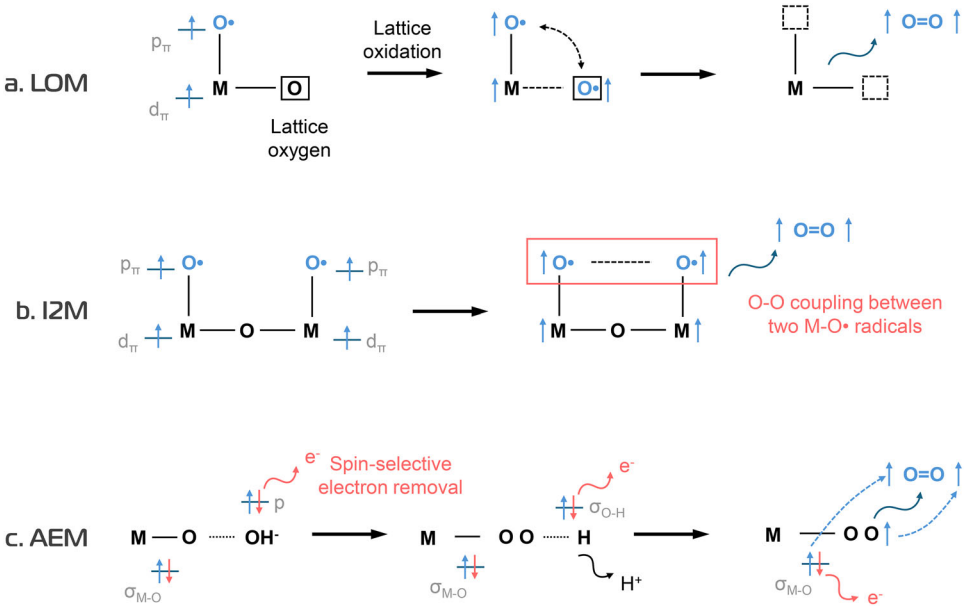

Figure 5. The schemes of O-O coupling and triplet O_2 turnover process. a) LOM, where spin alignment in an adsorbate M-O· radical and a lattice oxygen M-O· radical enables direct formation of the triplet O_2. b) I2M, where spin alignment in nearest-neighbor M-O· radicals enables direct formation of the triplet O_2. b) AEM, where spin-selective electron removal enables direct formation of the triplet O_2. Inspiration taken from ref. [4].

FM/antiFM, PM/antiFM) can be a key factor in OER activity. It is hypothesized that this effect can be attributed to accelerated spin-selective electron transfer into the catalyst.[104,105]

Besides effects arising from changes within the catalyst, the behavior at the solid-electrolyte interface plays a significant role in determining the field induced OER enhancement. For instance, beyond the magnetic field's effects on mass transport of charged species in the electrolyte,[75] strong magnetic field gradients at the electrode–electrolyte interface might enhance activity through enhanced electron transfer, as even in non-spin-dependent reactions like the hydrogen evolution reaction magnetic fields effects have been reported.[106] Moreover, recent studies demonstrate that OER enhancement depends strongly on the electrolyte pH and is most pronounced under strongly basic conditions.[12,68,107] This behavior was attributed to the formation of M-O· radicals with unpaired electrons, which are spin-polarized and activate spin-selective OER pathways.[4] Building on this, it was proposed that spin-polarized OER is particularly relevant for multi-site mechanisms such as the lattice oxygen mechanism (LOM) and the interaction of two metal sites (I2M), though it also influences the adsorbate evolution mechanism (AEM) (**Figure 5**).[108]

Lastly, the magnetic properties of the support material used in electrochemical cells can play a critical role. Nonmagnetic materials'such as coated glass, carbon-based electrodes, or stainless steel–typically exhibit negligible magnetic enhancement in OER activity when used as working electrodes.[12,94,107] Consequently, they are unlikely to contribute meaningfully to magnetic enhancement when serving as supports. In contrast, FM electrodes–particularly those that are intrinsically active for the OER, such as Ni foil or Ni foam–can show significant field-induced activity enhancements when used as working electrodes, and thus can substantially contribute to magnetic enhancement when employed as supports.[12,99,101,105] This highlights the need to distinguish between substrate-induced and catalyst-induced effects when investigating thin film or nanoparticulate catalysts deposited on conductive and possibly also magnetic supports. Additionally, FM supports can amplify magnetic field effects through magnetic coupling with magnetically ordered catalysts.[105]

Spin state and Intrinsic Magnetic Order Induced OER Enhancement: An alternative strategy for enhancing magnetic effects in the OER involves optimizing the intrinsic magnetic order of the catalyst. This approach is particularly advantageous as it eliminates the need for external magnetic influences, which would otherwise necessitate complex reactor designs and may introduce undesirable side effects. Consequently, to clarify the relationship between intrinsic magnetic order and OER activity, extensive research has been dedicated to investigating the role of the intrinsic magnetic order by modulating magnetic properties through various spin engineering techniques.[84,109]

Catalysts exhibiting larger intrinsic magnetization from increased spin exchange interactions or long-range FM order generally showed higher OER activity (Figure 4e).[72,78,80,110] For most cases, increased spin-polarization, which can be induced by a change in oxidation state, doping, or a transition from low to intermediate or high electron spin states, contributed positively to catalytic activity (Figure 4c,d).[71,102,111,112] However, because the spin configuration of the unpaired d-electrons within the catalyst is intrinsically linked to the filling of its e_g orbitals, unfavorable occupancy in certain high spin states can decrease OER activity,[97,113] highlighting the complexity of the spin-dependent effects.

One of the most utilized spin engineering techniques to alter spin state and magnetic order is the use of dopants or substituents which can induce changes in the chemical

environment, electronic properties and crystal coordination of the active site, and affect the spin state and long-range magnetic order through distortions, charge redistribution and spin exchange interactions.[84,109] Another technique that has been widely used involves modifying the magnetic properties of the catalyst through variations in synthesis conditions,[114] the size of the catalyst,[68,113] the strain,[36] and the exposed crystal facets.[112] These approaches have been applied to a variety of materials including layered materials,[95,115,116] single atom catalysts[71,97] and bulk magnetic compounds like metal-oxides[117–119] (Figure 2). A key limitation of these techniques is that changes in magnetic properties are often accompanied by modifications in catalyst composition, crystal structure, or symmetry, making it challenging to isolate the intrinsic effects of the spin state and magnetization of the active site on catalytic activity.

To mitigate these concerns, other studies have adopted spin and long-range magnetic order engineering techniques to selectively tune magnetic order and increase remanence with minimal alterations of other parameters. Studies on catalyst systems which show magnetic coupling via the proximity effect,[80,120,121] spin pinning,[85,104] alignment to stray fields from nearby magnetic particles,[110] metal-support interactions,[109] and spin transmission through spin-dependent electron transfer governed by quantum spin exchange interaction in magnetic van der Waals heterostructures[94] have enabled the decoupling of magnetic order induced effects and confirm the role of spin-polarization and intrinsic magnetization. Moreover, these studies demonstrated that FM coupling reduces the charge transfer resistance[94,120] and that small local magnetic fields[121] and spin filtering[94,104,121] at the interfaces with different magnetic order can enhance spin-selective electron transfer.

Another method to directly influence the magnetic order with minimal alterations of other parameters uses temperature variations to induce magnetic order transitions (Figure 4e). This method has enabled the observation of in situ OER enhancement with a PM to FM transition in the catalyst.[72,78] Additionally, it has been shown that the antiFM to PM transition in a catalyst with an PM/antiFM interface boosts OER activity by promoting spin disorder at the interface.[85] These results highlight that long-range order is crucial for improving OER activity and that the activity follows the trend: FM> FiM> PM> antiFM.

The above-mentioned approaches to tune the intrinsic magnetic order have thus enabled the identification of clear relationships between long-range magnetic order and spin-polarization of the active site to the OER activity. However, the explanation of those relationships varies across different studies, such that the exact origin of the enhancement effect remains to be pinpointed. Identified key factors range from more moderate absorption energies, regulated by stabilizing QSEI interactions,[72,94,110] local magnetic fields of the long-range ordered catalysts,[106] shorter metal-oxygen bonds or formation of spin-selective transport channels[68,78,117,119] to a higher amount of unpaired electrons,[71] or more optimal orbital filling reducing occupation of antibonding orbitals.[71,111,112] Additionally, enhanced spin spillover from the active sites to the intermediates[68,95,116,117] and reduced spin flip energies,[115] both of which enable the direct formation of triplet O_2 and effective oxygen coupling at the surface[36] and lower charge transfer energies,[72,94,120] are hypothesized to affect OER enhancements.

2.2.3. CISS Enhanced OER

The discovery of the CISS effect[122] has revealed that electron transfer reactions and electron displacements in chiral molecules are strongly spin dependent, even at ambient temperature, and this insight has led to the use of chirality to bias the OER toward the formation of triplet oxygen ($^3\Sigma$), rather than singlet byproducts (H_2O_2, and singlet O_2, $^1\Delta$).[10] The body of work on the OER is now substantial and has revealed the benefits of spin control for reaction efficiency and selectivity via the CISS effect in a large variety of chiral materials (Figure 2), as detailed in Table 2. In contrast to these general approaches, less common, material specific approaches exploit spin-selective carrier properties, either inherent to the catalyst or through engineering spin-polarized defect sites on the catalyst.[123–125] While magnetically enhanced OER efforts have primarily focused on electrochemical enhancements, the CISS effect has also been observed in a variety of photoelectrochemical (PEC) systems.

The initial report of CISS effects in OER by Mtangi and Naaman[5] used chiral molecular adsorbates to enhance reaction yields in PEC water splitting. In the following years, chiral electrocatalysts were found to enhance water splitting performance by reducing the OER overpotential and improving reaction selectivity, especially near neutral pH (Figure 4f). A variety of strategies have been employed to introduce and tune chirality in OER catalysts, including the self-assembly of chiral molecules, such as DNA strands, amino acids, or helicenes, on electrode surfaces, the use of intrinsically chiral inorganic materials, and the synthesis of nanostructured materials via chiral templating agents (Table 2). Although the use of chirally-imprinted or chiral electrocatalysts are better known, advances in CISS studies of OER have shown that chiral additives or chiral spin-transport layers can be used with established achiral catalysts and enhance the OER performance (Figure 4g).[74,126,127]

Several experimental studies have shown that imparting chirality onto electrocatalysts improves the Faradaic efficiency toward products involving spin sensitive intermediates and enhances the catalytic activity.[74] Accordingly, the Faradaic efficiency of O_2 production is increased, as systems incorporating CISS-active components exhibit markedly lower H_2O_2 yields compared to achiral analogs. This suppression of reactive oxygen species like H_2O_2 is particularly valuable for enhancing long-term catalyst stability. Studies with chiral electrocatalysts show that the specific (and mass) activities of chiral electrocatalysts can be 5 to 10 times better than their achiral counterparts (Table 2).

While chiral electrocatalysts can be prepared in many different ways and have been shown for metals, metal oxides, and chiral semiconductors, they possess important constraints. For example, many metal oxides are not stable at pH values <10 and the challenges of developing syntheses for each new chiral catalyst provides a barrier to progress. In contrast, recent developments show that chiral molecular films on electrode surfaces, which provide extremely high spin-polarized electron currents (approaching 100 %), can be fabricated.[128,129] The separation of the chiral material used to spin filter electrons from the composition and structure of the electrocatalyst promises to improve performance greatly because it will allow optimization of the electrocatalyst without the need for it to retain its chiral structure. That is, by using a buried chiral spin-transport layer to ensure

the spin-polarized electron transfer at the active catalyst, the benefits of spin-polarization on the redox chemistry can be ensured. For instance, chiral hybrid organic-inorganic oxides, known to act as spin filters,[130] could be used as spin transport layers in PEC water splitting. Chiral molecules and polymers have been used as spin transport layers as well; NiO_x catalysts were deposited on top of helicene monolayers, and the spin-polarization was shown to enhance OER compared to achiral samples[74] and chiral polyaniline coated electrodes were used as a spin transport layer.[131]

Confirming the presence and role of chirality in these systems requires careful characterization.[132] In addition to the electrochemical methods mentioned above, the chirality and spin-selectivity must be assessed. Circular dichroism (CD) spectroscopy, which measures the differential absorption of left- and right-circularly polarized light, is commonly used to verify optical activity. In thin films or nanostructures, CD can also confirm the retention of chiral ordering after material processing. To directly assess spin-selective transport properties, magnetic conductive atomic force microscopy (mc-AFM) is frequently employed. This method reveals differences in current as a function of magnetic orientation, indicating spin-polarization. Complementary techniques such as spin-resolved photoelectron spectroscopy (SR-PES) provide direct evidence of spin-polarized electron emission from chiral surfaces, particularly under ultraviolet or X-ray excitation. Additionally, conventional structural characterization methods, including scanning electron microscopy (SEM), transmission electron microscopy (TEM), and atomic force microscopy (AFM), can be used to evaluate morphology, nanostructure, and surface roughness, which can influence or correlate with the expression of chirality, especially in templated systems.

Despite growing evidence for CISS-mediated enhancements, a notable challenge in interpreting spin-dependent catalysis lies in disentangling true spin effects from other structural or surface-related phenomena. For instance, improvements in performance might stem from increased surface area, altered wettability, or changes in double-layer capacitance associated with chiral templating. To ensure the validity of CISS-related interpretations, rigorous experimental controls are essential, including the use of achiral analogs, enantiomers, and consistent electrode fabrication protocols.

2.2.4. Comparison and Combination of CISS and Magnetism in OER

Comparing activity enhancements in the CISS and magnetically enhanced OER fields is valuable, as each involves distinct phenomena that can account for the observed behavior. In chiral catalysts, improvements are usually linked to spin-polarized charge transport, which can either facilitate spin-selective electron removal from intermediates or induce spin polarization directly at the active site. In magnetic catalysts, the situation is more complex: beyond spin-polarized transport, exchange interactions across sites and layers can alter adsorption energies, establish spin polarization at active sites, and modify spin structures within the catalyst. Domain behavior, MR, and, under external fields, MHD effects can further contribute to activity increments.

Direct comparisons of overpotential and current density increments in the two approaches could thus provide insights into which factors dominate OER enhancement. Reported enhancements, however, vary widely. At 10 mA cm^{-2}, overpotential reductions range from 9 to 130 mV for external-field effects, 20–120 mV for intrinsic magnetism effects, and 25–150 mV for chiral catalysts. Current density increases span 0.4–320%, 35–500%, and 85–500%, respectively. From the current increments it seems intrinsic magnetism effects and CISS effects yield slightly larger enhancements, pointing to the central role of spin polarization at active sites, spin-dependent transport, and exchange coupling. However, the broad spread of reported values makes firm conclusions difficult, likely reflecting variations in catalyst composition, morphology (powder vs thin film), electrolyte, and applied field strength.

For Ni-Fe catalysts, external-field-driven domain wall removal or magnetoresistance effects lead only to modest improvements, with overpotential reductions of 16[93] and 14 mV[115] at 10 mA cm^{-2}. Ni-Fe oxides in chiral form achieve far greater enhancements, showing a 100 mV reduction.[133] A similar trend emerges when chiral molecules are introduced beneath NiOx: the resulting OER enhancement was about five times greater than that obtained under an external field.[74,134] Together, these observations suggest that for Ni-Fe catalysts intrinsic spin polarization of charge transport has a stronger impact on activity than external-field-induced effects.

A comparable pattern is seen in Co-Fe oxides, where activity gains are mainly attributed to intrinsic spin polarization at active sites through spin alignment, rather than domain effects. Here, reported overpotential reductions of 39,[70] 30,[121] and 21 mV[116] are of similar magnitude to those of chiral counterparts (28 mV).[73] External magnetic fields can further enhance activity via a reduction in MR, with larger decreases observed at very high fields–for example, a 69 mV reduction at 14 000 Oe[69] The similarity of enhancements at low fields between magnetic and chiral systems suggests that field effects may also generate spin-polarized current pathways, invoking a mechanism akin to CISS. At stronger fields, MR amplifies the enhancements.

In contrast, Fe_3O_4 shows a strikingly different behavior. Although the enhancement from the intrinsic magnetic transition from PM to FM can increase spin of electron transport, the observed effect is small: the overpotential is reduced by only 9 mV for 100 mA cm^{-2}.[117] Chiral Fe_3O_4 materials, however, exhibit much larger improvements, with a 150 mV overpotential decrease at 10 mA cm^{-2}[135] and a 3.5× increase in current density in another study[136] This stark contrast indicates that the dominant mechanisms can vary significantly between materials, with CISS-type intrinsic polarization often playing a stronger role than field-induced magnetic effects.

These examples highlight the potential for mechanistic insights when comparing CISS and magnetic effects under similar experimental conditions. However, more systematic studies using comparable setups are needed, as direct head-to-head comparisons remain scarce. Furthermore, a synergistic combination of both strategies could potentially enhance OER efficiency even further. When such an integrated approach is applied, both intrinsic spin polarization and field-induced effects may act together, offering a route to maximize catalytic performance.

When such a strategy is applied and both effects are integrated, the outcome is highly dependent on the materials and conditions used. Moreover, if their contributions are comparable, a difference in current is expected between opposite magnetic field orientations (North vs South pole), with the behavior depending on the enantiomer used. In this case, a stronger enhancement is expected when the magnetic field polarizes the spin in the same direction as favored by the chiral molecule.

Another intriguing example is the case of sPM iron oxide nanoparticle catalysts (s-Fe_3O_4) decorated with chiral diamines for water splitting.[137] Both the decoration with chiral molecules and the application of external fields independently enhanced OER activity. But their combination resulted in the highest observed enhancements, reaching up to 89%, thereby underscoring a strong synergistic effect. In a previous report, chiral cobalt oxide (CoO_x) only exhibited a magnetic field response after electrochemical treatment induced PM Co(IV) species,[86] emphasizing the importance of catalyst structure and oxidation states. In this case, no difference between the direction of the external magnetic field was observed, suggesting that the influence of the magnetic field on spin orientation appears to significantly outweigh the contribution from the CISS effect. Finally, in another work, electrodes obtained by electrodeposition of Ni on a magnet were used as working electrodes for the electrolysis of alkaline solutions containing chiral tartaric acid.[134] Here, reversing the magnetic field direction during electrolysis altered overpotentials, indicating chirality-induced spin effects.

The findings presented here underscore the potential of combining magnetization and the CISS effect to enhance catalysis.

2.2.5. Existing In Situ and Operando Methodology

To further advance the understanding of the mechanism behind spin-enhanced OER, and recognizing that the catalytic surface under OER conditions differs from the initial state of the catalyst, a limited number of pioneering studies have explored different in situ and operando techniques. We refer to experiments as in situ when they are performed under conditions similar to those of the OER measurements (e.g., using the same electrolyte), and as operando when they are conducted during the electrochemical reaction while simultaneously assessing catalytic activity. Operando X-ray absorption spectroscopy (XAS) has been widely used to determine the oxidation state, chemical environment, and crystal structure of active sites in dynamic catalytic surfaces. Additionally, operando Raman, infrared (IR), and UV–vis spectroscopies have been extensively applied to identify active sites, analyze intermediates and surface states, and investigate OER pathways. However, the use of these techniques to study the effects of magnetic order and external magnetic fields on these properties has only recently been explored by a few authors.[81,102,115,138–140] These works are highlighted below.

A combination of XAS and Raman spectroscopy demonstrated that application of an external magnetic field enhances the formation of reactive species on $NiFeO_x$, altering the reaction pathway and thereby improving catalytic activity.[139] Similarly, it was found that a magnetic field can alter reaction pathways and increase OER activity by shifting the RDS.[79]

Focusing on the spin state of the catalyst active site, it was found that enhanced electron density accumulation and increased spin-polarization under a magnetic field boosts OER activity in a Ni_1/MoS_2 single-atom catalysts.[102] Additionally, cobalt foam-based electrodes with an intermediate-spin state were shown to exhibit superior OER performance compared to those in a high-spin state.[140] This is attributed to the high spin state stabilizing electrophilic superoxo intermediates, which hinders reaction kinetics and decreases catalytic efficiency.

A study combining operando Raman spectroscopy with operando MFM revealed that higher potentials were required to form a FeOOH* intermediate in the domain walls of Fe_7Se_8 nanosheets compared to the potentials needed in the bulk of a magnetic domain. The subsequent removal of these domain walls ensured that FeOOH* formed at low potentials in both regions, showing that domain wall removal is the reason for the magnetic OER enhancement observed in these materials.[81]

These operando techniques evidently hold great potential for unraveling the mechanism of magnetically enhanced OER by directly correlating reaction pathways and intermediates with the catalyst's spin state, especially when multiple operando techniques are combined. However, broader use of these techniques, along with their application to well-defined model systems and direct comparison with computational studies, is required to fully realize their potential, a topic to which we will return later.

2.3. Magneto Hydrodynamic Effects

While our discussion so far has focused on spin-related phenomena in the catalyst and at the catalyst/electrolyte interface, it is also critical to account for the role of magnetic fields through MHD effects. These effects arise from the interaction between magnetic fields and moving ionic species in the electrolyte, potentially influencing experimental observations and their interpretation. Magnetic fields can alter the diffusion of reactants and products near the electrode surface, an influence that becomes especially significant when mass transport constitutes the rate-limiting step of the electrochemical process (Figure 4h).

When an electrochemical system is exposed to a magnetic field, various magnetic forces arise, affecting ionic motion, charge distribution, and fluid dynamics. The most relevant forces include:

1) *Kelvin Force*: The Kelvin force acts on PM species in a magnetic gradient field by exerting a force in the direction of the magnetic gradient.[141] Although it is often negligible in size, it becomes relevant when a gradient of PM species is present.[83] The Kelvin force can thin the diffusion layer and enhance electrochemical currents.[83,142]
2) *Lorentz Force*: The Lorentz force acts on charged species moving in a magnetic field and is perpendicular to both the magnetic field direction and the ionic current flow.[141] This force induces electrolyte convection, also known as MHD flow, which can enhance reactant transport toward the electrode,[75,143] remove gas bubbles from the catalyst surface, and decrease diffusion layer thickness, thus improving reaction efficiency. The force can take on complex shapes due to nonuniform currents at electrode edges,[142,144] complex

surface magnetization in magnetic catalysts,[145] adsorbed bubbles,[142] and non-ideal flat surfaces[145] which can enhance near-surface diffusion[141,142] while also making it crucial to carefully consider the direction of the force.[101]

3) *Maxwell Stress*: Magnetic fields can cause shape deformations in droplets containing PM species in the direction of the field, proportional to its strength. Therefore, recent studies hypothesize that this so-called Maxwell stress can modulate the electrochemical double layer (EDL) by altering the configuration of the ion cloud at the electrode-electrolyte interface.[83,142]
4) *DM and PM Forces*: Inhomogeneous magnetic fields can produce a localized magnetic buoyancy effect due to differences in magnetic properties between the liquid and gas phases. While this effect is usually negligible, it can become relevant under microgravity conditions.[146]

To date, most experimental studies have focused on establishing correlations between the strength and orientation of magnetic fields and the resulting enhancements in catalytic activity as the abovementioned forces are largely dependent on the direction of the applied field. By analyzing the directionality of the magnetic force in relation to the field orientation, current flow, ion movement, and electrode configuration, several authors have disentangled MHD effects from intrinsic spin-related effects within the catalyst.[72,75,101,147] However, to better understand the aforementioned effects in real electrochemical setups and quantify the potential OER enhancements associated with them, characterization methods capable of directly visualizing the motion of bubbles and ions in electrolytes under a magnetic field are essential. Several studies have employed optical microscopy to investigate oxygen bubbles in liquids, revealing that magnetic fields can enhance bubble velocity,[147–149] induce directional movement that depends on the orientation of the applied field,[75,147] facilitate bubble detachment,[147] and reduce bubble nucleation,[148] all of which can result in OER activity enhancement.[144] However, the size and the appearance of the effect depends on the shape of the cell, electrode and other geometrical considerations.

Investigating ion movement requires more complex setups. For this, Vensaus et al. employed a chemical dye that turns purple in alkaline environments to study the movement of OH^- in the electrolyte under a magnetic field. They demonstrated that the magnetic field induces a force on the ions, causing a rotational movement of the electrolyte, which induces bubble movement. Despite such changes in electrolyte mass transport which can assist in bubble removal, they show that the Lorentz force has a minimal impact on the overall OER current at relatively low current densities.[75] This could be explained by the fact that the reactants for OER are always in high concentration near the electrode[75] and that the transport of OH^- could not only be vehicular but also follow the Grotthus mechanism, such that water may act as the primary reactant, bypassing the involvement of charged species and thus reducing the influence of the magnetic field.[150] While the overall enhancement from MHD effects remains relatively small at low current densities, it could unlock new opportunities for industrial electrolyzers, where high current densities amplify the significance of mass transport and bubble removal.

Quantifying OER enhancement from a theoretical standpoint due to such MHD phenomena at the solid-liquid interface requires dynamic 3D modeling capable of resolving species velocities. This necessity arises from the complex interplay of magnetic forces, field lines, electrode geometry, and fluid trajectories, which collectively shape transport behavior in electrochemical systems.[151,152]

Building on this concept, Sen and co-workers[151] employed 3D computational fluid dynamics (CFD) to simulate flow fields and concentration gradients near electrode surfaces under the influence of magnetic fields. Their simulations, performed under both CV and CA,[151,152] incorporated reactant consumption, product formation, and hydrodynamic effects. The results revealed a decrease in diffusion layer thickness and enhanced species transport away from the interface, with flow behavior strongly dependent on magnetic field orientation–providing valuable insights into the role of MHD effects. However, this model still includes notable simplifications and, to our knowledge, remains the only attempt to address magnetic field-induced effects in full three dimensions. Continued model development is therefore critical to achieving a comprehensive understanding of MHD-driven enhancements in OER.

2.4. Key Principles for Spin Dependent OER

As described above, a variety of theoretical and computational models have predicted the influence of spin on OER catalytic activity, while experimental approaches have demonstrated its effect across a wide range of catalysts with different spin configurations. Based on this previous work we compile a list of key principles which may underlie the observed activity enhancements, which are summarized in **Figure 6**. These include: a) efficient electron transfer kinetics, b) favorable reaction energetics, and c) reduced spin-related electronic resistance via FM or spin-polarized pathways and d) liquid-phase transport effects.

a) Electron transfer kinetics. In a spin-ordered catalyst, spin-specific charge accumulation occurs on the surface, accompanied by spin exchange interactions between surface adsorbates and active sites, as well as between different sites within the catalyst.[18,45,102] Both these factors can increase reaction kinetics by changing electron transfer energies.[8,41] Additionaly, spin-polarized, surface-trapped polarons can facilitate electron transfer at the catalytic interface.[153] These effects provide a route for favoring spin-aligned intermediates during reaction by lowering the injection barrier or reducing charge transfer resistances[72,154] for the majority spin as displayed in Figure 6a. This in turn can result in more efficient production of energetically favorable spin-aligned triplet oxygen.

b) Energetics of reaction intermediates and transition states. The spin configuration at the atomic level of a catalyst and the chirality of a chiral catalyst influence the electronic structure of the active sites of the catalyst, e.g. via the orbital filling. Moreover, long-range spin order in magnetic catalysts induces strong QSEI and QEXI between catalyst and adsorbates.[8,9] In the case of chiral catalysts and catalysts with surface polarons, the spin polarization at the surface can stabilize certain spin states of the adsorbates and intermediates.[63,153] All these factors can result in changes in adsorption free energy of reaction intermediates and transition state energies and imply deviations from the typically assumed linear scaling of the transition state and chemisorption

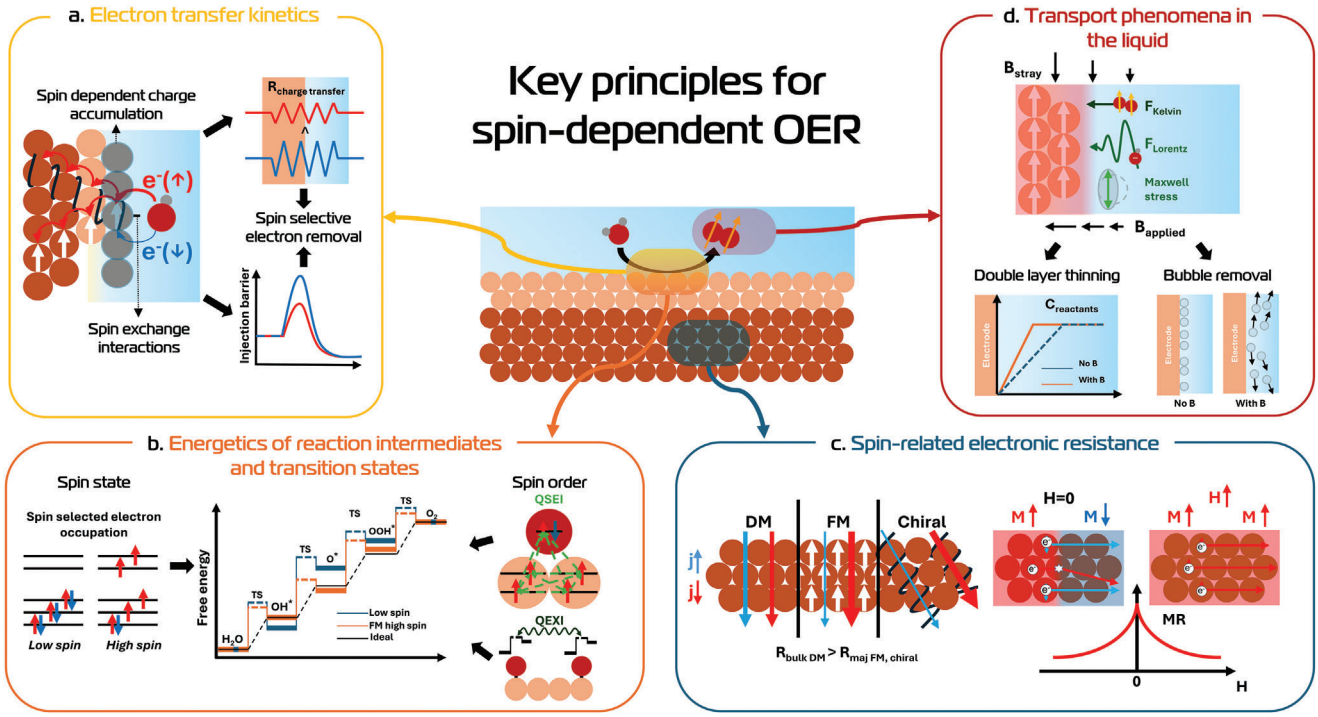

Figure 6. A schematic representation of the key principles which may underlie the spin induced OER enhancement. The different regions within the catalytic system where these effects play a role are indicated within the center image. a) Spin-dependent electron transfer kinetics effects. Spin-dependent charge accumulation and spin exchange interactions at the interface induce asymmetry in both the injection barriers and the charge transfer resistance for spin-up and spin-down electrons. These effects can lead to spin-selective electron removal. b) Spin effects on OER energetics. Variations in spin ordering modulate the free energies of reaction intermediates and transition states via quantum spin exchange interaction and quantum excitation interactions. Additionally, spin-selective orbital occupation further reshapes the free energy landscape. c) Spin-related electronic effects. The formation of spin-polarized conduction channels and the emergence of negative MR can lower resistance-induced electronic losses. d) Magnetic field-induced alteration of transport phenomena in liquids. Stray or applied magnetic fields (in or out of plane) can give rise to MHD effects– such as the Kelvin force (F_k) and Lorentz force (F_L), which can modify ion transport, alter the thickness of the electrical double layer, and facilitate bubble removal at the electrode interface. The orientation of the magnetic field strongly dictates the direction and magnitude of these forces; the illustration presents one representative case.

energies of the intermediates[9,36] as schematically depicted in Figure 6b. More favorable binding energies of the intermediates and lower transition state energy barriers enhance activity by getting closer to the ideal electrocatalyst given by the Sabatier principle.

c) Spin-related electronic resistance. Intrinsic spin order in magnetic materials and spin polarization in chiral materials give rise to spin polarized conduction channels leading to a low resistance for the majority spin which is lower than the bulk resistance for their non spin polarized counterparts.[96,114,118,119] This, in turn, can enable spin-selective electron removal, thereby generating spin-aligned intermediates. Moreover, magnetic order can induce MR effects, leading to higher electronic resistance in the bulk of a magnetic catalyst during electrocatalysis in the absence of an external field due to domain wall formation. Applying an external magnetic field can reduce this resistance.[99–101] Both these effects decrease electronic losses and can thus enhance catalytic activity. However, it is important to distinguish between them: in one case, magnetic order directly enhances intrinsic activity; in the other, magnetic order initially hinders activity by increasing resistance (compared to DM materials), and this loss can be reversed by applying an external magnetic field. These principles are summarized in Figure 6c.

d) Transport phenomena in the liquid. Magnetic fields influence the transport of reactants, products, and electrolyte species during electrochemical reactions[75,101] through MHD effects. Lorentz, Kelvin and DM and PM forces alongside Maxwell stresses can modify the movement of ions toward and oxygen gas bubbles away from the electrode surface and change the EDL structure under certain magnetic fields and magnetic field gradients as shown in Figure 6d. This enhanced mobility can improve oxygen bubble detachment and dispersion and thinning of the EDL, ultimately boosting OER activity.[75,101,151]

3. Open Questions and Challenges

While we can identify several key principles which can potentially underlie spin-enhancement in OER, determining which principle predominantly drives the effect remains a challenge, leaving the exact mechanism elusive. One significant challenge lies in disentangling the various overlapping effects described above. These include kinetic effects (Figure 6a), thermodynamic effects (Figure 6b), spin-dependent changes in the electronic transport properties of the bulk material (Figure 6c), and field-induced mass transport phenomena in the electrolyte (Figure 6d). These effects must be separated not only from each other, but also from

numerous other processes that may occur during OER and, while not inherently spin-dependent, could still influence the reaction outcome. To harness the effect and establish design principles for future catalysts, it is thus still essential to pinpoint the fundamental concepts that dominate spin-enhanced OER. In this section, we explore the open questions and challenges that must be addressed to close this gap. We start the discussion focusing on the previously identified key principles, after which we highlight some more general considerations and potential directions for investigating spin-enhanced OER.

3.1. Electron Transfer Kinetics

The effect of electron transfer kinetics in spin-enhanced OER has been studied using techniques such as Tafel plots, electrochemical impedance spectroscopy, Hall measurements, and by investigating changes in OER activity when tuning the spin-polarization at the surface through catalyst design. However, as discussed above, isolating electron transfer kinetics remains challenging in these experimental approaches. To address this challenge, theoretical models and computational studies have offered a promising route to isolate and study the electronic charge and spin-polarization of catalyst sites and adsorbates, and their impact on electron transfer kinetics. However, these models often require simplifications due to the complexity of real systems. A key unresolved challenge is incorporating angular momentum conservation, crucial for spin-dependent OER, into computational frameworks.

Moreover, accurately representing the dynamic electrochemical environment remains difficult. In practice, catalyst surfaces evolve, adsorbates exist in dynamic equilibrium, spin states fluctuate, and the electrochemical interface continuously changes. Capturing these transient phenomena computationally is currently not feasible. Additional complexity arises from modeling the effects of applied potential and electron transport across the catalyst. Realistic modeling also requires accounting for long-range magnetic order, grain boundaries, structural defects, and compositional variations, necessitating multiscale approaches that are computationally demanding. Furthermore, most models omit realistic operating temperatures, limiting their relevance to experiments. Moreover, on the experimental side, operando measurements are needed to investigate the system under such dynamic electrochemical conditions.

Lastly, because the field of polaron-mediated catalysis remains largely unexplored, the role of localized electrons or holes at lattice sites acting as local spins, characteristic of polaron systems, in determining the activity of OER catalysts remains poorly understood. This gap arises primarily from the complex nature of polaron behavior, as polarons often exist in multipolaronic environments rather than as isolated entities. Additionally, their thermally activated hopping mobility is not yet fully understood, obscuring the role of polarons in electron transport at catalytic interfaces.

Together, these challenges hinder the accurate simulation of spin-dependent, dynamic charge transfer processes at catalytic interfaces and make it difficult to correlate the theoretical predictions with experimental observations. Key open questions which remain include: i) how do intrinsic and induced spin order, chirality, and polarons affect charge transfer energies and spin-specific electron injection barriers, ii) what are the specific mechanistic steps along the reaction pathway where singlet-to-triplet transitions in intermediates occur, iii) what is the influence of electron transfer on this transition, iv) what is responsible for the conservation of angular momentum during the reaction, and v) what is the relationship between the energy scales of spin-flips and the charge transfer energies.

Addressing these aspects could help us understand whether the angular momentum conservation can pose a significant limitation for electron transfer. Finally, it is essential to determine whether long-range spin order (spin-alignment) is necessary for these effects or if local spin-polarization at the active site can independently influence these parameters.

3.2. Energetics of Reaction Intermediates and Transition States

Spin control of binding energies and transition states has been indirectly investigated experimentally in both magnetic and chiral systems. These studies have explored the effect of intrinsic spin order on adsorption and desorption dynamics of various molecules or ions on catalytic surfaces, the rate-determining step through Tafel analysis, and the reaction selectivity. Moreover, pioneering studies have explored how spin order influences the OER mechanism. For example, researchers have tried to investigate the effect of spin order on the type and concentration of reaction intermediates through operando spectroscopy (Section 2.2.5).

However, such studies are still limited in number and complexity, and a major challenge remains in the direct experimental observation of individual reaction intermediates. Many intermediates are either short-lived or closely resemble surrounding species, such as OH^- and water in the electrolyte, or = O and —OH terminated surfaces, making them difficult to detect. Moreover, such measurements are experimentally complex to realize and the dynamic behavior of the intermediates on the active catalyst surface is not well understood. This complexity is heightened by the possibility that interactions between intermediates and the catalyst may depend on the local spin order of the catalyst and the magnetic environment in the liquid. Additionally, the need to resolve the spin states of intermediates to study their interaction with spin order and reaction pathway adds significant complexity to examining spin-enhanced OER.

From the theoretical and computational standpoint, spin-polarized DFT+U has proven reasonably successful in predicting how local spin-polarization influences the electronic structure and adsorbate interactions, which in turn leads to favorable energetics and nonlinear scaling of intermediate energies in spin-polarized OER systems. Building on this, recent studies have begun integrating spin-polarized DFT+U into free energy calculations for key OER steps on oxide catalysts, in an effort to better align computational predictions with experimental observations (see Section 2.1.1).[8,26,31–35,37] However, while increasingly adopted, this integration is still not universally applied, and its omission in some studies leads to free energy predictions that do not fully account for the physics of strongly correlated systems. Furthermore, to the best of our knowledge, the effect of different long-range spin orderings in catalysts has not been systematically studied using such computational approaches.

While these advances mark important progress, it is crucial to recognize that spin-polarized DFT+U methods still face fundamental limitations that restrict their predictive accuracy. Due to the static mean-field treatment of both the Kohn-Sham potential and the Hubbard U correction, spin polarized DFT+U cannot capture dynamic magnetic fluctuations and fails to reliably describe PM insulating phases. Additionally, the reliance on a frequently empirically tuned U parameter and the simplified static treatment of electron correlations due to its single-determinant framework, can compromise the accurate description of local spin excitations and other many-body effects beyond an effective static potential. These limitations can be partially lifted by employing more advanced approaches, such as calculating U using the constrained Random Phase Approximation[155] or hybrid functionals, although these methods typically come with increased computational cost. These shortcomings become particularly pronounced at elevated temperatures or in systems that exhibit dynamic behavior, such as catalytic environments. As a result, these limitations can introduce significant inaccuracies, in the adsorption, reaction and transition state energies as well as in free energy calculations.

The frameworks of quantum spin-exchange interactions (QSEI) and quantum excitation-induced interactions (QEXI) and including them into free energy and transition state energy calculations, as discussed in reference,[9] offers a conceptual bridge between spin-polarized DFT+U results and experimentally observed spin effects in OER catalysis; However, these frameworks remain qualitative. Including explicit energy decompositions, allowing for the quantitative separation of contributions from different interactions to the total energy - such as spin exchange, Coulomb interactions, and correlation effects– can potentially help quantify the role of spin-dependent interactions.[156] Moreover, approaches beyond spin-polarized DFT+U can offer improved (and self-contained) descriptions of such effects, which we will discuss in detail in Section 4.1, though at significantly higher computational cost. Nonetheless, many of these advanced methods have matured and are increasingly being applied to realistic catalytic systems.

Moreover, it is important to acknowledge that despite the widespread use, the free energy calculations utilizing the method suggested by Rossmeisl et al. (see Section 2.1.1) face fundamental challenges that go beyond the intrinsic limitations of the underlying DFT method impacting both accuracy and applicability.

First, the widespread use of scaling relations may lead to inaccurate predictions. This limitation arises because spin interactions, such as QSEI and QEXI, between the catalyst and reaction intermediates can significantly affect both the adsorption free energies of intermediates and the energies of the transition states (Figure 6b)[9] and thus can potentially lead to breaking of scaling relations. Moreover, the formation of surface polarons might affect the scaling relationships of the binding energies of reaction intermediates.[43] As a result, the assumed linear relation between reaction energies and activation barriers, the Brønsted-Evans-Polanyi relation, may break down, especially in systems where magnetic effects or open-shell species are involved. When this assumption does not hold, the predictive power of volcano plots determined using the scaling relations is compromised because activation barriers cannot be ignored, potentially resulting in misleading conclusions in catalyst screening and design. This implies that accurate modeling must explicitly account not only for the energies of intermediate states but also for those of transition states. Moreover, recent studies indicate that although scaling relationships generally hold for magnetic oxide catalysts, more complex binding geometries than the assumed single-site adsorption can result in overpotentials that lie even beyond the top of the volcano.[32]

Second, spin transitions, like the conversion from singlet −OOH to triplet O_2, add further complexity by introducing constraints related to the conservation of angular momentum, as well as the need to incorporate spin-polarized transition states in simulations. Yet, mostly used computational approaches to calculate potential determining steps neither explicitly treat the formation of the O_2 molecule nor its desorption from the catalyst surface, thus failing to account for this critical spin transition.

Lastly, including pH effects and realistic potentials requires approximations (e.g., the CHE), which neglect charge redistribution at the interface and may wrongly estimate reaction energetics.

Due to these limitations, the explicit role of intrinsic spin order or chirality in determining the binding energies and transition states of key intermediates under realistic conditions and their connection to the experimentally observed spin-enhancement of the OER, remains largely unquantified.

Key open questions are: i) How does spin polarization of the active site influence the reaction free energy landscape, including transition states? ii) How do interactions between adsorbates on a spin-polarized surface affect this landscape? iii) How does this relate to the rate-determining steps? iv) To what extent does spin influence the free energy landscape differently across possible OER pathways? v) Can spin effects be systematically exploited to break traditional scaling relationships, as hypothesized in emerging frameworks like the QSEI (quantum spin exchange interaction) and QEXI (quantum exchange interaction) models,[9] which use qualitative space-time diagrams? Another important aspect is investigating the relationship between the energy scales of spin-flips and the heights of transition barriers between OER intermediates, as this may reveal how significantly spin-flips can influence overall reaction energetics.

Additional open questions include identifying which spin order is most favorable, assessing whether the directionality of spin order or chirality plays a significant role, exploring the influence of external magnetic fields on the aforementioned reaction thermodynamics, examining whether magnetic order or spin-polarization affects reaction selectivity by altering the formation energies of main products versus side products, and determining whether spin-spin interactions dominate over other electronic interactions between adsorbates and catalysts.

3.3. Spin-Related Electronic Resistance

The occurrence of spin-polarized conduction channels has so far been investigated by comparing intrinsic resistance and its anisotropy in materials with varying magnetic order. However, this approach does not directly measure the spin-polarization in conduction channels and thus cannot be used to verify that such channels can enhance OER. Theoretical models describing spin-polarized conduction channels exist in DFT-based calculations,

however, the link to experimental work remains difficult due the above-mentioned lack of inclusion of realistic catalytic environments. In the case of the CISS effect, experimental methods are mainly based on the observation of spin-dependent electron transfer. While it has been shown that electron transport through chiral molecules, chiral semiconductors, and chiral metals is spin-polarized, its impact on overall sample conductivity remains unclear. Moreover, a theoretical description of the relationship between chirality, spin polarization of currents, and OER activity is still lacking.

Thus, both for magnetic and chiral materials it is still uncertain whether spin-polarized channels can affect the bulk resistance under OER conditions to such an extent that a significant decrease in electronic losses occurs. Moreover, it is still unclear how the direction of the spin channels is related to the OER enhancement. Such insights could provide design rules for future catalysts and electrolyzer systems utilizing these effects.

Moreover, several studies have investigated the MR influence on the OER and found that it greatly depends on the geometries of both the experiment and the sample due to its anisotropic nature. In principle this allows studying MR effects by carefully considering the directionality of the spin-enhancement in experiments, however, it remains challenging to determine the exact contribution of MR in OER enhancement due to the complex shape of real catalysts and OER conditions.

A key question remains: how are the MR induced effects in catalysts influenced by the complex morphology of real catalyst surfaces, liquid-solid interfaces, and intricate current flows, especially under operando conditions where dynamic processes occur.

Efforts to probe MR induced effects using EIS under varying magnetic fields have yielded valuable insights into the direct link between charge transfer during the reaction and the MR within the catalyst bulk. However, these techniques face limitations, as they cannot easily disentangle MR contributions from other changes in series resistance, including those arising from electrolyte transport properties. It is thus still unclear how the magnitude of MR effects compare to the extent of the other key contributions

3.4. Transport Phenomena in the Liquid

Experimentally, MHD effects under magnetic fields have been demonstrated through two approaches: i) direct visualization of bubble and ion motion,[75,147,149] and ii) finding correlations between activity enhancements and the orientations of the magnetic field, current, and electrodes.[72,101] Together, these findings provide strong evidence that magnetic fields have the potential to influence mass transport via MHD mechanisms. However, reported results show considerable variability, with some studies indicating measurable enhancements in performance[101] while others observe negligible changes.[75] These discrepancies may arise from differences in experimental conditions, such as variations in magnetic field strength, current densities, electrode design, electrolyte composition, cell geometry, or catalyst hydrophobicity. Extensive and systematic studies investigating these variables are therefore needed to accurately characterize the effects of magnetic fields on mass transport phenomena. Furthermore, many studies do not consider MHD effects and thus conflate them with spin-related phenomena, underscoring the need for clearer distinctions in experimental analysis.[105,157]

Theoretical models offer valuable insights into the mechanisms behind these phenomena. For instance, Lorentz forces are predicted to enhance mass transport by compressing the double layer, thereby increasing the supply of electroactive reactants to the electrode. This effect can result in higher limiting currents under an applied magnetic field. However, integrating these effects into simulations which can predict the qualitative effect of the spin-induced forces on electrolyte species in 3D using e.g. CFD simulations or multiscale models is inherently complex due to the dynamic and multifaceted nature of electrochemical systems. Real-time variables, such as bubble growth, evolving electrolyte composition, and fluctuating reaction conditions add further complexity, making static theoretical models inadequate for capturing the full scope of magnetic field effects.

When studying magnetic catalysts, the effects of external magnetic fields may be altered by the formation of magnetic field gradients near catalyst surfaces. The inherent magnetism of the catalysts themselves can generate Lorentz forces, leading to changes in mass transport. These effects could significantly impact local mass transport and should be investigated further through both theoretical modeling and experimental studies.

A major challenge in the field is disentangling the roles of Lorentz forces, Kelvin forces, DM and PM forces, and Maxwell stress, and spin-related effects in enhancing OER activity. A key question is how the strength and orientation of magnetic fields influence these mechanisms. Additionally, the dynamic nature of the boundaries between electrochemical regions during reactions necessitates a thorough understanding of how these forces evolve under operando conditions. Furthermore, the interaction between external magnetic fields and the various media they traverse can profoundly affect the resultant forces, raising the question of how magnetic field lines behave in realistic OER systems.

3.5. General Considerations

Besides the specific questions and challenges related to the key concepts discussed above, there are several broader open questions which are important to answer for advancing the mechanistic understanding of spin-related effects in OER catalysis. They cannot be directly attributed to any single key principle, but can have an influence on both the interpretation of experimental results and theoretical studies.

1) **Dynamic Catalyst Surfaces**. It is known that most catalysts change dynamically under operating conditions even if they convert back to the initial state after the potential is removed. Such transformations can drastically alter their activity and stability. These transformations may include oxidation-state changes, surface reconstruction,[26] amorphization, leaching and dissolution, or the formation of new surface phases, particularly under anodic conditions in alkaline or acidic environments. Such structural and compositional changes typically originate at the topmost atomic layers, where interactions with electrolyte species and reaction intermediates are strongest. These surface modifications under operando

conditions can alter the spin state, spin polarization and spin order of the active sites and its surroundings, such that relying on the properties of the pristine catalyst could lead to incorrect spin-activity correlations.

2) **Role of long-range order**. An important question to consider is how different types of long-range spin order will specifically influence the OER. As described in Sections 2.1 and 2.2 it has been theoretically and experimentally shown in literature that antiFM and PM materials, unlike FM, do not exhibit the activity enhancement effect under magnetic fields and often have lower activity than their FM counterparts (Section 2.2.2 Spin state and Intrinsic Magnetic Order Induced OER Enhancement). However, long-range magnetic order may arise from interactions between multiple magnetic sublattices within a material, leading to complex structures that cannot be fully described by a single order type. For example, FiM and A-type antiFM combine both antiFM and FM orders within the same material, making it difficult to attribute OER enhancement to a specific magnetic order. Thus, the exact relationship between long-range spin order and OER enhancement remains unknown in such materials prompting the question: on what length scale does long-range order play a critical role?''
3) **Spin-polarization of the active site**. Two key questions remain: do the OER enhancements stem solely from long-range spin order across the material, or can they also arise from spin-polarization at the active site alone, independent of interactions with neighboring atoms? Can bulk spin-order enhance OER even if the active site itself is not spin-polarized, e.g. a non-spin-polarized site embedded in a spin-ordered lattice?
4) **Differences and similarities in chiral and magnetic catalysts**. So far, we have described the open questions for the fields of chirality and magnetic-enhanced OER as if they are identical. However, the driving forces behind spin order in these two systems are fundamentally different, suggesting that the mechanisms behind their respective enhancements may also differ. It is therefore essential to treat these fields as interconnected while carefully considering their distinctions. From this, different key questions arise: Are all the interactions and effects discussed above equally applicable to both systems? Can the CISS effect be used to rule out certain mechanisms as the dominant driver of magnetic OER, and vice versa? And, can we use a combination of these material classes to combine different enhancement strategies and thus further optimize the OER activity?
5) **Timescales**. Spin-spin interactions–such as spin flips and relaxation times in spin-ordered materials–typically occur on the nanosecond timescale. Other magnetization-related phenomena, including domain wall motion, domain annihilation, and magnetization switching in sPM particles, span a broader range from nanoseconds to milliseconds. In contrast, chemical steps involved in catalytic processes–such as adsorption, desorption, electron transfer, and ion or liquid movement–often occur on much slower timescales, extending up to seconds. This mismatch between the fast dynamics of spin-dependent interactions and the slower kinetics of electrochemical reactions raises important questions about the relevance and influence of spin effects in catalysis, particularly: on what time scale does spin play a critical role?

3.6. Focus Points for Future Research

Based on the above discussion, the field still has several open questions that need to be explored in more detail through combined experimental and theoretical efforts. The following points outline potential directions for future research in the field:

1) **Improved experimental and theoretical methods**. Future research should prioritize mechanistic studies to clarify the contributions of the different key principles. Experimentally, methods must be improved to identify the different intermediates and their spin state and electron injection barriers during the fundamental reaction steps of the different OER mechanisms. Moreover, methods to identify the effect of spin order on electron and ion transfer within the catalyst and the electrolyte should be established. Theoretically, the gap between quantum mechanical theories of spin-dependent transfer energies, binding energies of intermediates and transition state barriers, and real-world systems with magnetic and chiral properties where angular momentum conservation is critical and dynamics play a role, should be bridged. Moreover, models to investigate electron transfer in chiral or magnetic catalysts, as well as catalysts with surface polarons, under operating conditions, including the effects of MR and spin-polarized channels, and models describing transport phenomena in the liquid under the influence of external fields should be applied and developed for spin-dependent OER.
2) **Separate spin-related effects**. It remains difficult to tune the magnetic or chiral order of a catalyst material without altering other properties. Changes in composition, morphology, crystal structure, as well as microstructure and defect structure resulting from the synthesis pathway, inevitably affect not only the magnetic but also the electronic and structural properties of the active site. They must therefore be carefully considered, and thorough analysis on the electronic state and conductivity within the catalyst, orbital overlap between catalyst and adsorbate, and determination of the active site is essential. We should switch to experimental techniques that can simultaneously investigate the spin order and these secondary materials properties, which would allow the effects arising specifically from changes in spin structure to be distinguished from those driven by other factors. Another route is using experimental approaches that alter the desired physical properties of the materials, in a controlled manner, while minimally affecting others. This approach allows the relative importance of all the spin-related effects to be determined.
3) **Operando characterization**.Building on the understanding that catalyst surfaces dynamically restructure during operation, it is imperative to characterize the spin, chiral, and magnetic properties of the actual active site under OER-relevant conditions. However, current methodologies remain underdeveloped, with most spin-sensitive and chirality-resolved techniques limited to ex situ measurements. As previously discussed, this limitation can lead to incomplete or misleading spin-activity correlations. To address this gap, there is an urgent need to adapt these analysis techniques for in situ and operando electrochemical conditions. This approach is essential for directly tracking the evolution of spin states and spin order during catalysis, ultimately enabling a mechanistic

understanding of how magnetic and chiral properties govern OER activity and uncovering currently inaccessible correlations.

4) **Cell design and comparability**. The design of OER experiments has a large influence on the result. For example, different cell designs will introduce variations in the transport of species in the electrolyte processes upon application of an external magnetic field; likewise different techniques to apply a magnetic field will result in variations in field gradients and MR phenomena. Thus, there is a need to establish standardized experimental procedures to enable better comparison and reproducibility in the field.

4. Perspective

In the following section we will explore opportunities for advancing the field in terms of mechanistic understanding, experimental approaches, and theoretical frameworks, based on the points discussed above. We propose future research directions and methodologies, and explore emerging pathways within the field, outlining potential avenues for their further development.

4.1. Improved Theoretical Methodology

Advancing the field of spin-dependent OER and achieving a fundamental understanding of its underlying principles requires in-depth knowledge of spin-dependent electronic structure, strong electron correlation effects, and interfacial dynamics–both within the catalytic material and in its interactions with adsorbates. This section of the perspective outlines emerging theoretical, computational, and data-driven strategies designed to compute these properties and address the challenges discussed in the previous chapters. These methodologies are summarized in **Figure 7**, which outlines the required input parameters, provides a schematic representation of the modeling approaches, and highlights the key outputs that can be obtained.

4.1.1. DFT+U Studies

DFT+*U* and associated free energy calculations have been instrumental in revealing the role of local spin polarization in shaping the energetics of reaction intermediates and overpotentials, as well as in tracking the evolution of spin states along catalytic pathways. But many exciting opportunities remain underexplored. Several key aspects of spin-enhanced catalysis, where these methods hold significant potential for quantitative insight call for systematic and focused investigation.

Systematic comparison of overpotentials and intermediate free energies related to different long-range magnetic order (FM, FiM, and antiFM) within the same catalyst system could provide valuable insights into how magnetic order mediates catalytic behavior (Figure 7a). Moreover, extending spin-polarized DFT+*U* calculations to more complex OER mechanisms is essential, as different reaction pathways may exhibit different spin dependencies (see Figure 5). Similarly, studies exploring the effect of spin-orbit coupling in OER are necessary, especially for catalysts that contain heavier elements such as 4d and 5d transition metals. A further incentive is to include kinetic effects by explicitly calculating transition states using methods such as the Climbing-Image Nudged Elastic Band (CI-NEB) or metadynamics that can help reveal how spin exchange interactions and spin conservation influence kinetic barriers and thereby OER activity (Figure 7a).[36]

Finally, recent advances allow explicit modeling of applied magnetic fields within DFT, providing a unique opportunity to directly investigate how external fields influence the magnetic configuration at active sites and modify overpotentials. These studies could reveal if external magnetic fields enhance catalytic activity by mediating the spin states of the active site, neighboring ions, and adsorbates. This would be an important contribution toward disentangling the specific effects of an external magnetic field at the reaction sites from micromagnetic phenomena that may also lead to OER enhancements under magnetic fields. These include long-range MR effects or increased exposure of active sites due to domain wall removal. These micromagnetic effects, on the other hand, can be assessed using alternative computational methods, which will be discussed below.

In addition to exploring these new directions, current computational DFT+*U* approaches for spin-dependent OER can be further refined to more accurately capture spin-dependent properties. Improved treatment of electronic correlations–particularly spin-spin interactions–using hybrid functionals or meta-GGA functionals can yield a more realistic representation of the magnetic and electronic structure of the active site than the currently widely used GGA functionals. To capture spin excitation effects and spin-polarized polarons, the inclusion of electronic excitations within the framework of many-body perturbation theory (MBPT) is also promising. This involves quasiparticle effects treated within the GW approximation and excitonic effects by solving the Bethe-Salpeter equation. However, due to their high computational cost, these methods have so far been mostly restricted to bulk materials.[158–160] Additionally, incorporating solvation effects in spin-dependent energy calculations–through implicit models like VASPsol[33] or explicit solvation models–will be important for realistic electrochemical modeling. Finally, including the applied potential in these calculations will be essential to accurately capture the spin properties under OER conditions.[38]

The integration of the aforementioned spin-polarized DFT+*U* techniques with emerging methods such as quantum computing and machine learning, and exploring innovative combinations of these approaches, holds great promise for accelerating the discovery of spin-sensitive catalysts. These developments will be further discussed in the following subsections.

4.1.2. DFT+DMFT Calculations

A current limitation of the above-mentioned methods lies in their treatment of inhomogeneity of magnetic order and dynamic or fluctuating magnetic moments, which are essential in order to describe the phenomena occurring within complex redox-active catalyst materials for the OER. Moreover, to gain a realistic understanding, models must operate at temperatures relevant for catalysis, typically from room temperature to 80–90 °C. Meeting these requirements demands a method that goes beyond spin-polarized DFT+*U*.

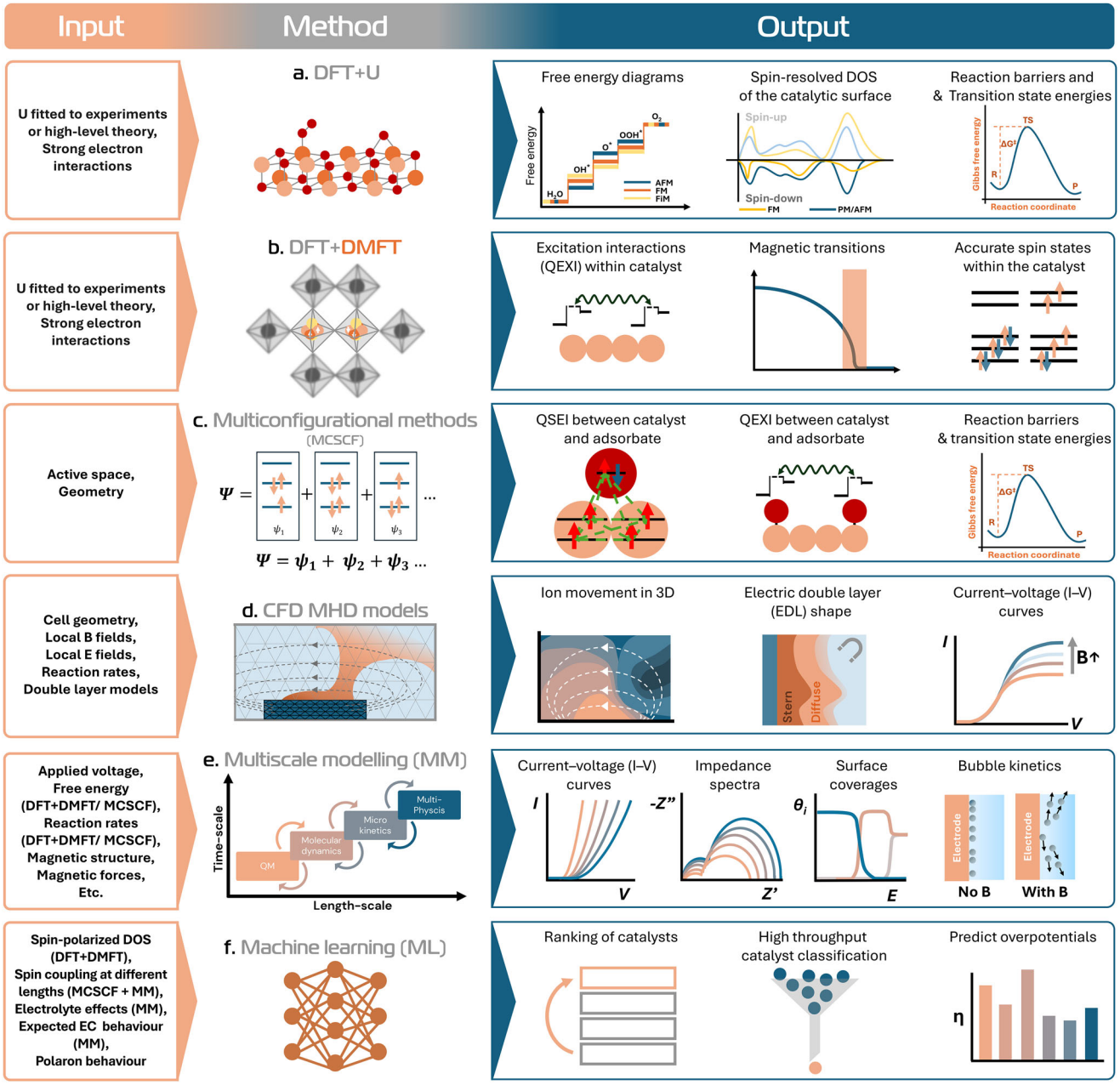

Figure 7. Schematic overview of proposed theoretical approaches, including required inputs and expected outputs, for advancing spin-dependent OER research. a) Spin polarized DFT (DFT+*U*), b) DFT combined with DMFT, c)MCSCF methods capturing complex electron correlations, d) CFD models based on finite element methods (FEM) combined with MHD effect models (CFD-MHD) for macroscopic spin and fluid dynamics, e) multiscale modeling integrating phenomena across different length and time scales, and f) ML techniques to accelerate discovery and as a unifying framework for OER catalyst discovery.

Embedding strategies, such as DFT combined with dynamical mean-field theory (DFT+DMFT), enable this. In this approach, the original lattice many-electron problem, constructed starting from DFT band-structure calculations, is mapped onto a quantum impurity in a self-consistent bath. The latter is obtained with the constraint that the quantum-impurity self-energy equals the local self-energy of the original problem.

The DFT+DMFT technique captures the transition from itinerant to localized electronic behavior, and thus the physics of the Mott metal-insulator transition, both in the PM and long-range ordered (e.g., FM or AntiFM) magnetic phase. (Figure 7b). In DMFT, the key approximation is that the self-energy is frequency but not momentum dependent. Long-range order can however be obtained by simple local-cluster extensions at no additional computational cost. More complex non-local effects can be also accounted for, however via advanced non-local extensions, which typically also have a much higher computational price. The DFT+DMFT approach and its non-local extension are currently

the most advanced techniques for describing strongly-correlated materials and have so far been very successfully used to study the nature of the Mott transition, the origin of magnetic and orbital ordering, and much more (see, e.g., Ref. [161] and references therein). While DFT+DMFT has thus been primarily employed to study the electronic structure of such systems, particularly those with complex spin and orbital characteristics, its ability to capture dynamical fluctuations makes it a promising framework for exploring strong correlation effects and charge-transfer dynamics in catalytic systems.

Although explicitly including adsorbate interactions or reaction pathways in DFT+DMFT calculations remains computationally challenging and expensive, especially in realistic settings, the method can provide critical insights into the local electronic environment and spin polarization of metal atoms within the catalyst, which may serve as active sites during catalysis. In particular, the electronic and spin structure of the active site, shaped by dynamic correlations, plays a crucial role in governing electron-removal steps and determining the energetics of key OER intermediates. These insights can prove valuable for understanding spin-dependent OER.

By accounting for dynamic correlation effects–such as fluctuating magnetic moments and local charge fluctuations–DFT+DMFT is well-suited to model paramagnetic phases and catalytic redox centers, where transition metal *d*-orbitals fluctuate between oxidation states. Together, these capabilities enable a representation of the properties of the active site that more closely reflects its magnetic properties. For example, for the representative catalyst $LaCoO_3$ both DFT+U and DFT+DMFT correctly predict the low-spin ground state.[162,163] However, while DFT+U can be applied to larger systems and is therefore the current method of choice for studying complex reconstructions,[162] surface effects, and OER activity,[37] the DFT+DMFT approach–by properly capturing dynamical fluctuations–is better suited for describing key phenomena such as the subtle energy balance between the different spin states and the associated finite-temperature spin-state transitions.[163]

Looking ahead, advances in computational techniques (e.g., the development of more efficient quantum impurity solvers) or in hardware (supercomputer abilities) can in the future make computing structural relaxations and accurately capturing adsorbed intermediates more accessible. This could enable a more realistic description of the behavior of both the active site and adsorbates, as well as their evolution under near-operando conditions. Moreover, because DFT+DMFT can accurately capture the temperature dependence of magnetic ordering and describe the PM state, it enables a detailed investigation into how both PM phases and the transition from a FM or AntiFM to a PM phase influences the spin and electronic structure of the active site and nearby adsorbates. This capability allows not only for an assessment of how FM, AntiFM and PM ordering affect the energetics of the OER, shedding light on the role of long-range spin order, but also for an exploration of how the magnetic phase transition itself, and the associated spin fluctuations near the critical point, may impact catalytic performance. In particular, this approach can help explain the temperature-dependent behavior of OER activity observed around the magnetic transition, as discussed in Section 2.2.2 Spin state and Intrinsic Magnetic Order Induced OER Enhancement.

A major limitation of the DFT+DMFT technique is its high computational cost, which currently prevents it from accurately describing adsorbates and thus limits its applicability to catalytic systems. Although DFT+DMFT builds upon the DFT+*U* framework, it is significantly more demanding numerically because it involves solving a many-body quantum impurity problem. For real materials, the latter is typically solved using methods like Quantum Monte Carlo on massively parallel supercomputers. Consequently, the size of the system that can currently be realistically treated, such as the number of orbitals and sites included in the DMFT calculations, remains limited.

4.1.3. Multiconfigurational Methods

Another approach for more accurate calculation of adsorption energies, transition state barriers and reaction energies and the resulting free energies including strong correlation and spin-specific effects, is the use of multiconfigurational quantum chemical methods, such as multiconfigurational self-consistent field (MCSCF) techniques. Like DFT+DMFT, they aim to capture strong electron correlation, but they differ fundamentally in how the active region is treated. MCSCF methods explicitly construct fully correlated wavefunctions within a defined active space. MCSCF methods enable precise control of spin and electronic states by variationally optimizing both orbitals and configuration interaction coefficients, providing an advantage in targeting specific spin or excited configurations.[164] MCSCF methods are therefore valuable for investigating the active region in strongly correlated systems (Figure 7c).

In this context, MCSCF, in the form of the embedded correlated wave method[165] for example, provides a rigorous framework for computing localized spin states, adsorption energies, activation barriers, and electron transfer kinetics in spin-enhanced OER systems (key principles a and b in Figure 6). By resolving the multireference character of electronic states, especially during charge transfer and spin transitions, these methods offer a way to accurately model spin-selective adsorption processes and the associated energy barriers between spin states.[166] Although these studies are still in their early stages, developments in this research area is surging. This capability could aid in exploring how spin polarization influences catalytic performance by altering reaction energetics and electron transfer pathways, and may also hold promise for modeling spin transitions in reaction intermediates, such as the conversion from singlet −OOH to triplet O_2.

Moreover, MCSCF methods offer significant potential to advance the modeling of complex, spin-coupled catalytic processes by incorporating conceptual frameworks such as QSEI and QEXI. Integrating these specific frameworks enables a deeper understanding of spin-dependent phenomena in OER (Section 2.1.1 Key Results and Methodological Limitations)[9] (Figure 7c).

QSEI arise from spin-dependent electron interactions governed by the Pauli exclusion principle: electrons with parallel spins tend to spatially separate, reducing Coulomb repulsion and stabilizing open-shell configurations. These effects influence the orbital occupancy and spin states of the catalyst, as well as the energy barriers associated with adsorption, intermediate forma-

tion, and transition states during the OER. Wavefunction-based quantum chemical methods, such as MCSCF methods, can be used to investigate these interactions by analyzing spin states and the multiconfigurational nature of the electronic structure, which includes exchange and correlation effects.

QEXI, on the other hand, involve multiconfigurational electron excitations that minimize repulsion via transient promotion to higher-energy orbitals. This behavior cannot be captured by a single Slater determinant and instead requires a linear combination of configurations:

$$|\Psi_0\rangle = c_0\,|\Phi_0\rangle + c_1\,|S\rangle + c_2\,|D\rangle + c_3\,|T\rangle + \ldots \quad (1)$$

where $|\Phi_0\rangle$ is the reference state, and $|S\rangle$, $|D\rangle$, and $|T\rangle$ represent single, double, and triple excitations. Such correlation effects are poorly treated in mean-field methods, like Hartree–Fock or spin polarized DFT +U. Again, high-level MCSCF methods, can explicitly include these excitations, providing much-needed accuracy. However the factorial scaling associated with these methods renders them impractical for large catalytic systems.

MCSCF methods yield accurate energetics for strongly correlated systems but come with additional limitations. Applying these methods to complex catalytic interfaces is especially challenging due to their high computational cost and the inherent difficulty of modeling extended surfaces and dynamic electrochemical environments. Having said that, recent advancements in algorithm and hardware have rendered these methods more realistic and useful tools for modeling catalytic systems.[167] Moreover, they are often system-specific and still largely disconnected from realistic catalytic operating conditions, although they can offer more accurate energetics and spin-state descriptions than conventional spin-polarized DFT+U approaches.

To overcome these limitations, embedding strategies have been developed that integrate the strengths of MCSCF methods with DFT, allowing strongly correlated active sites to be treated with high-level accuracy while embedding them in an environment described by a lower-level theory.[165,166] For example, a recent study, using embedded correlated wavefunction (ECW) theory, showed that the differing CO_2 reduction activities of Cu(111) and Cu(100) arise from distinct CO hydrogenation pathways, emphasizing the role of ECW in understanding surface morphology effects on selectivity.[168] Another study on IrO_2(110) used an embedded multireference approach and showed that the O_2 release barrier–a critical step in OER–was significantly influenced by the breaking of π-bond between O_2 and Ir, and its interaction with adjacent electrophilic Ir-oxo species.[166] These details were missed in standard DFT but captured with multireference methods.

Looking forward, quantum computing presents a promising pathway to overcome the scaling limitations of MCSCF calculations, particularly as system sizes approach regimes intractable for these methods on classical supercomputers. Emerging hybrid quantum-classical embedding approaches, which are conceptually similar to DFT+DMFT, are being explored for accurate and scalable modeling of spin-resolved catalysis and strongly correlated materials.[169] Although current quantum hardware and algorithms are not yet mature for routine application to chemically realistic OER systems, continued developments in both MCSCF methodologies, embedding strategies and quantum computing are expected to enhance their practical applicability in the future.[169]

4.1.4. Computational Fluid Dynamics Models

Understanding spin-induced effects on dynamics within the electrolyte and mass transport, like the MHD effect, requires extending theoretical studies to models that incorporate solvent effects and field gradients. Such extensions are crucial for capturing transport phenomena at relevant scales within realistic cell geometries but introduce significant complexity. CFD models using FEM, as previously discussed, offer a flexible and physically grounded framework to tackle these challenges (Figure 7d).

To more accurately capture the dynamic and heterogeneous nature of electrochemical systems, it is essential to include the detailed structure of the EDL and its role in ion transport. Incorporating Helmholtz, Gouy–Chapman, or Stern models into the framework proposed by Sun et al., or a similar model, could help overcome existing limitations.[151,170–173] Another limitation of the current CFD model is its oversimplified treatment of redox reactions. Including a more accurate representation of the OER and its kinetics would improve realism.

Another promising next step is to include local magnetic and electric fields. These fields, affected by gradients in magnetic susceptibility, electrode geometry, and stray fields, can significantly alter ion motion.[174] We propose using FEM or hybrid FE/boundary element methods to model the spatial distribution of magnetic fields generated by both the catalyst and external sources, see Figure 7d. These techniques are well-suited for handling complex geometries, temperature effects, and anisotropic or inhomogeneous materials, and have been effective in modeling magnetic force induced motion,[175] magnetic domain motion[176] and stray fields.[177] Similarly, electrode morphology, charge accumulation at interfaces, and applied potentials result in locally varying electric fields. These can also be modeled using FEM[178] or simpler numerical methods.[179] Finally, extending the model to incorporate Kelvin forces, Maxwell stress, complex cell geometries, and bubble formation could substantially improve our understanding of MHD effects, as it would enable a more comprehensive investigation of the interactions among these phenomena and the Lorentz force.

4.1.5. Multiscale Modeling

Multiscale modeling offers the opportunity to bridge quantum-level insights with experimentally observable electrochemical behavior (Figure 7e). Spanning multiple length and time scales by combining methods such as molecular dynamics, kinetic Monte Carlo, and continuum modeling,[180–182] overcomes the limitations commonly associated with purely atomistic models. Continuum modeling, in particular, encompasses a diverse range of approaches: from solvation models and implicit electrolyte models at the atomistic level,[183,184] to microkinetic modeling of the electrochemical interface[185–189] up to multiphysics modeling at the component or device level.[190–193] Given these advantages, the need for multiscale modeling is increasingly recognized, with more studies emerging in this area.[180,181]

New approaches based on nonlinear state-space models and microkinetic modeling have recently been developed, allowing a direct connection between electrochemical models and experimental data. These approaches address a key limitation in electrochemical measurements: while electrical quantities such as potentials, currents, and impedances are applied and measured, they are not directly linked to the underlying (electro)chemistry or the electrochemical models.[180,181] Examples of such efforts have been published in the context of solid oxide fuel cell electrodes[194–196] and, more recently, for the OER.[187–189,197,198] We propose that a deeper understanding of spin-dependent OER can be achieved by incorporating spin-dependent (sub) models into such multiscale approaches. For example, the microkinetic modeling approach from Bieberle-Hütter et al.[186,187,198] could use spin-dependent DFT data, i.e. spin-dependent free energy data for the different de-protonation steps in OER. The free-energy data is used as input for the estimation of the rate constants and, hence, spin dependence is included in the reaction mechanism. By simulating current-voltage curves, surface coverages, and impedance data from spin-free and spin-dependent free energy data, the impact of spin on the electrochemical data can thus be simulated (Figure 7e). The results can be directly compared to experiments and the impact of spin could be assessed. Similarly, magnetic and non-magnetic materials can be systematically compared to identify the impact of the long-range magnetic order on the electrochemical activity and performance of energy materials. Another promising direction is the incorporation of alternative reaction mechanisms,[199] beyond the classical four-step pathway proposed by Rossmeisl et al.,[24] to investigate how spin influences different catalytic routes.

It is also crucial to assess how these spin-dependent effects influence macroscopic behaviors. This requires combining DFT based models for describing metal electrodes with classical molecular dynamics,[200] solvation models, microkinetic or multiscale approaches to simulate solid-liquid interfaces and interactions within the electrolyte. Such an approach would enable exploration of a broad range of phenomena, including the influence of spin polarization on bubble motion, electrolyte flow, and the electrochemical interface's structural dynamics–such as electrode degradation or surface transformations, and restructuring within the EDL. Sensitivity analysis can support such studies and identify limiting parameters as has been shown in [201].

Such computational advancements offer the potential to move beyond static models, capturing the evolving electrochemical environment more accurately. The integration of these methods with operando and spin-resolved experiments can help guide the rational design of spin-engineered catalysts, improving both electrochemical activity and selectivity. Additionally, incorporating magnetic effects, such as, models that describe the Lorentz force (as discussed in Section 4.1.4), or micromagnetic models that describe magnetic domain wall movement under magnetic fields, can provide insights into the role of magnetic fields in electrochemical performance. However, scaling these models to 3D systems or integrating them into CFD models remains challenging. These models may currently thus be better suited for assessing the impact of simplifications in less complex frameworks.

Limitations of these methods are related to the multiple input parameters, such as pre-exponential factors or surface reorganization energy, which are needed to carry out the simulations but are often not known a priori, see.[189] Moreover, the assumption that spin-polarization and order can change independently is possible in simulations, but might not reflect reality where changes in magnetism might change other materials or process parameters.

4.1.6. Machine Learning

Machine learning (ML) has become an indispensable tool in electrochemical research, particularly for OER, due to rapid advances in algorithms, model architectures, data accessibility, and computational hardware (Figure 7f).[202–204] Unlike traditional ab initio methods like DFT, ML models learn patterns from data, enabling the discovery of complex correlations, reducing computational costs and accelerating catalytic material screening. To date, ML has mostly been used to enable faster catalyst discovery by learning complex structure-property relationships.[205–207]

Beyond material screening, ML holds great promise for advancing spin-enhanced OER modeling by bridging electronic structure, spin dynamics, and experimentally measurable properties across multiple scales. However, the incorporation of spin effects into ML models for OER remains virtually unexplored, and even in general materials modeling, such integration is still limited. Existing efforts include ML-based prediction of magnetic parameters,[208] ordering in 2D materials,[209] and magnetic materials discovery.[210–212]

At the atomic scale, several descriptors have been proposed for the evaluation of catalysts using ML.[202] Recent reviews highlight ionization energy, electron affinity, and charge transfer as key features.[203,204] with ionization energy and electron affinity emerging as particularly important. However, standard DFT often underestimates these values due to self-interaction errors.[213] Corrections such as DFT+U and hybrid functionals can mitigate these issues, offering improved accuracy for charge localization and transfer.

A promising application of ML in spin-dependent OER research lies in uncovering the relationship between spin configurations and key catalytic properties such as charge transfer rates, adsorption energies, and work functions, factors critical to understanding and optimizing spin-selective electron transfer. However, accurately modeling the dynamic, spin-dependent charge transfer processes at catalyst-adsorbate interfaces poses significant computational challenges. Recent advances in ML offer potential solutions specifically for polaron systems: novel model architectures now enable accelerated exploration of the multipolaron configuration space, facilitating rapid and accurate identification of ground-state spatial charge distributions.[214,215] Furthermore, the integration of spin degrees of freedom into machine-learned interatomic potentials[216] extends ab initio spin-polaron simulations to the nanoscale, enabling more realistic modeling of catalytic processes under operational conditions. Developing analogous approaches for chiral and magnetic catalysts would be highly valuable for deepening our understanding of spin effects on charge transfer mechanisms.

Another promising direction is the application of machine learning as a unifying framework for multiscale modeling,[217] with the potential to simultaneously capture a wide range of spin-related phenomena. This includes spin-spin interactions

such as QSEI and QXEI, both within the catalyst and at the catalyst-adsorbate interface; long-range magnetic ordering, including FM, antiFM, and FiM phases; and micromagnetic effects such as spin channels, domain structures, and stray magnetic fields. Modeling these phenomena within a single framework would allow for comprehensive investigations into their combined influence on energy barriers, transition states, electron transport, and overall OER activity. In this context, a particularly exciting direction is the development of unified ML architectures such as the All-atom Diffusion Transformer, which can generate both molecules and materials within a common framework.[218] Such models could enable generative design of spin-active catalytic interfaces by learning from multiscale data and simulating complex phenomena like spin-polarized charge transport and magnetically modulated reaction energetics.

Moreover, in polaron-mediated catalysis, where spin states and charge localization play a critical role in determining activity and selectivity, ML can help uncover complex structure-property relationships that are computationally inaccessible with traditional methods. Recent efforts suggest that machine-learned force fields could be designed to explicitly capture spin-dependent polaron dynamics, particularly in systems with adsorbates or magnetic ordering.[219] These models can be trained on accurate quantum chemical data and extended to simulate realistic interfacial environments with defects, solvent effects, and thermally activated hopping processes–factors that directly affect spin-dependent electron kinetics. Initial studies recommend validating these approaches on minimal systems before progressing to more complex geometries relevant to OER.

Despite the significant potential of ML, its reliability fundamentally depends on the availability of high-quality datasets, which are often limited or derived from DFT, with known errors in correlated oxides and transition metal surfaces. Experimental data remain scarce and are not standardized.[205] Traditional scaling laws often fail for complex catalysts, and spin, charge transfer, and magnetic effects are still underexplored. ML frameworks such as self-learning algorithms[205] and generative models[220] offer promising strategies for data augmentation and transferability across catalytic environments, addressing this key bottleneck in data availability. Integrating ML with benchmark datasets that include spin information and charged defect configurations could significantly enhance model generalization and predictive accuracy.

Together, these developments illustrate a path forward for machine learning as a unifying framework to model spin-enhanced OER (Figure 7f), one that connects atomic-scale spin effects to mesoscopic observables, and ultimately, to experimentally relevant catalytic behavior. Realizing this vision will require tight integration of ML with accurate quantum chemistry data, careful treatment of spin-related phenomena, and validation against controlled experiments.

4.1.7. CISS Enhanced OER

The theoretical state-of-the-art regarding the CISS effect remains largely phenomenological, and the field lacks a consensus on a predictive, first-principles model. Nevertheless, significant theoretical advancements are expected as the fundamental mechanisms underlying the CISS effect continue to be elucidated. For example, as mentioned in Section 2.1.2, theoretical models that go beyond the independent-particle approximation and incorporate electron correlation effects into the theoretical framework have been able to more accurately capture the singlet nature of the molecular states within a chiral material. A solid understanding of such fundamental physics underlying the CISS effect is essential for elucidating its influence on chemical processes. However, current ab initio calculations remain inadequate because they fail to quantitatively or even qualitatively reproduce the physics of the CISS effect. Nevertheless, emerging theoretical frameworks that describe spin-polarization in chiral molecules, particularly at metal interfaces and under non-equilibrium conditions, hold promise for advancing our understanding of spin-dependent phenomena in catalysis, including reactions such as CISS enhanced OER.

A promising pathway forward lies with the incorporation of non-adiabatic effects into current ab initio models.[221–224] In this approach, the role of nuclear motion, i.e. vibrations, is included by constructing a Berry force, which can be incorporated in the electronic single-electron part of the Hamiltonian as an effective gauge potential **A**. This shifts the momentum operator $p^2 \rightarrow (p - \gamma \mathbf{A})^2$. In this way, the molecular nuclear motion acts as an effective magnetic potential (**A**) that directly modifies the electron wave functions. Since electron–vibron and electron–phonon coupling related to this molecular nuclear motion arises directly from particle-particle interactions, the development of such models may enable the description of correlated states that can explain spin polarization in molecules, potentially advancing the field toward a more quantitative understanding of the CISS effect.

Another recently proposed feature of the CISS effect is its ability to generate highly spin-polarized triplet currents.[62,225,226] In the context of the OER, such spin-polarized currents could enhance activity by favoring spin-aligned intermediates by selectively removing two-electron triplets of a specific spin-projection, as discussed in Section2.4 External Magnetic Field Enhanced OER. Extending the model which describes this polarization effect, to include electron transfer from the reactant to the catalyst, both with and without spin-polarization of the currents within the catalyst, could offer valuable insights. In particular, it would allow for evaluating the total energy required for the four electron transfer steps involved in the OER and help assess whether spin-polarization contributes to enhanced activity. A key advantage of this approach is that it allows the investigation of electron transfer kinetics independently of the other effects discussed in Section 3.

To advance our understanding of how the CISS effect influences the OER, there is a need for reaction-specific theoretical models. Thus far, however, most theoretical studies have concentrated on the ORR. This emphasis stems from two main factors: the more direct link between spin-polarized electron transfer–central to the CISS effect–and electron supply in the ORR, and the broader availability of experimental data for validation.[63,67,225,226] While these models were originally designed to explain the spin-selective reduction of triplet O_2 to singlet products in the ORR, they also offer valuable insights for the OER, where the formation of triplet O_2 imposes analogous spin constraints. Key transferable hypotheses include: 1) simultaneous two-electron transfer to mitigate angular momentum

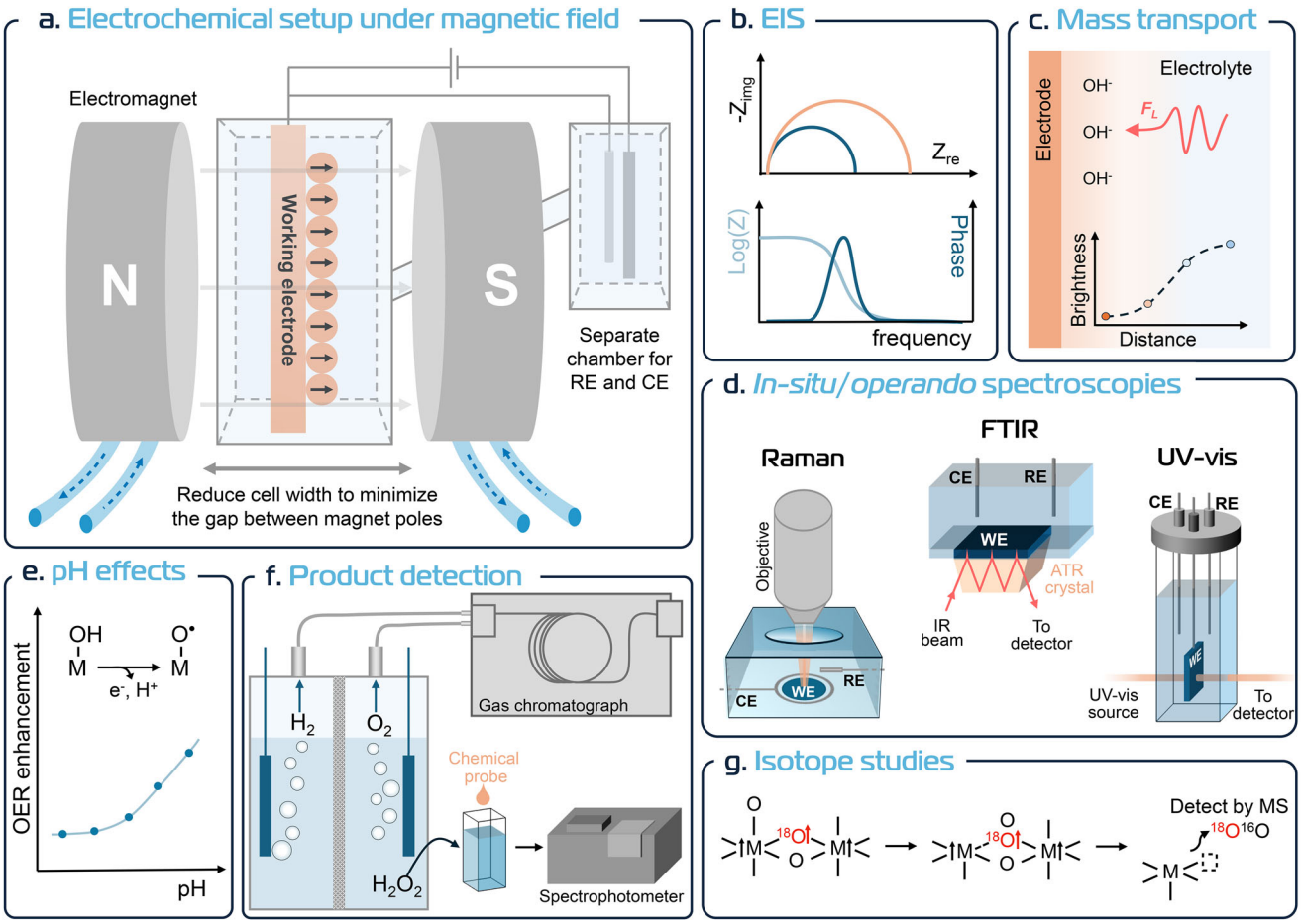

Figure 8. Methodology to study effects of spin and magnetic fields on electrochemical processes. a) Schematic of an electrochemical cell integrated with an external magnetic field, used to probe magnetically induced spin-polarization during OER.[75,93] The narrow cell width minimizes the gap between magnetic poles to enhance field strength at the working electrode. b) EIS enables analysis of charge transfer processes. The Nyquist (top) and Bode (bottom) plots permit the identification of individual contributions to the overall electrochemical process. c) Optical probes of mass transport can identify gradients in concentration near the electrode surface, impacted by the MHD effects.[75] d) In situ/operando vibrational and optical spectroscopies (Raman, FTIR, UV–vis) offer molecular-level insight into intermediate species under working conditions. e) pH-dependent studies reveal changes in OER activity, which can be linked to proton-coupled electron transfer steps and spin-dependent reaction pathways.[11] f) Product detection via gas chromatography and spectrophotometry aids in quantifying selectivity and efficiency. g) Isotope labeling combined with mass spectrometry helps trace oxygen atoms and identify mechanistic pathways.

constraints;[63,225,226] 2) spin-polarized electron removal to reduce activation barriers potentially enabling access to a triplet reaction surface[63] and 3) defined chirality to lower entropic barriers by limiting the number of accessible reaction channels.[63]

4.2. Prospective Experimental Methodology

In this section, we propose different methodologies for future experimental work that could enable researchers to shed further light on the spin-dependent OER mechanism. We give a short description of each method and discuss its proposed relevance for the field. Moreover, we highlight some considerations about current methodology which we believe are crucial to enable accurate and reproducible observations. **Table 3** and **Figures 8**, **9**, and **10** summarize the proposed methods for spin-enhanced OER research, highlighting their key parameters, advantages, limitations, and suitable environments. These summaries serve as a practical guide for readers to identify techniques most relevant to their research interests and to direct further detailed reading within this chapter for a deeper understanding of each method's functionality and potential. The overview presented in this chapter is intended to guide the design, implementation and application of future methodologies in the study of spin-dependent OER.

4.2.1. Electrochemical and Spectroelectrochemical Characterization

Electrochemical Techniques—Most Utilized Techniques for OER Activity Characterization: Accurate electrochemical measurements are crucial for identifying spin effects on OER under magnetic fields (Figure 8a). As discussed before, OER activity under magnetic field is normally measured by three electrochemical

Table 3. Summary of experimental methodologies relevant to spin-dependent OER studies: measured parameters, variable parameters, possible applications, environment, probing depth/resolution, and limitations.

Method	Measured parameters	Variable parameters	Possible application for spin dependent OER	Environment	Probing depth and resolution	Limitations
Electrochemical Impedance spectroscopy (EIS)[76,77]	Complex and absolute impedance and phase angle	Frequency of sinusoidal voltage perturbation	Investigate effect of spin on electrochemical interface and charge transfer; Direct comparison to microkinetic model output	operando, OER electrolyte	Surface up to entire electrochemical system	Direct link to chemical reactions requires extensive models
Raman spectroscopy[81,139]	Vibrational frequencies of electrode (phonons), surface intermediates, surface terminations, surface adsorbates, near surface molecules in the electrolyte crystal structure changes, surface reconstructions	Excitation wavelength, electrolyte composition	Investigate spin effects on surface intermediates, adsorbate concentrations and reconstructions	operando, OER electrolyte	adsorbate surface sensitive, bulk electrode properties, $<1\ cm^{-1}$ (<0.3 meV)	Similar Raman shift for similar metal ions; Interference from the electrolyte; Low signal; relies on SERS effect
Infrared (IR) spectroscopy[235,237]	Vibrational frequencies of electrode surface terminations, surface adsorbates, molecule concentration in the electrolyte near the electrode (micrometer distance). Local pH	Spectrometer wavelength, Attenuated total reflectance, external reflection, electrolyte composition	Investigate MHD effects and spin effects on product formation and adsorbate concentration	operando, OER electrolyte	Probing depth depends on configuration but interface sensitivity can be achieved; ATR: 1-5 micrometer evanescent wave, IRRAS: through electrolyte; <1 cm-1 (<0.3 meV)	ATR: relies on SEIRAS effect; IRRAS: highly confined thin layer electrolyte; Interference from electrolyte
UV-Vis spectroscopy[79]	Changes in optical density by catalyst reconstruction	Spectrometer wavelength, electrolyte composition	Investigate spin effect on surface intermediates and reconstructions	operando, OER electrolyte	Bulk sensitive	Low signal strength; Requires optical changes during operation

(*Continued*)

Table 3. (Continued)

Method	Measured parameters	Variable parameters	Possible application for spin dependent OER	Environment	Probing depth and resolution	Limitations
pH-sensitive dyes[75,143]	Local OH^- concentration near the WE	Dye type, concentration, excitation wavelength, pH values	Study mass transport by MHD effect under magnetic field	operando, OER electrolyte	Localized, µm-scale probing	Limited to optically accessible setups
Isotope labeling studies[108,248]	Product signals (e.g., $^{16}O^{18}O$ and $^{16}O_2$), OER enhancement by magnetic fields	Isotope types (D, ^{18}O, etc.)	Investigate effect of spin on OER pathways	Isotope-labelled electrolyte	Molecular or atomic scale probing	Requires high-sensitivity techniques (e.g., mass spectrometry)
Gas Chromatography (GC)[250]	O_2 concentration, evolved gas composition	Carrier gas, flow rate, sample collection time	Investigate effect of spin on activity and selectivity	operando, OER electrolyte possible	Entire electrochemical system; Detection limit ppm; Temporal resolution minutes	Low time resolution
Differential electrochemical mass spectroscopy (DEMS)[251]	O_2 evolution rate	Electrolyte	Investigate effect of spin on selectivity; Real-time response of O_2 formation to spin order changes	operando, OER electrolyte possible	Surface-near (10-100 µm); Time resolution ms-s	Complex setup, calibration needed
Optical Oxygen Sensing[252]	Dissolved O_2 concentration	Sensor material, light source intensity, integration time	Investigate effect of spin on selectivity	operando, OER electrolyte	Entire electrochemical system; Temporal resolution ms	Sensitivity to pH/temperature; Gas bubbles disrupt signal
Colorimetric assays or UV-vis spectroscopy using chemical probes[250]	H_2O_2 concentration	Probe type, pH, reaction time	Investigate effect of spin on selectivity	operando, OER electrolyte	Entire system	Probe selectivity and stability affect accuracy; No real-time data
Rotating ring disk electrode (RRDE)[253]	Faradaic currents at disk and ring (O_2 at disk, H_2O_2 at ring)	Rotation rate, ring potential	Investigate effect of spin on selectivity	operando, OER electrolyte	Electrode surface (µm); Time resolution ms-s	Requires careful calibration; Only near-surface detection; H_2O_2 collection efficiency variable

(*Continued*)

Table 3. (Continued)

Method	Measured parameters	Variable parameters	Possible application for spin dependent OER	Environment	Probing depth and resolution	Limitations
Scanning tunnelling microscopy (STM)[234,256–265,268]	Local crystal and electronic structure of surface and adsorbates, adsorption geometries	Bias voltage, tunneling current, tip/sample potential, environment, tip functionalization	Investigate electronic structure of active site and adsorption kinetics	UHV/ambient	Sub-nm to atomic resolution; Surface sensitive	Complex setup; Needs well defined, flat, low-noise surfaces
spin-polarized STM (SP-STM)[266,267]	Magnetic structure, spin-polarized density of states	Tip spin-polarization, bias, magnetic field orientation	Investigate spin-polarization of electronic structure; magnetic structure	UHV	Sub-nm to atomic resolution; Surface sensitive	Limited environment flexibility
Electrochemical STM (EC-STM)[271–278] and noise EC-STM[270,275–278]	Surface morphology, active site identification	Potential, electrolyte, scan rate, tip-sample distance	Investigate spin effect on catalyst restructuring and the role of different atomic sites under operando conditions	Solid/electrolyte (EC-STM), Operando conditions for noise-EC-STM	Sub-nm to atomic resolution; Surface-sensitive	Challenging tip stability; Needs smooth surfaces
(Electrochemical) Atomic force microscopy (EC-AFM)[281–283]	Surface topography, conductivity, ionic environment, hydration forces, EDL structure	Tip properties, electrolyte composition	Investigate spin effect on local surface reconstructions, conductivity, EDL under operando conditions	operando, normal OER electrolyte possible although most tips only allow moderate-pH electrolytes	Surface only and first liquid layers; Atomic to nm scale (topography) tens of nm scale (ionic) lateral resolution	Limited temporal resolution; Crosstalk with noise; Lack of chemical specificity
Magnetic conductive AFM (mc-AFM)[132]	spin-polarization in charge transport	Tip magnetic coating, bias, force setpoint, scan rate	Investigate spin-polarized electron transport in chiral catalysts	Typically ambient atmosphere but moderate-pH electrolytes possible in specific sample configuration	Tens nm lateral resolution	Interpretation of spin effects requires careful control; Complex setup

(*Continued*)

Table 3. (Continued)

Method	Measured parameters	Variable parameters	Possible application for spin dependent OER	Environment	Probing depth and resolution	Limitations
Magnetic force microscopy (MFM)[81]	Local magnetic domain structure	Tip properties, electrolyte composition, stray field strength	Investigate local magnetic domain structures under operando conditions	operando, normal OER electrolyte possible although most tips only allow moderate-pH electrolytes	50 nm lateral resolution (10-20 nm possible)[393]	Crosstalk with noise; Only for significant stray fields; Non-trivial role of liquid on tip-sample force
Kelvin probe force microscopy (KPFM)[288]	Local workfunction and surface potential	Tip properties, electrolyte composition	Investigate spin effect on chemical potential under operando conditions	operando, moderate-pH electrolytes with salts	Tens nm lateral resolution	Very noise sensitive; Complex liquid tip-sample interactions
Scanning electrochemical probe microscopies (SECM,[291,292] SICM,[293] SECCM[293,294])	Local activity, topography, ion/electron transfer, electrochemical environment	Tip properties, electrolyte composition	Investigate local activity, ion movement, electron transfer	operando, OER electrolyte	Lateral resolution few µm to hundreds nm	Complex setup; Limited spatial resolution
X-ray absorption spectroscopy (XAS),[296] X-ray magnetic circular dichroism (XMCD),[297] X-ray magnetic linear dichroism (XMLD)[298]	Oxidation state, local geometry, spin order, anisotropies of charge, spin and angular momentum	Photon energy, light polarization, sample-beam orientation	Investigate effect of spin on active site oxidation state and local geometry; Probe electronic structure, spin order and activity simultaneously	Ambient and operando, OER electrolyte	Soft X-rays: 100 nm probing depth (fluorescence yield), 5 nm (electron yield); Hard/tender X-rays bulk sensitive	Mostly done at synchrotron facilities; Complex cell/sample designs especially for soft X-rays
Fresnel mode Lorentz transmission electron microscopy (LTEM) [306]	Magnetic domain walls, magnetization direction (indirect)	Sample tilt, defocus, magnetic field	Investigate magnetic structures and domain walls, possibly in situ	UHV or ambient, recent advances in in situ holders	10-20 nm lateral resolution (down to 2 nm)[394,395]	Limited quantification; Defocus blurs features; Sensitive to thickness/contamination
Off-axis electron holography (EH)[307,309,396]	Electrostatic and magnetic field distribution (phase shift mapping)	Biprism voltage, magnetic field	Investigate magnetic structures and domain walls, possibly in situ	UHV or ambient, recent advances in in situ holders	2-5 nm routine lateral resolution[397] (<1 nm possible[398])	Complex setup; Tradeoff resolution vs field of view; Requires thin samples
Electron magnetic circular dichroism (EMCD)[311,312]	Element-specific magnetic moment	Beam tilt, energy loss, collection angle	Investigate magnetic structures and domain walls in magnetic catalysts	UHV	1-5 nm lateral resolution TEM,[311] <0.2 nm STEM[312]	Weak signal; Thin samples required; Precise diffraction conditions; Limited operando

(*Continued*)

Table 3. (Continued)

Method	Measured parameters	Variable parameters	Possible application for spin dependent OER	Environment	Probing depth and resolution	Limitations
Photoemission electron microscopy (PEEM)[322,324]	Spatial resolution of chemical and magnetic properties, using X-rays: Spatial resolution of XAS and XML(C)D signal	UV-vis or X-ray source, photon energy, light polarization, kinetic energy of secondary electrons, energy filters	Investigate magnetic structures and domain walls in magnetic catalyst while simultaneously probing electronic structure	UHV, ambient pressure and liquid environments under graphene membranes	5 nm probing depth with soft XRays; Hard/tender X-rays bulk sensitive; <3 nm lateral resolution possible	Relatively flat and electrically conducting sample surface
Low energy electron microscopy (LEEM)[320]	work function distribution, structural contrast	low-energy electron beam energy, kinetic energy of secondary electrons	Investigate spin effect on surface dipoles, electronic states, and adsorbate-induced charge transfer (probed by changes in work function); Combined with PEEM: Correlate magnetic domain structures with surface morphology and electronic contrast	UHV and ambient pressures	3-5 nm probing depth for secondary electrons; Spatial resolutions <20 nm	Relatively flat and electrically conducting sample surface
Magneto optical Kerr effect (MOKE) microscopy[325]	Relative magnetization, magnetic anisotropy field, coercivity, anisotropy, remanence	External magnetic field, magnetic sensitivity direction	Investigate catalyst domain structure, magnetic and optical properties under operando conditions	Ambient or operando, OER electrolyte	Probing depth 30 nm; Lateral resolution 250 nm	Requires smooth, reflective surfaces
Electron paramagnetic resonance (EPR) / Ferromagnetic resonance (FMR)[328]	Spin concentration, redox state, magnetic moment, magnetic anisotropy, Curie temperature	Magnetic field, microwave power	Identify paramagnetic species; Investigate effect of spin on transport processes (EDMR); Identify transient states and intermediates	operando, OER electrolyte	Bulk and surface sensitivity depend on microwave penetration depth	Size restrictions (mm-scale samples); Conductive materials problematic

(*Continued*)

Table 3. (Continued)

Method	Measured parameters	Variable parameters	Possible application for spin dependent OER	Environment	Probing depth and resolution	Limitations
^{57}Fe Mössbauer spectroscopy[337–339]	Hyperfine interaction parameters (isomer shift δ_{iso}, quadrupole splitting ΔE_Q, magnetic field H)	Applied magnetic field	Track spin state evolution under operando conditions at active sites; Study influence of magnetic fields on these processes	operando, OER electrolyte	Bulk technique with high sensitivity for electronic and coordination environment changes	Requires sufficient surface/volume ratio and ^{57}Fe isotope enrichment; Limited to Fe-based systems; Long measurement times for lab-based setups; Synchrotron Mössbauer faster
Vibrating sample magnetometry (VSM) and superconducting quantum interference device (SQUID) magnetometry[104]	Magnetization, magnetic hysteresis, total magnetization, magnetic anisotropy, exchange interaction between layers	Magnetic field	Understand complex magnetic structures and link spin order to activity; operando characterization of magnetic order	Ambient and operando, OER electrolyte	Bulk technique	Not element specific
Circular dichroism (CD) spectroscopy[104]	Differential absorption between left- and right-circularly polarized light	Spectrometer wavelength	Investigate chiral properties under operando conditions	operando, OER electrolyte	Bulk sensitive	Limited to optically accessible setups
Mott polarimetry[132]	spin-polarization of electrons traveling through chiral structures	Electron energy, sample angle	Investigate spin-polarization and selectivity in chiral catalyst electrodes	UHV	Surface sensitive (1–2 nm)	Requires chiral material deposited on substrate with strong spin-orbit coupling
Hall Effect methods[132]	Hall voltage resulting from spin injection	Bias voltage; provides 3D voltammogram (charge current, spin, voltage)	Monitor spin-dependence of anodic current under operando conditions	operando, OER electrolyte	Bulk sensitive	Requires Hall bar integrated into sample design
Magnetic circular dichroism extreme ultraviolet (MCD-XUV) spectroscopy[124]	spin-polarization of d-electron states	Wavelength, light polarization	Investigate spin-polarization in d electrons in catalyst electrodes	Currently restricted to near surface in UHV	Surface sensitive; Few nm probing depth	Requires XUV source

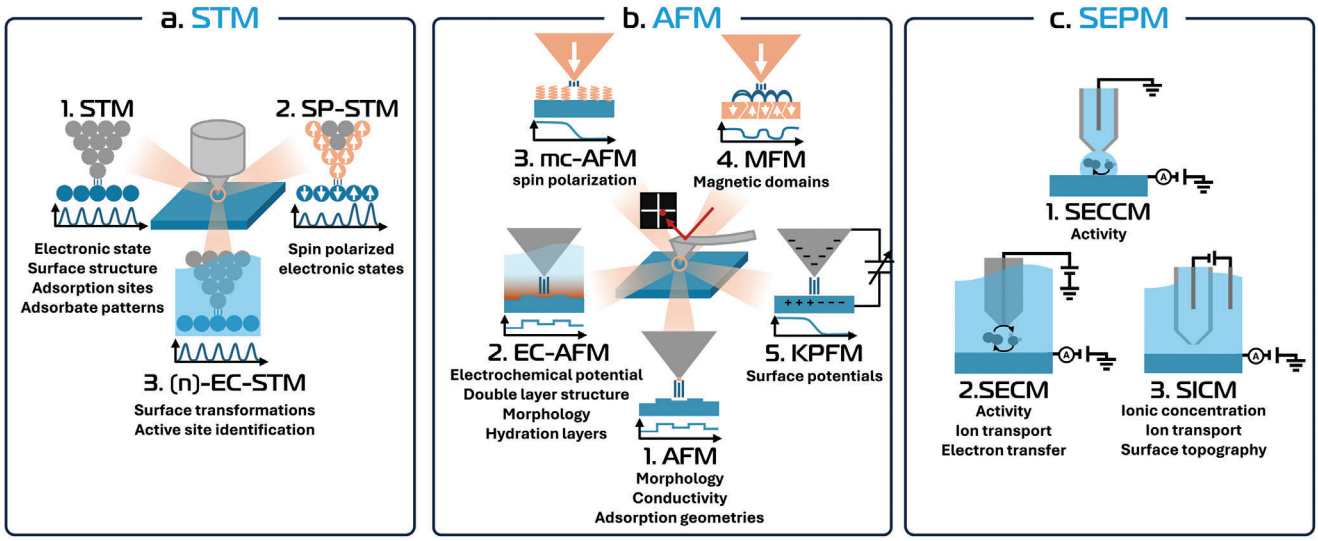

Figure 9. Schematic summary of scanning probe microscopy techniques for future spin-dependent OER research. The images illustrate the working principles of each method. The key properties probed by each technique which are relevant to this field are indicated below each schematic. The figure serves as a visual guide to complement the discussion of detailed working principles in the corresponding sections, helping readers navigate and explore the techniques most relevant to their interests.

methods: CV, LSV, and CA. Reliable OER measurements require initial surface stabilization, as the change in surface chemistry greatly influences the OER activity. To compare the OER activity with and without a magnetic field, one should be cautious in using LSV. The magnetic field can induce mass transport and spin-related charge accumulation near the EDL. Such a change in EDL may cause a shift or distortion in the non-Faradic region of an LSV curve,[149] interfering with the estimation of magnetic field-enhanced OER. On the other hand, the OER activity measured by CV, after *iR*-correction and background corrections,[227] provides a more accurate estimation of magnetic field effects. Moreover, as mentioned in the review, steady-state CA provides complementary insights to CV by adding time resolution, enabling the disentanglement of effects that tend to become convoluted over the longer timescales of a full CV cycle.

OER kinetics are often analyzed using the Tafel plot, where the Tafel slope is only kinetically meaningful within certain potential ranges. At high overpotentials, OER activity is influenced by non-kinetic factors, such as mass transport limitations and bubble formation.[89] This is especially true when applying magnetic fields where MHD effects largely enhances mass transport and bubble removal, such that the Tafel analysis at high overpotentials is less reliable for assessing the change in spin-related kinetics. Thus, fundamental studies on spin-related OER kinetics should be performed at low overpotentials/current densities to minimize the non-kinetic effects.

MHD effects can alter mass transport at the solid-liquid interface. To decouple these influences from genuine spin effects, control experiments under stagnant and stirred conditions,[228] as well as the use of microelectrodes or hydrodynamic simulations, are recommended.

Comparing or fitting the experimental results obtained from the different electrochemical characterization methods discussed above with the outcomes of multiscale models, as outlined in Section 4.1.5 can help establish a direct link to electrochemical models and mechanisms. This, in turn, can deepen our understanding of the influence of spin on the fundamental processes governing the OER.

Impedance Spectroscopy: Next to the above discussed most commonly used methods, further systematic studies combining EIS with spin engineering techniques of chiral and magnetic systems may allow for the investigation of the relationship between spin order, electron transfer, and adsorption of intermediates (Figure 8b). Additionally, a limited number of studies have demonstrated that EIS can differentiate between bulk MR effects and spin-induced changes at the electrochemical interface, such as variations in charge transfer resistance and adsorption kinetics.[72] By performing EIS measurements in a three-electrode configuration (working, counter, and reference electrodes) and analyzing uncompensated resistances, which reflect contributions from the electrolyte and catalyst, it becomes possible to correlate the magnetic field-dependent trends with those observed in bulk MR measurements and OER activity under magnetic fields. Widespread application of this approach, combined with advanced impedance data fitting techniques described above, may enable quantification of the extent to which MR contributes to OER enhancement.

Furthermore, electrode architecture can provide deeper insight into MR-related effects. In systems where electron transport is governed by lateral resistance across magnetic domain walls, MR is likely to play a more prominent role than in configurations where a non-magnetic, conductive subsurface supports a magnetic catalytic surface. Investigating EIS responses under magnetic fields in such systems could help clarifying the conditions under which MR significantly influences OER performance.

Lastly, EIS data is typically interpreted by fitting to equivalent circuit models.[76,77] However, determining the correct circuit models remains a challenge, particularly when attempting to understand complex phenomena like spin effects in OER.

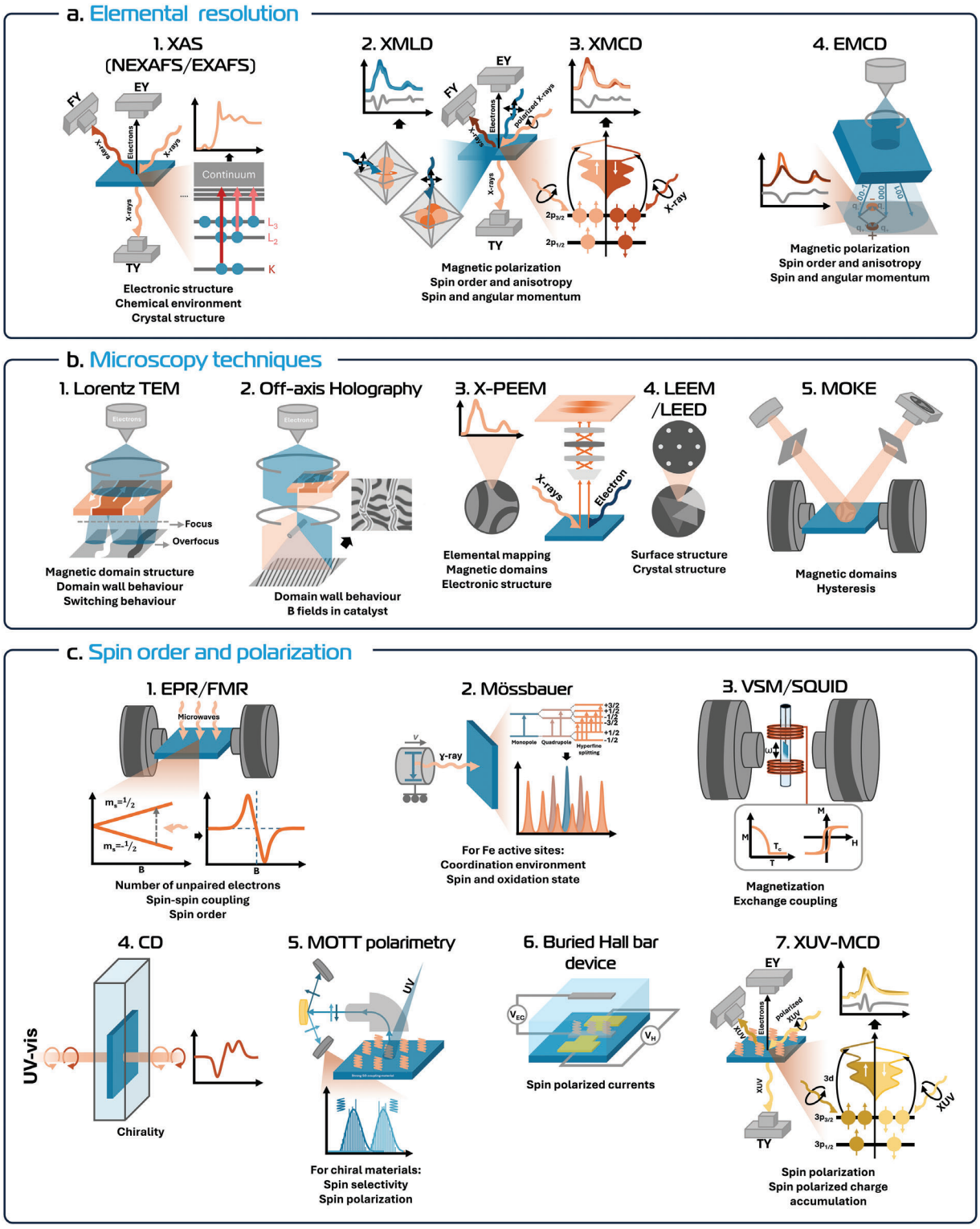

Figure 10. Schematic summary of proposed characterization techniques for measuring magnetic and chiral properties relevant to future spin-dependent OER research. The images illustrate the working principles of each method. The key properties probed by each technique, relevant to this field, are indicated below each schematic. The figure serves as a visual guide to complement the discussion of detailed working principles in the corresponding sections, helping readers navigate and explore the techniques most relevant to their interests. The techniques are grouped into three categories: (a) methods with elemental resolution that enable direct investigation of active sites; (b) microscopy techniques that provide spatially resolved imaging to reveal local properties; and (c) techniques capable of probing spin order and spin-polarization, which are essential for establishing direct spin-activity relationships.

An alternative way to perform a physical analysis of impedance data is the transformation of the impedance to a distribution function of relaxation times (DRFT).[229,230] Boukamp[230] critically reviewed the DRFT method, several inversion methods, applications of DRFT in energy research, and its advantages and disadvantages. Even though DRFT is a good way of deconvoluting the dispersive processes in electrochemical applications, it does not allow for interpretation with electrochemical quantities and models. To overcome this limitation, fitting procedures can be extended to include microkinetic models in combination with state-space models,[194–197] which is described in more detail in Section 4.1.5. These approaches enable a more mechanistic analysis by directly linking impedance features to elementary reaction steps and associated kinetic parameters.

Experimental Protocols for External Magnetic Field Studies: To observe and identify the spin-enhancement in OER, standard protocols for applying magnetic fields during electrocatalysis are critical for minimizing the activity enhancement via secondary effects like MHD. First, a uniform magnetic field should be used to avoid Kelvin force from field gradients affecting mass transport. Second, for catalysts with a rough surface, the magnetic field should be applied perpendicular to the electrode surface (parallel to the current) to minimize the macroscopic Lorentz force.[101,144] For catalysts with magnetic anisotropy, the external field should be applied along the easy axis to maintain a stable magnetization with a lower field. Third, the magnetic field strength at the working electrode should exceed the saturation field (H_S) to ensure a fully aligned magnetic moment in FM catalysts. Importantly, the magnetic field should be applied only after the surface is stabilized by electrochemical pre-treatment and a comparison before and after demagnetization and magnetization of the catalyst layer is desired to confirm that the observed enhancement indeed arises from magnetization.[103]

Electrochemical results under a magnetic field can be influenced by the composition of the electrolyte, which is primarily associated with the ion distribution and transport during the reaction. Previous research suggested that the type of anions affects the bubble dynamics during the bubble growth and detachment in electrochemical reactions,[231] which varies the MHD effect under magnetic fields. Besides, different cations in alkaline conditions are also reported to influence OER activity by interacting with the oxygen intermediates,[19] potentially affecting the spin-related OER pathway. We suggest to use identical electrolyte composition for comparison of spin-related effects within the same or across various catalyst materials and electrochemical cells. To detect such ion transport effects under magnetic fields, pH-sensitive dyes, such as phenolphthalein dye[75] or metacresol purple[143] could be used for monitoring the electrolyte motion according to the coloring (Figure 8c).

Furthermore, proper electrochemical cell setups under a magnetic field are important for ensuring accurate and reproducible measurements (Figure 8a). A temperature control and monitoring system is essential for investigating spin-related OER under a magnetic field, as it helps minimize temperature fluctuations in the electromagnet coil and maintain a stable temperature in the electrochemical cell. The electrochemical cell should be designed to minimize the gap between the electromagnet poles to further limit the Joule heating. The temperature of the cell and the region between the poles should be monitored. Any observed increase in activity should be carefully examined for correlation with temperature changes to determine whether thermal effects contribute to the enhancement. For a typical three-electrode electrochemical system, only the working electrode (WE) should be placed under magnetic fields, while the counter electrode (CE), the reference electrode (RE) and the wiring should remain in a separate chamber with minimal magnetic fields to avoid additional or parasitic effects.[75,150] In order to get quantitative measurements, the system should also incorporate forced convection to minimize uncontrolled mass transport arising from the interplay between natural transport processes in electrochemistry and MHD flows.[228] Moreover, the positions of the electrodes relative to the directionality of magnetic field lines should be considered.[101]

Operando Raman, Infrared, and UV–Vis Spectroscopy: In situ Raman, FTIR and UV–vis spectroscopy offer ease of availability and accessibility and rapid data acquisition relative to X-ray-based synchrotron methods, and these spectroscopic techniques provide a largely untapped avenue to detect subtle, magnetically induced changes in electrocatalytic OER (Figure 8d).

Raman spectroscopy uses a laser to induce inelastic scattering of light from a material - such as an OER electrocatalyst. This process can excite a variety of vibrational modes, including the electrocatalyst's phonon modes (typically within the low-frequency range of 100–700 cm^{-1}) and vibrations associated with surface adsorbates (e.g., −OH, −OOH, H_2O, and multiatomic cations/anions) typically observed in the mid-infrared region. Owing to its low scattering cross-section, Raman spectroscopy is relatively insensitive to the electrolyte; however, it is highly sensitive to interfacial species and the catalyst's bulk properties, making it a key technique for in situ/operando investigations of electrochemical water oxidation.[232] Raman spectroscopy will therefore be crucial to elucidate the influence of magnetic fields on the formation of reaction intermediates and on the catalyst physical properties.

Regarding the detection of reaction intermediates, initial in situ Raman microscopy experiments during OER on a NiFe catalyst under a magnetic field revealed alterations in the O-O stretching vibration region, which have been linked to the formation of Ni-O-O-Fe bridges.[139] Similarly, studies on an FeSe water oxidation electrocatalyst under a magnetic field demonstrated a 100 mV earlier onset of FeOOH vibrational features, attributed to spin ordering of the catalyst surface.[81] Further experiments by doing scan rate-dependent and time-resolved measurements, as well as using isotope-labelling can further strengthen these hypotheses and can elucidate the relationship between the temporal behavior of spin processes and catalytic activity.

For the characterization of catalyst properties, Raman studies on magnetic systems, such as MoS_2, $SrCr_2As_2$, and perovskite manganites, have already demonstrated that applying magnetic fields can induce measurable shifts in Raman peak positions and variations in intensity. These spectral changes are often linked to lattice expansion or contraction, providing a sensitive probe for detecting subtle modifications in the intrinsic properties of magnetic materials. Consequently, it would be interesting to explore whether similar in situ/operando Raman spectral changes can be observed and correlated with variations in OER performance. Finally, magnetic fields can influence the mobility of the surface species, potentially impacting surface reconstruction processes. Raman spectroscopy serves as a valu-

able tool to investigate alterations in these processes. However, in combination with magnetic field-induced dielectric polarization, such changes may also lead to enhanced Raman signal intensities.[233,234] This enhancement could make interpretation of Raman signals more difficult since the appearance and increase in intensities could be misleadingly correlated to new intermediates.

Unlike Raman spectroscopy, Fourier transform infrared (FTIR) spectroscopy is based on the absorption of infrared radiation by all components along the optical path between the source and the detector. This technique has distinct advantages and limitations which depend on measurement configurations, such as differences in surface sensitivity, electrode morphology (porous vs smooth), and mass transport considerations. FTIR spectroscopy inherently enables the capture of electrochemical conversion effects on the near-electrode electrolyte composition. For OER research usually attenuated total reflection FTIR is used.[235,236] For example, the technique allows for straightforward quantification of local pH changes,[237] determination of local ion concentrations, and detection of products evolving and diffusing away from the electrode surface. For these reasons, in situ/operando FTIR studies have been extensively used to study OER.[235,236]

FTIR spectroscopy will likely prove useful in elucidating the impact of MHD effects, which can cause significant changes in interfacial concentrations of ions, water, and O_2. These changes may not only affect the stability of reaction intermediates but also alter local concentration gradients, thereby shifting Nernstian overpotentials and improving or worsening conversion rates. Consequently, capturing dynamic changes within the diffuse double layer, caused by the external magnetic field or catalyst spin order, offers a promising opportunity to further disentangle the local MHD effects.

Lastly, if changes in the optical densities of the electrode material or the electrolyte constituents in the UV–vis/NIR regime are expected during OER, then spectroscopy in this spectral range can be employed to elucidate the impact of magnetic fields.[79] Moreover, UV–vis spectroscopy can enable characterization of catalytic responses across multiple timescales–from femtoseconds to seconds–allowing detailed kinetic analyses. By monitoring the concentration of oxidized species responsible for driving water oxidation, UV-vis measurements can be used to extract key kinetic parameters such as rate constants and reaction orders, thereby offering direct insight into the dynamic evolution of active sites under operando conditions.[238–240]

Experimental Variables and Measurable Outputs—Temperature Dependent Studies: As discussed in the review part of this paper, determination of the temperature dependence of catalytic activity has proven to be a powerful tool for probing in situ changes in magnetic order and their influence on OER activity even in the absence of external magnetic fields. However, elevated temperatures also increase reaction rates by thermal activation and affect other electrochemical processes–such as water adsorption and dissociation, surface species dynamics, electrolyte conductivity, oxygen vacancy migration, and catalyst degradation.[241–243] To isolate magnetic effects, it is thus advisable to compare materials with similar electronic structures but different magnetic transition temperatures,[72] or to perform in situ characterization of these secondary effects.

Expanding the temperature range for measurements would greatly enhance our ability to investigate how magnetic transitions influence OER activity. While most studies concentrate on temperatures near ambient conditions, alkaline electrolyzers can operate above 150 °C, with some systems–particularly those using metal alloys, spinels, or perovskite oxides–tolerating temperatures up to 160 °C.[244] Advanced electrolyzer designs can even reach temperatures as high as 700 °C,[242] making high-temperature measurements a promising direction for future research. From a fundamental science perspective, studying OER at sub-zero temperatures could offer valuable insights into exotic magnetic states and novel quantum or topological phenomena such as skyrmions, which emerge only at these low temperatures. However, to our knowledge, OER electrolyzers capable of stable operation below 0 °C have yet to be developed.

pH-Dependent Studies: As discussed in the review section, M–O· oxyl radical species are crucial in the LOM and I2M pathways (Figure 5),[4,108] where spin alignment between the metal orbital electron and the oxygen's unpaired electron–facilitated by favorable interactions within the catalyst–enables direct triplet oxygen formation. In contrast, the AEM does not form such radicals and relies solely on spin-selective electron removal (Figure 5).[4,108] Since the stability of M-O· radicals depends strongly on pH,[4] LOM and I2M mechanisms show pronounced pH dependence (Figure 8e),[108] whereas AEM does not. Investigating how pH affects spin effects on OER activity can therefore help identify which pathway the reaction follows, which key species are involved, and how spin influences them. Furthermore, designing catalysts to follow a specific pathway and studying their pH response can deepen our understanding of the specific role of spin within each of these pathways.[108] Moreover, spin-related effects under acidic conditions remain relatively unexplored, owing largely to the limited stability of most FM transition metals and their oxides in such environments. This instability necessitates the deliberate design of magnetic or chiral catalysts to withstand acidic media and enable meaningful measurements. Despite these challenges, reductions in Tafel slope and overpotential have been reported under acidic conditions both with and without magnetic fields[245,246] and with chiral modifications.[126,247] Further studies could extend the investigations across broader pH ranges, spanning acidic to alkaline conditions, to elucidate how spin interactions influence key oxygen intermediates such as M–O· and M = O species.

Isotope Studies: Beyond pH-dependency, spin-related OER pathways (Figure 5) could also be investigated by isotope labeling of the catalyst or electrolyte, combined with product detection, e.g. in mass spectrometry (Figure 8d). For example, heavy water (D_2O) has been used to study the spin-polarized proton-coupled electron transfer process in the AEM pathway under a magnetic field,[248] which implies that the cleavage of O-H could be affected by the magnetic field. Additionally, ^{18}O-isotope labeling could be performed to detect the participation of lattice oxygen in the magnetically-enhanced LOM pathway (Figure 8g).[108] This approach thus presents possibilities for studying spin-related OER mechanisms at the atomic level.

Furthermore, understanding the key intermediates for spin interactions may enable the strategic use of chemical probes during OER under magnetic fields, such as phosphate[248] or

tetramethylammonium cations (TMA^+),[249] to selectively detect specific oxygen species, enabling precise identification of reaction pathways and providing deeper mechanistic insights into the role of spin in OER.

Product Detection: Conventional metrics such as current density obtained from CV or CA represent the sum of all interfacial processes occurring within the electrochemical cell, including side reactions and electrode degradation. Consequently, these measurements alone cannot definitively distinguish between true water oxidation and the formation of undesired byproducts. Accurate identification and quantification of both gaseous and liquid, dissolved products are therefore critical (Figure 8f). Spin effects, as demonstrated in the CISS field, have been shown to modulate product selectivity during water oxidation. However, the spin-dependent faradaic efficiency, particularly the ratio of O_2 to H_2O_2 produced, remains largely unexplored in the context of magnetically enhanced OER. For O_2 quantification, well-established techniques like gas chromatography,[250] differential electrochemical mass spectroscopy[251] or optical oxygen sensors[252] offer direct means to quantify O_2 evolution. To detect H_2O_2, colorimetric assays or UV–vis spectroscopy using chemical probes are commonly employed.[250] Complementary techniques, like rotating ring-disk electrode (RRDE) setups, further enable sensitive, simultaneous monitoring of both H_2O_2 and O_2 via their respective reduction reactions.[253]

4.2.2. Scanning Probe Microscopy Techniques

The OER strongly depends on surface active sites and intermediate species that undergo transformations under reaction conditions. Scanning probe microscopy (SPM) techniques are emerging as essential tools for characterizing these phenomena with high spatial resolution, under both ultra-high vacuum (UHV) and electrochemical environments. These methods, summarized in Figure 9, provide valuable insights into the relationships between surface morphology, electronic structure, spin-dependent properties, and catalytic performance.

Scanning Tunneling Microscopy: Scanning tunneling microscopy (STM), allows the investigation of the structural and electronic properties of catalyst surfaces at the nanoscale, and even at the atomic level. By exploiting the fact that quantum tunneling depends exponentially to the distance within a sharp conductive tip and a conducting or semiconducting sample, STM provides information about the local density of states (LDOS) within an energy window around the Fermi level (determined by the bias voltage applied between the tip and the sample) (Figure 9a.1). This enables atomic-resolution imaging of surface structures, such as step edges, terraces, defects, and adsorbates that determine the performance of oxygen catalysts.[254–256] Under UHV conditions, STM has successfully revealed adsorption geometries and electronic properties of O_2 molecules, as well as water dissociation at cryogenic temperatures on several catalytic surfaces.[257–262] As mentioned before, OER catalysts often exhibit surface transformations and restructuring, which are crucially influencing activity and necessitate experimental evaluation of surface characteristics. UHV-STM has proven effective in identifying surface sites before and after OER that are highly susceptible to structural rearrangement and can thus be used to anticipate operando transformations.[263,264] Moreover, scanning tunneling spectroscopy (STS) can probe the electronic band structure, surface states, and Fermi-level alignment with nanometer precision.[256,265] In summary, using STM to investigate how spin engineering of catalysts, external magnetic fields, or temperature-induced changes in spin order affect the structural and electronic properties and processes, and linking these effects to catalytic activity, can provide deeper insight into spin-driven influences on the OER.

Spin-Polarized STM (SP-STM): Employing magnetically coated tips extends the STM capability to probe spin-dependent electronic states at surfaces (Figure 9a.2). UHV studies demonstrated the effectiveness of SP-STM in elucidating magnetic interactions in catalytic reactions, providing critical insights into spin-dependent adsorption and catalytic mechanisms.[266,267] To demonstrate the influence of spin fluctuations on enantioselectivity, SP-STM has been used to probe enantioselective adsorption of chiral molecules on magnetic islands,[268] under UHV conditions. Adapting SP-STM to electrochemical environments remains challenging because of limited tip stability under reactive conditions and thermal noise. Nonetheless, many CISS studies mimic spin-selective detection, by using magnetic substrates and non-spin-polarized STM tips as proxies.[132,269]

Electrochemical STM (EC-STM) and Noise EC-STM extend STM capabilities to in situ electrochemical conditions, allowing for atomic-scale imaging of electrode surfaces under potential control in an electrolyte environment.[270–272] While EC-STM has been used to characterize surface reconstruction during several electrocatalytic reactions,[273,274] the most promising application of EC-STM in the context of this perspective is the use of the noise fluctuations in the tunneling signal in noise EC-STM (n-EC-STM)[275] to track catalytic active sites down to the atomic scale under operando conditions (Figure 9a.3).[270,276,277] Remarkably, this technique is not limited to well-defined single crystal surfaces, and has been extended to identify OER active sites on transition metal oxide layers.[278]

Atomic Force Microscopy: AFM measures surface topography and interactions by detecting forces between a sharp or functionalized tip and a sample (Figure 9b.1). Examples going beyond pure topographic imaging include the functionalization of the tip with a terminal O atom under UHV to identify oxygen adsorption geometries[279] and injection and imaging of polarons[280] using non-contact AFM, opening the possibility to study polaron mobility at catalytic interfaces.

AFM, even in its fast-speed variations (time resolution ≈milliseconds), is a slow technique for characterizing reaction intermediates (timescale typically in the picosecond to sub-millisecond range) but it remains invaluable for providing spatially resolved insight into long-lived reconstructions on the catalytic surfaces which determine the surface activity. Moreover, combining AFM with liquid flow cells offers the possibility of measuring dynamic processes at constant concentrations, from the first seconds of the reaction to days, potentially allowing investigation of surface reconstructions and degradation, including their behavior under applied fields.

Electrochemical AFM (EC-AFM) further extends AFM capabilities to the investigation of electrochemical interfaces during reaction, enabling subnanometer resolution measurements of surface morphology, double-layer structure, local electrochem-

ical environments, hydration layers, and nanoscale surface reconstructions (Figure 9b.2).[281–283] Combining EC-AFM with spin engineering or external magnetic fields can thus enable nanoscale exploration of the effects of spin on surface reconstruction and catalyst electronic properties. Force-distance curves can be used to characterize the electric double layer structure /ref and such studies could be extended to model catalysts with engineered domains exhibiting defined spin ordering (e.g., through patterning or thickness gradients) Moreover, potential-sensing EC-AFM enables operando mapping of surface electrochemical potentials with nanoscale resolution.[284] As this technique enables direct probing of electrochemical activity in a specific region within a catalyst, it offers a promising route to establish direct spin order-activity relationships using model catalysts with engineered domains, as described in the previous section). **mc-AFM** can determine the degree of spin-polarization by measuring spin-dependent currents with either magnetic tips or chiral molecule-functionalized AFM tips in contact mode (Figure 9b.3). The tip is brought into contact with a magnetized surface. The force of interaction between the tip and substrate is measured as a function of magnetization direction. When using chiral molecules, a difference in adhesion or force curves when the magnetization is flipped indicates spin-dependent interactions- a signature of the CISS effect.[285]

Magnetic Force Microscopy (MFM), in contrast, uses magnetically coated tips operated in non-contact or tapping mode to detect magnetic domains through stray magnetic field gradients (Figure 9b.4). Recent operando MFM studies revealed direct correlations between magnetic domain wall dynamics under magnetization and catalytic activity during OER,[81] offering a promising pathway to better understand the link between local magnetic order and OER activity, especially if this technique could be combined with local activity probes like EC-AFM or Scanning Electrochemical Probe Microscopies (SEPM). Moreover, modeling these measurements using DFT calculations and comparing them with experimental results can help quantify magnetic exchange forces at the electrochemical interface.[286]

A further possibility is to use **Frequency-modulated Kelvin Probe Force Microscopy (FM-KPFM)** in which the contact potential difference between the tip and sample is detected by measuring shifts in the cantilever's resonance frequency, enabling highly sensitive and high-resolution mapping of surface potentials (Figure 9b.5).[287,288] A recent study employed FM-KPFM to simultaneously measure quantum capacitance and surface potential in monolayers of α-helical peptides.[288] The research demonstrated that both the magnetic polarization of the substrate and the chirality of the peptides influenced the measured surface potentials. Since surface potentials can potentially alter the OER catalytic process and contribute to its spin dependence, utilizing KPFM for spin-enhancement studies holds significant promise. However, although recent efforts have extended KPFM to aqueous solutions,[289] true operando OER measurements are not yet feasible.

Scanning Electrochemical Probe Microscopies: SEPM are advanced techniques that enable precise, high-resolution imaging and electrochemical measurements at the nanoscale. A detailed description of these techniques can be found in a recent review.[290] **Scanning electrochemical microscopy (SECM)** uses a micro- or nanoelectrode tip to scan surfaces, measuring electrochemical processes like electron transfer, ion transport, and catalytic activity in real-time under operando or in situ conditions (Figure 9c.2)[291,292] and SECM imaging can thus identify active regions, which promises to make it a valuable tool for exploring magnetism and chirality effects on OER activity.

Scanning ion conductance microscopy (SICM) employs nanopipettes to map the surface topography, ion flux, and changes in local electrochemical environments with high spatial resolution. This technique could be used for studying the ionic transport dynamics and local variations in concentration, such as the consumption of OH^- during the OER (Figure 9c.3).[293]

Scanning electrochemical cell microscopy (SECCM) enables nanoscale electrochemical measurements by rastering a nanopipette with a small droplet of electrolyte over the surface at speeds of tens to hundreds of μm/s, providing high-speed, high-resolution electrochemical imaging, recording electrochemical data at each contact point of the nanopipette (Figure 9c.1). It enables the distinction of individual facets and nanoparticles in catalytic materials, offering a fine-scale view of how localized electrochemical reactions occur.[293] This capability is especially useful for studying heterogeneous catalysts and understanding the effects of small-scale structural features on the OER.[294] While SECM is the most commonly used SEPM technique due to its adaptability and versatility, SECCM offers higher lateral resolution and enables high-throughput data acquisition. One of SECCM's key advantages is that it confines the electrolyte to a small area of the sample, minimizing exposure and thereby reducing the risk of degradation. However, maintaining the stability of the electrolyte droplet at the SECCM tip can be challenging, making the experimental setup and operation more demanding.

Together, these SEPM techniques allow for the exploration of spatially resolved electrochemical properties, particularly for studying local variations in surface morphology, ionic composition, and catalytic activity. Scanning across chiral regions, magnetic domains, or domain walls may reveal localized variations in catalytic performance. Future advancements could include the use of spin-selective redox mediators or tips functionalized with chiral molecules, or magnetic tips in SEPM, designed to interact specifically with the spin states of OER intermediates, offering deeper insights into spin-dependent catalytic mechanisms.

Complementary Techniques and Multimodal SPM Approaches: Since no single technique can resolve all challenges and open questions related to oxygen electrocatalysis, a multimodal approach is essential. SPM techniques are commonly used in combination with spectroscopy (X-ray photoelectron or absorption spectroscopy, Raman) and ab initio calculations to achieve a comprehensive understanding of OER processes on surfaces. Moreover, EPR-STM is emerging under UHV and cryogenic conditions as a technique that combines atomic-resolution imaging with the detection of single-electron spin transitions.[295] Although the technique is in its infancy, we anticipate that it could offer a powerful approach to investigate spin-dependent processes and transient intermediates in oxygen catalysis, with unprecedented detail.

On the solid/liquid front, the study of spin-polarized samples with EC-STM and noise-based techniques represents a significant opportunity to explore spin-dependent intermediate adsorption and activation under operando conditions. Additionally,

the combination of EC-STM and SECM with spin-engineered samples can provide deeper mechanistic understanding at electrochemical interfaces. Thus, future advancements in scanning probe methodologies, especially when equipped to characterize physical and chemical surface properties under operating conditions, are poised to significantly advance our understanding of the spin-related phenomena driving the OER.

4.2.3. Characterization of Magnetic Properties

Careful characterization of the magnetic properties of the catalyst is crucial for fully understanding the spin effects in the magnetically enhanced OER. Advanced magnetic measurement techniques enable the construction of a comprehensive picture of the magnetic order, including depth profiles, spatial variations, exchange-coupled regions, and surface magnetic states (Figure 10). These features can then be directly correlated with OER performance. Moreover, studying these properties under operando conditions is essential for accurately linking the actual magnetic ordering to the catalyst's electrochemical behavior.

X-ray Absorption Spectroscopy, X-ray Magnetic Circular Dichroism and X-ray Magnetic Linear Dichroism: X-rays can interact with the core electrons of a material, with a consequent electronic excitation toward an empty molecular orbital, leaving a core-hole (absorption process). Thus, X-ray absorption spectroscopy, which measures absorption intensity within a defined photon energy range near an absorption edge, provides information about the local chemical environment of the absorbing atom (Figure 10a.1).[296]

In general, soft X-ray photons (100–2000 eV) probe mainly K edges (1s to 2p transitions) of low Z (<13) elements, and L edges (2p to empty states transitions) of first row transition metals; the study of these so-called Near Edge X-Ray Absorption Fine Structure (NEXAFS) spectra can provide useful information about the oxidation state, spin state and local geometry of the material, with chemical selectivity and relative surface sensitivity. On the other hand, medium and hard X-ray photons (> 2000 eV) mainly probe K edges (1s to empty states transitions) of medium-high Z elements with bulk sensitivity (because of the higher penetration depth combined with the transmission mode acquisition popular in this energy range). In this energy region, in addition to the oxidation state, it is possible to obtain structural information looking at the so-called extended X-ray absorption fine structure (EXAFS) region, where multiple scattering effects dominate the absorption process.

When NEXAFS is performed with polarized light, the absorption will change according to the different orientation between the incident light polarization vector and the quantization axis of atoms in a material; this property can provide additional information about local anisotropies of charge, spin and angular momentum around an atom in a material. This aspect of XAS gave birth to other related spectroscopies through which other physical properties can be investigated. In X-ray magnetic dichroism (XMD) spectroscopies, the use of left/right circularly (XMCD)[297] or horizontally/vertically linearly (XMLD)[298] polarized light combined with the dichroic response of p to d electronic transitions in magnetic materials allows one to quantitatively determine their FM or antiFM properties respectively, with chemical selectivity (Figure 10a.2,3).

XAS, when used in operando conditions, enables monitoring the dynamic evolution of the electronic structure of a catalytic system under working conditions, allowing to identify the role of the sites involved in the catalytic reaction mechanism.[299] With the advent of fourth-generation Synchrotron facilities, ambient pressure and operando XAS have gained traction. The first experimental setups were dedicated to the study of catalytic processes occurring at the gas-solid interphase, ongoing developments aim to extend operando XAS techniques to liquid-phase environments.[300] This advancement will enable direct observation of electronic and structural dynamics–such as changes in oxidation state and local coordination–at solid-liquid interfaces under realistic catalytic conditions, including electrocatalysis. Both approaches have demonstrated the ability to provide direct evidence of oxidation state and spin state variations under reaction conditions.[301,302] For such measurements, it is important to recognize that the probing depth is largely determined by the detection mode. Transmission mode is bulk-sensitive, while total electron yield (TEY), which detects emitted electrons, is highly surface-sensitive (≈5 nm). Fluorescence yield is less surface-sensitive (≈100 nm) than TEY. Since catalytic processes primarily occur at the surface, selecting the appropriate detection mode is crucial to capturing surface changes during catalysis.

Combining these operando measurements with spin-engineered catalysts or applied external fields would enable the study of the effect of spin order on these properties. However, due to the experimentally complex setups, ambient pressure XAS in the soft X-rays regime is available only in a few of the world's beamlines.[303] Moreover, these setups pave the way for the use of Soft-XMCD/XMLD techniques under catalytic conditions, which is appealing because they are generally performed at the L edges of transition metals. At these edges, the XMCD signal is significantly stronger than at the K edges, which are usually probed in hard-XMCD/XMLD experiments. This difference arises because the core hole excited at the L edge experiences spin-orbit coupling, whereas the core hole at the K edge does not.

Operando XMCD/XMLD are unique and very promising tools for spin-dependent OER studies because they could allow us to discriminate the role of electronic and magnetic property modifications of the catalyst - with elemental resolution - and of the reactant molecules during OER. We expect that such experiments will provide fundamental information regarding the spin-related effects in spin-enhanced reactions. As an example of its potential, XMCD has been used in operando conditions by Yu et al.[304] to provide insights on the gating mechanism of electric double-layer transistors, by measuring Co $L_{2,3}$ edge XMCD and O_K edge during bias application. The experimental setup developed by Guerrero et al.[305] shows the possibility of using circular polarized light to measure the Fe $L_{2,3}$ edge XMCD signal of a Fe film at 1 bar of total pressure. Thus, operando XMCD offers a powerful approach for investigating solid/gas or solid/electrolyte interfaces in electrochemical systems involving magnetic materials. By directly correlating OER activity with spin states, electronic structure, and their modifications under catalytic conditions, deeper insight into spin-enhanced OER mechanisms can be achieved.

Lorentz Transmission Electron Microscopy, Off-Axis Holography and Electron Magnetic Circular Dichroism: TEM enables simultaneous access to microstructure, electronic structure, chemical composition, electrostatic and magnetic properties, thus enabling correlative studies that provide insight into structure-property-activity relationships. Magnetic imaging in TEM is based on the interaction of high-energy electrons with the magnetic fields within and surrounding a sample. To avoid distortion of magnetic domains by the ≈2 T objective lens in standard TEM, Lorentz microscopy (LTEM) disables the objective lens and uses a mini-lens or transfer lens to achieve field-free imaging conditions. In this section, we will introduce two commonly used phase contrast techniques in LTEM: Fresnel mode and off-axis electron holography, and one spectroscopic TEM based technique: electron magnetic circular dichroism (EMCD).

Fresnel mode LTEM utilizes the Lorentz force, which causes charged high-energy electrons to deflect sideways as they pass through magnetic domains with varying orientations (Figure 10b.1). This deflection creates regions of electron density excess, or deficiency, immediately below the sample, resulting in lines of black and white contrast at domain walls when imaging with under-focus, or over-focus, conditions, as shown in Figure 10b.1 [306]. Importantly, magnetization parallel to the beam produces no Lorentz deflection; thus out-of-plane magnetic domains (parallel to the electron beam direction) are invisible unless the sample is tilted to project an in-plane component.

Off-axis electron holography provides the ability to quantify the magnetic phase shift and electrostatic potential. Electron holography records the interferences of coherent electron waves, allowing for the recovery of both the amplitude and the relative phase. The two waves then overlap and interfere, producing a hologram with interference fringes (see Figure 10b.2). The phase shift of the electron wave can be reconstructed from the holograms and quantitative phase information with high spatial resolution about the projected in-plane magnetic fields and electrostatic fields in a sample can be extracted.[307–309] Furthermore, when combined with a model-based approach, a quantitative magnetization distribution can be resolved.[310] However, the associated procedures can only be fully quantitative if the experiments are carefully designed and great care is taken to avoid introducing artifacts.

Different from phase contrast techniques mentioned above, EMCD does not require a field-free condition and can be implemented using standard TEMs. Moreover, EMCD detects out-of-plane magnetic components, offering complementary magnetic sensitivity to other TEM-based techniques. EMCD is conceptually analogous to XMCD but it uses electrons instead of circularly polarized X-rays. While XMCD relies on differential absorption of left- and right- circularly polarized photons, EMCD uses the interference of electron scattering paths within a crystalline sample to produce a dichroic effect.[311,312] Figure 10a.4 shows the setup of TEM-EMCD. The EMCD signal is obtained by acquiring electron energy-loss spectra (EELS) from symmetric Bragg reflection (±g) positions in the diffraction plane and calculating their difference. It enables quantification of element-specific spin and orbital magnetic moments.[311]

Table 3 summarizes the key characteristics of the three TEM-based magnetic imaging techniques described above. The comparison includes spatial resolution, phase resolution, field of view, key limitations, and in situ measurement capabilities. Fresnel-mode LTEM provides real-time imaging of magnetic domains with moderate spatial resolution and wide field of view but is limited to qualitative contrast. Electron holography offers quantitative phase mapping of both magnetic and electrostatic phase with high phase sensitivity and nanometer-scale spatial resolution, though it requires a coherent setup and is less compatible with chemically reacting systems. EMCD, in contrast, enables element-specific quantification of spin and orbital moments with atomic resolution in optimized STEM configurations but suffers from weak signal intensity and limited operando capability. Together, these techniques offer complementary strengths for probing magnetism in catalytic systems.

In spin-enhanced catalysis research, TEM studies have so far been limited to investigating the crystal structure. However, the techniques described above have demonstrated strong capabilities in probing magnetic structures in metals, oxides, and chiral magnets across various sample types.[313] These methods therefore offer valuable insights into the correlation between this magnetic structure and catalytic behavior. For example, electron holography can reveal domain reconfigurations before and after OER, while EMCD provides element-specific spin and orbital moment data that complement oxidation-state maps from STEM-EELS. Such imaging is particularly important for OER catalysts, where the spin and valence states of transition-metal cations critically influence activity. Although in situ applications remain challenging, recent advances in environmental TEM holders and phase-reconstruction techniques are substantially enhancing the ability to image materials under near-operando conditions[314] even using Lorentz TEM and off-axis electron holography.[315] Such developments hold significant potential for the direct observation of magnetic flux and electrostatic charge distributions in catalyst materials during reactive processes. These capabilities could provide new insights into the interplay between structure, magnetism, and catalytic performance at the nanoscale, thereby contributing to the rational design of next-generation functional catalysts.

Low Energy Electron Microscopy and Photoemission Electron Microscopy: Photo Emission Electron Microscopy (PEEM) is a full-field photon-in-electron-out imaging technique on the photoelectric effect, where monochromatic UV or X-ray light generates photoelectrons with defined momenta and energies (Figure 10b.3). This process begins when photons with energy $h\nu > \Phi$ (the material's work function) strike a conductive surface, causing the emission of photoelectrons and Auger electrons with a range of kinetic energies. These electrons undergo inelastic scattering, resulting in a strong low-energy secondary electron peak. Electron lenses, energy filters, and apertures then generate a 2D intensity map, with contrast arising from variations in electron emission. By tuning the wavelength and polarization of the incident light, PEEM can reveal chemical and magnetic properties of the sample's near-surface region with nanoscale spatial resolution across several microns. Modern PEEM systems–particularly those with aberration-corrected optics–achieve spatial resolutions below 3 nm, primarily limited by spherical and chromatic aberrations.

Combined with synchrotron x-rays (100–3000 eV), PEEM offers powerful chemical and magnetic imaging capabilities. Spatially-resolved X-ray Absorption Spectroscopy provides

chemical contrast, valence variations, local site-symmetry, and adsorbate coordination (Figure 10b.3). In spin-enhanced OER studies, this could help distinguish purely the electronic effects from spin effects, and provide a way to explore the effect of spin-polarization on the adsorbates. Particularly exciting for spin-dependent OER is the combination of polarized x-rays with PEEM, which opens up detailed magnetic imaging at <20 nm resolution. PEEM imaging with circularly or linearly polarized X-Rays, allows spatially resolved spectroscopy corresponding to X-ray magnetic circular and linear dichroism, which are discussed in detail in section 4.2.3. Thus, it can probe the FM and antiFM properties, respectively, offering the possibility to study the element-specific spin structures and to map the domain structure with several nm spatial resolution. These observations then could be related to the magnetic catalyst performance under OER conditions to gain valuable insight into the magnetic structure- electrochemical performance correlation.

In addition to PEEM, Low-Energy Electron Microscopy (LEEM) is another powerful technique which uses backscattered electrons, generated by illuminating the sample surface with a low-energy electron beam (Figure 10b.4) to map changes in Φ across a surface. These variations reflect changes in surface dipole, electronic states, and adsorbate-induced charge transfer, and could be influenced by spin order, which can impact OER activity. Investigating the spin-property relationship in OER catalyst could thus help to clarify the role of spin in OER enhancement. When used alongside XMCD/XMLD-PEEM, LEEM enables correlation of magnetic domain structures with surface morphology and electronic contrast, helping to distinguish between purely magnetic effects and structural or electronic contributions to catalytic behavior. Furthermore, Low-Energy Electron Diffraction (LEED) allows bright and dark-field imaging of domain orientation across a surface with a few tens of nm resolution.[316] Understanding such domain orientation and symmetry is crucial, as magnetic anisotropy can strongly influence spin-adsorbate interactions and thus affect spin-dependent OER performance.

PEEM and LEEM require stringent sample conditions and the probing depth is limited to just a few atomic layers (typically 3–5 nm). Nevertheless, modern systems routinely achieve element-specific full-field imaging over hundreds of microns while reaching spatial resolutions below 20 nm–and in some cases down to 3 nm–enabling detailed studies of electrode morphology, phase changes, and magnetic domains before and after electrochemical reactions.[317,318] Another advantage of LEEM and PEEM is the possibility of tracking structural, chemical and magnetic changes across a surface in real time and under in-situ conditions during heterogeneous catalytic reactions[319,320] and phase transitions.[321] Regularly, PEEM and LEEM require UHV conditions, impeding operando studies. But in recent years, several notable advances have been achieved, allowing PEEM to be extended to near-ambient pressure imaging[322] as well as imaging electrochemistry at solid-liquid interfaces in real-time using graphene windows.[323,324] Extending these capabilities to operando, spatially-resolved spectroscopy with polarized X-rays could open new avenues for understanding spin-enhanced chemical processes, as the measurements discussed above could then be performed directly on the active catalytic surface under OER conditions.

Magneto-Optical Kerr Effect Microscopy: Magneto-optical Kerr effect (MOKE) microscopy enables non-invasive, surface-sensitive domain structure observation and magnetometry (Figure 10b.5). MOKE refers to the change in the polarization state of light as it is reflected from a magnetic surface. In the context of linearly polarized light, this effect can be conceptualized as a rotation of the polarization plane depending on magnetization, which can be converted into a weak but observable change in light intensity by means of an analyzer in optimized full field polarization microscopes. MOKE microscopy requires smooth and reflective surfaces for optimal performance. For metallic surfaces, a probing depth of ≈30 nm can be attained. This method allows for the local measurement of magnetic hysteresis loops, the determination of magnetization directions, and the extraction of relative magnetization values. A comprehensive review of applied MOKE microscopy for the characterization of magnetic materials can be found elsewhere.[325]

The spatial resolution of MOKE microscopy is constrained by the optical diffraction limit. When combined with the employed optical apparatus, a resolution of ≈250 nm can be achieved. Magnetic analysis of smaller structures remains a viable option. The field of view can extend to several centimeters. Standard MOKE microscopy achieves a single-shot temporal resolution in the millisecond range. However, sub-picosecond temporal resolution can be achieved through the implementation of specialized setups. MOKE microscopy enables uniform imaging of magnetic domain structures of different catalyst materials used for the OER. As this can be carried out independently of electrochemical measurements and concurrently in operando during such measurements, MOKE microscopy holds great potential for spin-dependent OER studies. The direct identification of effects arising from spin order within the catalyst materials is made possible by correlating changes in the electrochemical properties with alterations in the magnetic properties and imaged magnetic structure of the catalyst. Furthermore, changes in the magnetic properties of the investigated catalysts due to degradation or redeposition processes can be probed during the OER. Notably, the successful in situ implementation of MOKE microscopy and magnetometry during electrochemical measurements not only demonstrates feasibility but also paves the way for future advances in magnetic operando analysis.[326,327]

Electron Paramagnetic Resonance and Ferromagnetic Resonance: EPR spectroscopy uses unpaired electrons to detect the presence of PM centers in a material by inducing transitions between energy states associated with different spin magnetic quantum numbers m_s in an external magnetic field (Figure 10c.1).[328] The intensity of the resonant microwave absorption, which is measured as a function of the magnetic field strength, provides information about the absolute number of unpaired electrons in a sample. Furthermore, the exact value of the external magnetic field at which a resonant transition occurs is sensitive to magnetic moments of nearby electron or nuclear spins and reports on the microscopic environment of localized PM centers by quantifying the coupling and distances to neighboring spins.

Magnetic resonance techniques can help to identify active sites, transient states and reaction intermediates as well as spin-dependent processes at catalytically active surfaces.[329] However, due to small signal strengths, conventional EPR is mainly considered a bulk characterization technique. Still, there are a few

examples of studies on PM centers on catalysis-relevant surfaces detected by EPR, using particularly long averaging times.[330]

Detailed insights into catalytic processes, in particular also magnetically-enhanced and chirality-enhanced OER, could be provided by combining EPR with electrical detection. The resulting technique, electrically detected magnetic resonance (EDMR) spectroscopy, has a much higher sensitivity than conventional (microwave-detected) EPR and can be pushed down to the single-spin level.[331] As EDMR detects changes in the electrical conductivity, this technique is ideally suited to study spin-dependent charge-transfer processes and identify current-limiting transient states and reaction intermediates.[332] This has, for instance, been demonstrated by detecting EDMR signals resulting from spin-dependent charge transfer at the interface between chiral electrodes and an electrolyte.[332]

Spin-resonant transitions can also be excited in FM materials, and probed in FMR spectroscopy. In contrast to EPR, which probes individual uncoupled spins, the magnetic moment that gives rise to a resonant signal in FMR is caused by many exchange-coupled electron spins and allows studying parameters like the magnetic anisotropy, the magnetic moment and the Curie temperature.[333]

The alignment of spins due to the FM order in FMR leads to much larger signals, providing the opportunity for studying ultrathin FM films down to a few nm and thus enable surface sensitive measurements. Many additional opportunities for magnetic resonance techniques thus open up when (spin-ordered) FM electrodes are used to explore spin-enhanced OER. Notably, in-situ FMR and EPR experiments offer a unique capability: beyond simply probing the spin states of catalysts and adsorbates, these resonant techniques can actively manipulate spin configurations by inducing transitions between spin states. This dynamic control provides a direct means of modulating spin-dependent conduction channels, should allow one to selectively "switch on or off" specific reaction pathways. The resulting change in catalytic activity can be directly observed as a change in current in the EDMR signal. Such experiments hold great promise for establishing a causal relationship between spin state and catalytic performance, and for enabling the disentangling of complex spin-related phenomena. FMR can also be applied to probe whether or not a nominally spin-ordered electrode is indeed FM and stays FM under reaction conditions. This is particularly relevant when potential-induced changes, prolonged exposure to OER conditions with corresponding degradation pathways or side reactions may modify the composition of the electrode surface and thus its magnetic properties.

^{57}Fe Mössbauer Spectroscopy: ^{57}Fe Mössbauer Spectroscopy is used for characterization of iron in various solid compounds. It studies the recoil-free nuclear resonance absorption and emission of γ rays (E = 14.4 keV) in ^{57}Fe nuclei. In lab-based Mössbauer spectroscopy a radioactive ^{57}Co source is used to generate the relevant γ rays. To match the energy of the nuclear excited and ground states in the sample and the source, the latter is given a small velocity of several mm s^{-1} (note 1 mm s^{-1} corresponds to an energy difference of ca 50 neV). If the resonance absorption occurs, in this velocity range, the amount of γ rays that are detected is lowered leading to characteristic absorption lines (Figure 10c.2).

The resulting Mössbauer spectra are plotted as relative absorption intensity versus Doppler velocity. The spectral features reflect interactions between the nucleus and its surrounding electric and magnetic fields, known as hyperfine interactions. These can lead to characteristic patterns depending on the local environment of the iron atom. A single absorption line appears if only an electric monopole interaction is relevant. The velocity at which the balance point of the line occurs is referred to as isomer shift, where the isomer shift (δ_{iso}) indicates changes in electron density at the nucleus, often related to the oxidation state. If there is an asymmetry in the local electric field–due to distorted ligand fields or non-cubic symmetry, additional electric quadrupole hyperfine interactions occur that appear as overlay to the electric monopole interactions, leading to a doublet pattern. The energy difference between the two lines is described by the quadrupole splitting (ΔE_Q). In magnetically ordered systems, a magnetic dipole interaction is additionally superimposed on the electric hyperfine interactions. These can split the nuclear energy levels further, producing a sextet pattern. This magnetic hyperfine splitting is quantified by the internal magnetic field (H_{int}). Each of these hyperfine parameters provides valuable insight into the chemical, structural, and magnetic environment of the iron sites being probed.

As such, Mössbauer spectroscopy offers great potential for in situ or operando characterization of iron-containing catalysts. Prior work has shown that the local environment of iron is affected by applied electrochemical conditions, resulting in spin and oxidation state changes.[334–336] For example, comparing the data on operando Mössbauer spectroscopy for NiFeOOH in the OER indicates that, depending on the Ni:Fe ratio, a different ferryl iron signature occurs in the spectra.[337–339] These findings demonstrate that Mössbauer spectroscopy can sensitively detect changes in spin state, oxidation state, and local coordination. In in situ or operando setups, the long measurement times - often several hours to days in laboratory based experiments – can limit its practical application.[340–342]

An option to overcome this limitation is provided by synchrotron-based Mössbauer spectroscopy that can be performed at selected synchrotrons as DESY, ESRF, Spring-8.[343–345] It enables much faster data acquisition and is thus more relevant for in situ or operando spectroscopy. This approach also allows for comparison of catalyst behavior with and without an applied magnetic field, helping to reveal mechanistic changes driven by spin effects.

Vibrating Sample and Superconducting Quantum Interference Device Magnometry: VSM and SQUID magnetometry are the most commonly used techniques for studying the magnetic properties of materials. In VSM, the sample is vibrated between pickup coils, which induces a voltage that is proportional to the sample's magnetization (Figure 10c.3). Most SQUID magnetometers also involve moving the sample through pickup coils. This movement induces a change in the magnetic flux of the Josephson junction-based SQUID sensor, which is transformed into a voltage signal proportional to the sample's magnetic moment. Both VSM and SQUID magnetometry enable precise measurement of magnetic moments across a range of external magnetic fields and, depending on the configuration, temperatures. The selection of either technique should be guided by their respective advantages and limitations. SQUID magnetometry offers sensitivity higher than that of VSM, making it particularly

suitable for detecting small magnetic signals or working with minute sample quantities. However, due to its reliance on superconducting components, SQUID instruments are typically restricted to operating temperatures below ≈ 400 K. In contrast, VSM systems are better suited for experiments requiring elevated temperatures, as they do not face the same thermal constraint.

The results of the experiments can be used to determine magnetic order, transition temperature, saturation magnetization, and coercivity. In cases of more complex sample geometries, like thin films or layered structures, both techniques can be used to determine magnetic anisotropies and to probe exchange interactions.[104] All of these properties can be systematically correlated with magnetically induced enhancements in OER activity. Such comparisons could probe the relationship between the catalyst's spin ordering at the surface and subsurface layers and its OER performance, as well as the influence of magnetic field directionality on catalytic enhancement.

While both VSM and SQUID have to date only been utilized ex situ to characterize the magnetic properties of the catalyst prior to catalysis, it is possible to adapt both techniques for operando measurements. Despite the previously discussed differences in operating principles, VSM and SQUID magnetometry support similar sample holder geometries, typically using hollow DM tubes ≈5 mm in diameter, in which the sample is suspended–thereby limiting the sample size to below 5 mm. By making these tubes leak-tight and filling them with electrolyte to submerge the sample while maintaining electrical contact with external instrumentation, operando measurements become feasible. This concept has already been demonstrated, using a sealed Teflon tube in a SQUID magnetometer to investigate redox-dependent magnetic behavior.[346] Using this approach, it should be possible to directly correlate the magnetic moment of the real active catalyst phase under operating conditions to the observed electrochemical dependencies and gain more insight into the actual role of the spin state in the OER. (**Table 4**).

4.2.4. Characterization of Chirality and Spin Filtering

Understanding the role of chirality in OER catalysis necessitates robust methods for characterizing chiral electrodes. A key objective is to elucidate how CISS influences electron transfer and catalytic activity. To date, inferences about the importance of spin-polarized radical intermediates in the OER reaction on chiral electrodes are drawn from circumstantial evidence, such as the correlation of spin-filtering properties of OER catalysts with their catalytic performance. Thus, developing and applying operando techniques capable of probing chirality, spin-polarization, and radical intermediates in real time will be essential to uncover the mechanistic impact of chirality on reaction pathways.

Chirality: CD spectroscopy, which measures the differential absorption between left- and right-circularly polarized light (Figure 10c.4), is the principal technique for the characterization of chiral systems. In the context of spin-dependent OER catalysis mediated by the CISS effect, operando CD spectroscopy presents a particularly compelling approach to monitor the dynamic evolution of chirality in electrode materials under working conditions. Recent studies suggest that this approach is highly promising. For instance, in a study involving chiral Fe–Ni metal oxides in alkaline solution, the evolution of the CD signal during electrocatalysis indicated that the OER-active sites formed in the chiral catalysts are spin-polarized centers and involved in the reaction.[133] Additionally, redox-triggered structural transformations in heme proteins have been investigated using operando CD spectroscopy coupled with electrochemistry and other operando optical methods,[347] highlighting the power of multimodal operando characterization.

While operando CD can thus provide real-time insights into the evolution of chirality under electrochemical conditions, a complete understanding of spin-polarization in catalysis requires direct correlation of the intrinsic spin-filtering properties of chiral materials with their catalytic behavior. In this regard, some studies have explored the relationship between the CD responses of chiral systems and their spin-selective electron transfer and charge transport characteristics.[348–350] However, establishing robust structure-function relationships remains an outstanding challenge.[351] Continued development of integrated operando techniques which combines CD with characterization techniques for spin filtering and polarization, will be critical for elucidating the intricate interplay between chirality, spin-polarization, and catalytic function in CISS-mediated OER systems.

Spin-Filtering and Spin-Polarization in Chiral Electrodes: The primary methods used to quantify the spin filtering properties of chiral electrocatalysts and chiral electrode films are Mott polarimetry and mc-AFM measurements.[132]

Mott polarimetry measures spin-polarization by analyzing the asymmetric scattering of electrons from a target with high spin-orbit coupling. In chiral systems, it is used to probe spin-selective electron transmission caused by the CISS effect. Electrons are excited in a substrate and pass through a chiral layer, which preferentially transmits one spin. Those electrons that pass are accelerated toward a second target, where their scattering pattern reveals the spin-polarization induced by the chiral film (Figure 10c.5). Though highly effective in probing spin-polarization and its correlation with OER activity, Mott polarimetry is constrained to ex situ measurements under UHV conditions.

Conventional **mc-AFM** employs a magnetized conductive tip to measure spin-dependent electron transport through a material (Figure 9b.3). In chiral systems, it detects the CISS effect by observing current changes as the tip's magnetization is reversed, thereby revealing spin-selective conductivity. However, the poor stability of magnetic tips in liquid environments prevents the direct application of mc-AFM under operando conditions.

A viable workaround involves using a standard conductive tip while magnetizing the substrate on which the chiral layer is deposited through a thin magnetic underlayer–such as a 5 nm gold film deposited on nickel–which can be magnetized either up or down. In this configuration, a non-magnetic AFM tip can be used and the magnetic layer is not exposed to the liquid environment, eliminating stability concerns.[352] This latter approach offers the potential for operando mc-AFM measurements. Other issues related to nanoscale imaging in OER conditions such as interference of electrical noise and potential fluctuations with the AFM signal, and disruptions due to bubble formation, would apply in this case.

MR of film electrodes, Hall effect, and other methods have also been used to study spin-filtered currents in the CISS community. Details of each of these techniques can be found in a recent

Table 4. List of abbreviations. Left two columns: methods and techniques; right two columns: phenomena, materials, components, and concepts.

Abbreviation	Method / Technique	Abbreviation	Concept / Phenomenon
AFM	Atomic force microscopy	antiFM	Antiferromagnetic
CA	Chronoamperometry	AEM	Adsorbate Evolution Mechanism
CASSCF	Complete active space self-consistent field	CE	Counter electrode
CD	Circular dichroism	CHE	Computational hydrogen electrode
CFD	Computational fluid dynamics	CISS	Chirality-induced spin selectivity
CI	Configuration interaction	DM	diamagnetic
CV	Cyclic voltammetry	EDL	Electrochemical double layer
DFT	Density functional theory	FM	Ferromagnetic
DMFT	Dynamical Mean-Field Theory	FiM	Ferrimagnetic
DRFT	Distribution function of relaxation times	HS	High-spin
EC-AFM	Electrochemical-AFM	I2M	Interaction of two metal sites
EC-STM	Electrochemical-STM	IR	Infrared
ECW	Embedded correlated wavefunction	KS	Kohn-Sham
EDMR	Electrically Detected Magnetic Resonance	LDOS	Local density of states
EELS	Electron energy-loss spectra	LOM	Lattice oxygen mechanism
EIS	Electrochemical impedance spectroscopy	LS	Low-spin
EMCD	Electron magnetic circular dichroism	MHD	Magnetohydrodynamic
EPR	Electron paramagnetic resonance	ML	Machine learning
FEM	Finite element method	MOKE	Magneto-optical Kerr effect
FMR	Ferromagnetic resonance	MR	Magnetoresistance
FTIR	Fourier transform infrared	OER	Oxygen evolution reaction
GGA	Generalized gradient approximation	ORR	Oxygen reduction reaction
KPFM	Kelvin Probe Force Microscopy	PEC	Photoelectrochemical
LDA	Local-density approximation	PM	Paramagnetic
LEED	Low-Energy Electron Diffraction	QEXI	Quantum excitation interactions
LEEM	Low-Energy Electron Microscopy	QSEI	Quantum spin exchange interactions
LSV	Linear sweep voltammetry	RDS	Rate-determining step
LTEM	Lorentz transmission electron microscopy	RE	Reference electrode
mc-AFM	Magnetic conductive AFM	SOC	Spin-orbit coupling
MBPT	Many-body perturbation theory	sPM	Superparamagnetic
MCSCF	Multiconfigurational self-consistent field	TSS	Topological surface states
MFM	Magnetic force microscopy	UHV	Ultra-high vacuum
PEEM	PhotoEmission Electron Microscopy	WE	Working electrode
SECCM	Scanning electrochemical cell microscopy		
SEM	Scanning electron microscopy		
SEPM	Scanning Electrochemical Probe Microscopies		
SICM	Scanning ion conductance microscopy		
SP-STM	Spin-polarized scanning tunneling microscopy		
SPM	Scanning probe microscopy		
SQUID	Superconducting quantum interference device		
SRPES	Spin-resolved photoelectron spectroscopy		
STM	Scanning tunneling microscopy		
STS	Scanning tunneling spectroscopy		
TEM	Transmission electron microscopy		
VSM	Vibrating sample magnetometry		
XAS	X-ray absorption spectroscopy		
XES	X-ray emission spectroscopy		
XMD	X-ray magnetic dichroism		
XMCD	X-ray magnetic circular dichroism		
XMLD	X-ray magnetic linear dichroism		
XUV	Extreme ultraviolet		

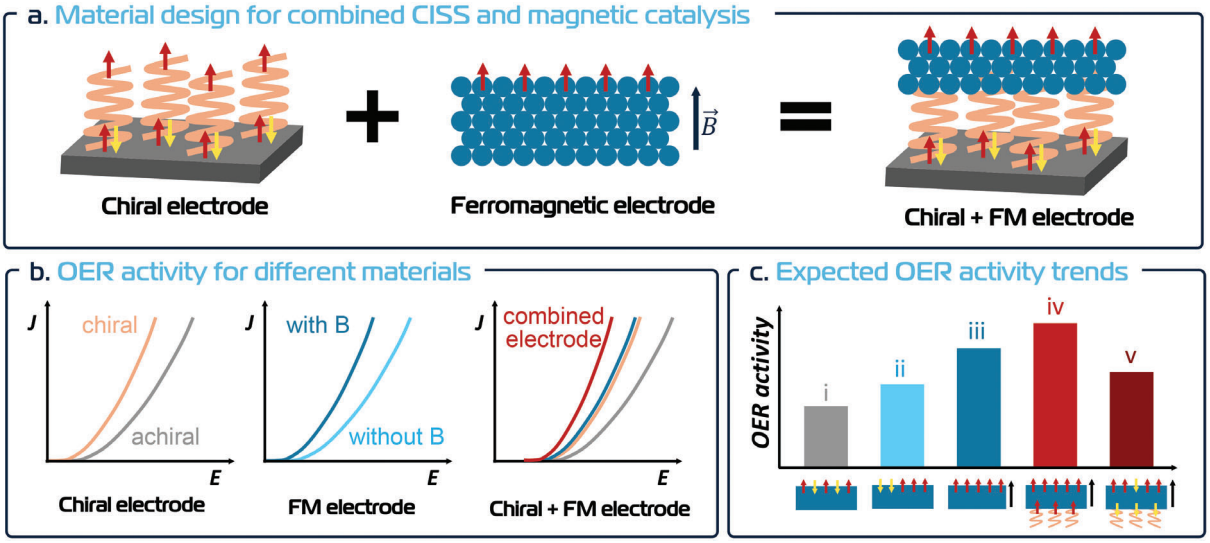

Figure 11. Illustration of the potential synergistic effects of combining the CISS effect with magnetism to enhance OER activity. a) A hybrid electrode combining a chiral spin transport layer with a FM electrode may enhance OER activity, as detailed in the LSV curves (b). c) Schematic comparison of expected OER activity for: (i) aPM electrode, (ii) a FM electrode, (iii) a FM electrode subjected to an external magnetic field, (iv) the same FM electrode functionalized with chiral molecules whose spin-polarization via the CISS effect aligns with the external magnetic field, and (v) the same FM electrode functionalized with the opposite enantiomer, producing spin-polarization opposite to that of the magnetic field. Such comparisons can provide insight into the relative contributions of magnetic and CISS effects, and offer strategies to maximize spin-selective charge transfer and catalytic efficiency.

review.[132] One promising operando method for probing spin-dependent electrochemistry involves preparing a catalyst film on a Hall bar device, as shown by Kumar et al. (Figure 10c.6).[353] While such measurements have not been performed for OER, it has been shown that the chiral OER catalyst CoO_x can be electrodeposited onto the surface of such electrodes,[354] thus highlighting the feasibility of this approach.

Several alternative approaches, although less explored, also offer promising avenues for investigating spin-polarization under catalytic conditions. First, operando EPR spectroscopy would provide a direct method to probe the spin-polarization of catalytic centers (see Section 4.2.3) and may also enable the detection of radical intermediates formed during the OER.[355] Second, magnetic circular dichroism (MCD) spectroscopy in the extreme ultraviolet (XUV), similar to the abovementioned XMCD but associated with M-edge transitions (Figure 10c.7), has recently shown potential for linking enhanced OER activity to the generation of a spin-polarized hole population.[124] Applying MCD in operando configurations could provide additional important information on the reaction mechanism and spin-polarization in the catalyst, however, to our knowledge, the technique is currently still restricted to vacuum conditions. Lastly, electron-based characterization tools (as mentioned in Section 4.2.3) could significantly enhance our understanding of spin-polarization in chiral materials, and although their application under in situ and operando conditions is challenging, recent advances suggest that this would be feasible in the near future, thereby holding great promise (Section 4.2.3)

4.3. Combination of CISS and Magnetism in OER

Since the observed OER enhancement due to the CISS effect and using magnetic materials share mechanistic motifs, a combination of the fields will provide a unique opportunity to further understand or distinguish these processes. However, this combination has been rarely addressed in the literature. Each approach brings distinct advantages: CISS enables intrinsic, molecule-level control over electron spin without the need for external fields, thereby avoiding MHD interferences. In contrast, magnetic materials offer external and tunable control over spin alignment through temperature and magnetic fields, enabling real-time modulation of catalytic performance. Moreover, their diverse range of long-range magnetic orderings can be leveraged to tailor exchange interactions and spin-mediated conductivity. By leveraging these complementary strengths, we envision that hybrid systems could not only maximize spin-mediated catalytic activity but also provide deeper insights into spin-dependent reaction mechanisms, as schematized in **Figure 11**.

To explore the hybrid space between these fields, comparative and combined experiments are essential. Early studies have shown that chiral molecules on FM substrates can exhibit enantioselective interactions via spin complementarity.[10] Comparing the OER response of opposite enantiomers on such magnetic substrates under identical magnetic-field strengths and orientations can reveal whether CISS and magnetic alignment act synergistically or antagonistically (Figure 11c iv and v). Similarly, varying the direction and magnitude of the applied field (e.g., parallel vs perpendicular to the chiral monolayer) could allow mapping of the vectorial interplay between CISS-driven and field-driven spin-polarization.

From a materials standpoint, integrating chiral assemblies onto magnetic substrates or employing these assemblies as embedding matrices for magnetic catalysts offer a compelling strategy for constructing hybrid electrodes that unite intrinsic molecular spin filtering with externally tunable, field-induced spin alignment (Figure 11a). Such systems hold the potential

for synergistic spin-polarization effects, where the combined effects of CISS and magnetic ordering could produce significantly enhanced OER activity[137] (Figure 11b,c). In addition, exchange coupling at the interface may "lock in" spin orientation (Figure 11c.v) even in the absence of an external field, pointing toward the development of room-temperature spintronic catalysts.

When designing such hybrid systems, experiments should include racemic and achiral or PM and DM analogues of the chiral and FM materials, respectively, to ensure that observed activity enhancements are attributable to spin effects rather than changes in surface area or electronic structure.[73,74] Moreover, to fully harness the potential of spin-based OER enhancement, a systematic exploration of material combinations is needed. This includes pairing a range of FM or FiM catalysts (e.g., Co- or Fe-based oxides, perovskites, spinels) with diverse chiral molecules, ligands, or polymeric additives, or via chiral templating.[133] Such a comparative framework would enable researchers to disentangle the relative contributions of CISS and magnetic alignment across different systems and uncover the conditions under which one mechanism dominates or the two act synergistically. This approach could reveal design rules for identifying optimal pairings that maximize spin-selective charge transfer and catalytic efficiency. Furthermore, by evaluating these combinations under controlled variables such as pH, ionic strength, and field orientation, deeper insights into spin-material-interface dynamics and the OER mechanism may be achieved. An interesting divergence in methodology between the two fields offers additional opportunities for cross-pollination. Magnetically enhanced OER studies have typically focused on benchmarking electrochemical performance through current density and overpotential metrics. In contrast, the CISS community has gone further by quantifying Faradaic efficiency, specifically the production ratios of O_2 and H_2O_2, as a proxy for spin-polarization effects. Adopting this approach in magnetic-field-enhanced studies could provide more mechanistic resolution and help identifying the specific contribution of spin-polarization to catalytic enhancement. Moreover, the CISS effect has been observed not only in electrochemical OER systems but also in photoelectrochemical cells. In contrast, the application of external magnetic fields in PEC systems remains underexplored, likely due to experimental limitations in combining magnetic fields with light-driven systems. This discrepancy highlights an opportunity to extend magnetic strategies into PEC systems and further explore spin effects under photoelectrochemical conditions.

4.4. Material Design and Model Systems

So far, magnetic powder inks, molecular chiral monolayers and chiral templated materials have been the most widely used classes of materials to study the influence of spin structure on OER activity. Such samples often reflect an ensemble of magnetically active particles or molecules, and thus reveal geometrically averaged information on the potential spin enhancement and electrochemical performances. While still being able to provide valuable insight into the spin-enhanced catalysis mechanism, there is a vast selection of alternative materials classes and geometries, that remain mostly unexplored and could proof beneficial for better understanding of the effect. A wide range of magnetically active and chiral material classes, along with diverse model systems featuring tunable parameters to systematically control, modify, and manipulate spin- induced properties of these system, as well as its geometrical appearance, are available. These materials and model systems offer promising additional or alternative avenues to explore the spin enhancement in electrocatalysis under well-defined conditions, as detailed below. The most promising material classes are shown on the left side of **Figure 12**, alongside the most promising tuning strategies for model systems on the right, both selected for their potential to yield valuable insights into spin-enhanced OER research.

4.4.1. Alternative Materials Classes

Beyond the typically explored powder and molecular catalysts, magnetism, chirality and more specifically the engineering and control of the spin properties is explored in many fields unrelated to catalysis research. Many of these material classes, such as the molecular-based magnetic materials or topological insulators, are yet unexplored (or less explored, like half-metallic magnets or topological chiral materials) for electrocatalysis, specifically for the spin-enhanced OER, and utilizing them could uncover new, yet undiscovered phenomena.

The presence of SOC in a system without inversion center leads to the appearance of a variety of the electron transport phenomena.[356] For examples, the possibility to control the spin states via electrical gating in **Rashba materials** (Figure 12a) could allow for a novel experimental approach in OER enhancement research. Thus, comparing activity changes induced by either voltage or external magnetic field in these materials could be of great insight to the origin of the spin induced enhancements. Examples of Rashba spin-orbit interaction include interfaces of $LaTiO_3$[357] and $LaAlO_3$[358] with $SrTiO_3$ and the $KTaO_3$ interface with Al.[359] However, due to the often ionic character of the involved materials, their OER activity may be low, yet still controllable, making them suitable for studying the spin-enhancement in model experiments. One has to keep in mind that the majority of the Rashba materials are not oxides, making a careful selection of an OER-stable compound crucial for the experimental design, though some non-oxide Rashba materials have already been investigated for water electrolysis, like MoS_2.[360]

Another promising class of materials is **half-metallic magnets** (Figure 12b). These are materials, exhibiting metallic behavior toward electrons with one spin direction and insulating/semiconducting behavior toward electrons with the opposite spin.[361] Such unique transport properties could make half-metals promising for understanding the role of the spin transport selectivity in the OER enhancement phenomena. Furthermore, the list of half-metallic magnets is vast and includes several transition metal oxides, like Fe_3O_4[104] or $La_{0.7}Sr_{0.2}Ca_{0.1}MnO_3$,[78] which have already been used to study the magnetically enhanced OER effect and are known to be both electrochemically stable and active.

Topological semimetals (Figure 12c),[362] characterized by conduction and valence bands that touch at discrete points or lines in momentum space, with properties governed by specific

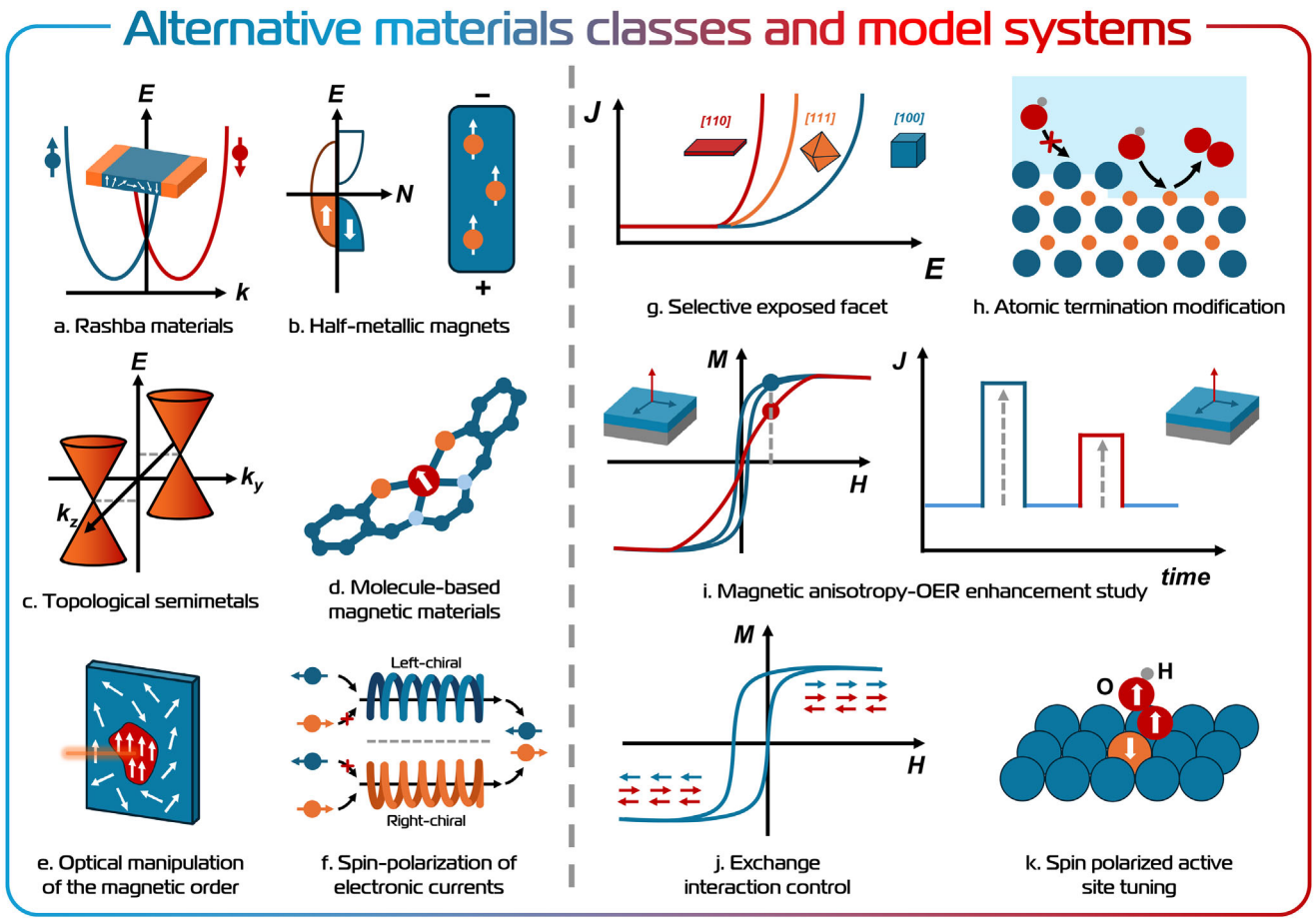

Figure 12. Schematic summary of the proposed alternative materials classes and the most promising tuning strategies within models systems, that could be utilized for the future advancement of spin- enhanced OER field. The alternative materials classes are on the right side of the figure. Each schematic demonstrates the core theoretical principle behind the materials class, highlighting its potential for the spin- enhancement studies. The core advantages of using epitaxial model systems are schematically demonstrated on the right side of the figure, highlighting their benefits for more controlled studies to isolate and investigate certain specific physical aspects, compared to more conventional experimental systems. Detailed discussions on how the chosen materials classes could be used in the spin enhancement research and the core advantages of the model systems can be found in the corresponding sections.

symmetries or their breaking, have recently gained attention for the OER. For example, $PdSn_4$[363] has been used for the exploration of both OER and HER fundamentals. The interest is driven by their exceptionally high charge carrier mobility and the presence of robust topological surface states (TSS) arising from the bulk band inversion. It is proposed that these features can enhance electron transfer and positively influence surface processes such as adsorption and desorption.[362,364,365] In the context of spin-dependent OER, the strong SOC in most topological semimetals is expected to be highly relevant, as it can induce spin-polarization in their TSS. Notably, **magnetic topological semimetals** offer exciting possibilities, particularly due to their intrinsic long-range magnetic order and electron delocalization.[362,365] The robustness of spin-polarized TSS, combined with the ability to dynamically modulate their topological features through symmetry alterations, using electric fields, magnetic fields, or circularly polarized light, makes these systems promising platforms for systematically exploring the role of spin and topology in catalytic processes with $Co_3Sn_2S_2$ already being utilized for OER studies.[365] Lastly, **topological chiral semimetals**, materials that combine crystal chirality with topological characteristic, can exhibit Fermi surfaces with monopole-like spin textures in the bulk state. These spin textures can generate spin-polarized carriers that could play a vital role in spin-dependent OER as has already been demonstrated on Ru-based compounds.[366,367]

To focus on the influence of the intrinsic spin properties on the OER activity, one might turn to **molecule-based magnetic materials** (Figure 12d).[368] A major advantage of such systems is the high degree of direct tunability of the magnetic properties via chemistry, opposed to more classical indirect property modulation approaches via doping or strain engineering that was discussed in more detail before. Examples of relevant molecule-based magnets include compounds composed of organic ligands and transition metals, which are not only potentially active for OER, but also offer a convenient platform for identifying the origin of magnetic active sites. For example, a $V(TCNE)_x\gamma(CH_2Cl_2)$ molecular-based magnet has been

demonstrated to possess ferromagnetic hysteresis even at room temperature.[369]

Materials that offer the possibility of **optical manipulation of the magnetic order** (Figure 12e) could provide a completely new approach to probe and exploit the spin-induced OER due to the versatility of physical properties they offer. Optical manipulation of the magnetic order is frequently performed on transition metals, their oxides or multilayers with the examples of Ni thin films,[370] CoO single crystals[371] and NiFe/NiO bilayers[372]) respectively, which presents a good starting point for exploring this approach for OER catalysis. Optical manipulation usually involves directing a short laser pulse of several mJ/cm^2 power at the material, then investigating the triggered spin dynamics or its impact on the spin order.[373] Coupled with electrochemical characterization, it would be possible to correlate optically-induced magnetic order fluctuations with electrochemical activity. While an operando approach would be preferable due to the short life span of most effect (e.g. antiFM-FM transformation occur on the picosecond timescale[374]), some laser induced changes could also be of permanent nature (e.g. laser pulse induced spin reorientation[375]), allowing for ex situ studies.

Another promising avenue, particularly relevant to the CISS field, is the exploration of material systems that exhibit nearly 100% **spin-polarization of electronic currents** (Figure 12f). Notable candidates include ultrathin films of metal oxides (e.g. Al_2O_3 with L- and D- alaninol),[130] metal-organic frameworks (e.g. Dy(III) and L-tartrate ligand - based MOF),[376] and covalent organic frameworks (e.g. Zn(salen)-based chiral covalent organic frameworks),[377] all of which have demonstrated such spin polarization, positioning them as promising platforms for investigating spin-enhancement phenomena. Verification of these spin-polarized currents can be performed using the buried Hall probe configuration described in Section 4.2.4.

The majority of the abovementioned materials classes have not been used before to study the influence of spin on OER, while others have only appeared in a limited number of studies, yielding initial insights into the effect. Further designing spin property-specific OER experiments for these classes could potentially uncover new phenomena, lead to new discoveries and potentially allow for deeper understanding of the enhancement effect.

4.4.2. Model Systems

Commonly studied OER powder catalysts inherently exhibit geometrical and structural complexity due to the ensemble of grain sizes, crystal orientations, exposed facets, grain boundaries, and the frequent use of binders and support matrices. This complexity often makes the interpretation of electrochemical data challenging and representative only of the collective behavior of the catalyst material. This is especially relevant for studies of magnetic order induced effects in OER catalysis, where the application of model systems is still lacking. At the same time, the often directional application of a magnetic field combined with undefined anisotropy in the catalyst adds even more variables to the system. These phenomena make the deconvolution of property descriptors for spin-dependent OER very challenging.

Designing model systems to probe the spin enhancement of OER and spin-induced effects within the catalysts could yield a solution to this challenge, by allowing more precise tuning and control of selected descriptors separately. Such model systems should possess defined structural properties and well-defined stoichiometry, as well as defined, tunable and well-characterizable electronic and magnetic properties, which can be thoroughly tested inside and outside the electrochemical environment. By design, these systems also more closely resemble the simplified models used in theoretical calculations, enabling more meaningful comparison between experiment and theory.

To select a model system for the experiment, one must first determine which descriptor to focus on. For example, the influence of the exposed crystal facet on the catalytic activity is well-known and can be tuned by several different approaches (Figure 12g). The most accessible one, which could be achieved with wet chemistry methods, would be the employment of systematically faceted nanoparticles and nanosheets.[378] By controlling the synthesis parameters, it is possible to select the thermodynamically favored crystal facets, implement them in a coherent manner on a support, and link these features to the OER performance of the material with and without applied magnetic field.

Another example of model systems that allow even more control over the material properties are single crystals[379] and epitaxial films.[380] Although more challenging to synthesize due to the need for high-temperature or vacuum equipment, atomically smooth surfaces of selected crystal facets can be obtained under carefully chosen synthesis conditions with the added possibility of tailoring the atomic termination. (Figure 12h).

The uniform crystal orientation of such single-crystalline or epitaxial systems opens the opportunity to explore the relationship between magnetic anisotropy and the spin enhancement mechanism, based on the defined and controllable relative orientation between the applied magnetic field and the model catalyst–something that cannot be achieved with powder or ceramic electrodes (Figure 12i). Moreover, epitaxial thin films provide the ability to tune magnetic anisotropy through strain engineering and crystallographic orientation.[381] These strategies opens new avenues to disentangle the effects of magnetic-field-induced spin order, which originate from the catalyst's intrinsic magnetic anisotropy, from MHD effects, which are not governed by such material-specific properties.[72,101] Another unique advantage of epitaxial systems is the ability to engineer long-range spin order by creating and tailoring heterostructure interfaces,[382] thereby enabling precise tuning of a material's response to external magnetic fields through exchange interaction effects (Figure 12j). While a similar effect can be achieved using core–shell nanoparticles,[104] a thin-film heterostructure approach enables nanometer-scale precision in controlling the layer thickness ratio and surface layer morphology.

Lastly, model systems can be used to tune and investigate the electronic and magnetic properties of spin-polarized active sites, as well as the coupling and interactions between these sites during the catalysis (Figure 12k). The emerging class of single-atom catalysts could enable such studies, as these systems allow for the placement of distinct spin-polarized atoms with specific properties into the support. Precisely controlling the density and spacing of the active sites allows for the systematic modulation of the

strength and nature of their coupling, which could offer a unique platform for spin-enhancement research.

While offering significant opportunities for a systematic understanding of catalytic processes, model system approaches typically have important limitations. Using faceted nanoparticles or core–shell particles for example does not eliminate size distribution, leaving conductivity and exposed area inconsistency untouched. Furthermore, the magnetic properties of the powder-based systems may depend on particles size and its distribution, e.g. coercive field, saturation magnetization or local spin-polarization. While this size dependence can be exploited to systematically tune magnetic behavior, it also underscores the need for precise control over particle size distribution in order to draw reliable and reproducible conclusions.

Even single-atom catalysts–often considered to possess the most well-defined active sites among catalytic systems–can be influenced by interactions between the active sites and their supports. These interactions could potentially alter the magnetic response of the single atom to an external field and add more descriptors to the system.[383] In thin films, for example, careful consideration must be given to thickness-dependent effects, such as surface and interface magnetic dead layers that can suppress magnetization at low thicknesses, as well as pronounced magnetic anisotropy, which depends on factors such as exact thickness, strain, and oxygen content. Lastly, one of the major downsides for epitaxial films and single crystals is their typically low conductivity or their electrical contacting within the electrochemical cell, typically limiting the absolute current densities that can be applied to these thin film model catalysts. However, a number of studies exists, demonstrating how to bypass this limitation.[382]

The use of model systems enables the design of experiments that precisely isolate and investigate specific physical properties of a material. When carefully selected, such systems allow for comprehensive data collection both inside and outside the electrochemical environment, facilitating the correlation of spin-induced properties with OER enhancement. While each model system presents its own challenges, vide supra, the choice of multiple complementary model systems for comparative studies can be particularly advantageous depending on the research question and available analytical techniques. The high degree of experimental control that model systems offer enables clearer interpretation of results and opens pathways to novel experimental strategies that are often unattainable with conventional catalytic systems.

4.5. Interdisciplinary Community Approach

Advancing spin-enhanced catalysis requires a deep understanding of how various physical properties behave under reaction conditions and how these relate to electrochemical performance. The challenges, opportunities and promising future pathways in this emerging field are intrinsically interdisciplinary, involving a broad spectrum of experimental and computational techniques. This diversity is evident not only from the range of approaches discussed above but also in the comparison between magnetically enhanced and CISS-enhanced OER. Bridging these related yet distinct domains holds great promise for accelerating progress and uncovering new insights.

Therefore, future breakthroughs will depend on collaboration between research teams with complementary expertise.[14] For example, the expertise of such teams could span: i) model system synthesis, ii) operando characterization, iii) ab initio modeling, iv) microkinetic or multiscale modeling, and v) electrochemical benchmarking and impedance spectroscopy. It is evident that multimodal operando characterization is key to identify the active state of the catalyst, its magnetic and chiral properties, and the electrochemical mechanisms and OER activity and selectivity. Future simulations should incorporate both static and dynamic solid-liquid interfaces, reaction intermediates, and micromagnetic effects, such that collaboration between theoreticians working on different system complexities, time scales and length scales is essential. Machine learning and quantum computing applied to computational materials science of strongly correlated, magnetic, and chiral systems–linking their physical properties to electrochemical behavior and performance–hold tremendous promise. On a different level of abstraction, experimental and computational surface scientists can provide crucial insights for identifying key steps in the spin-dependent reaction mechanisms, which then should be assessed by electrochemists.

Beyond such interdisciplinary collaborations based on the topics suggested in this perspective, close collaboration with applied and industrial research is essential for real-world impact. Assessing material sustainability early on, even on model system level, can further accelerate the transition from fundamental research to practical applications.[384] Even at the stage of fundamental research, given the breadth of coexisting or even competing phenomena and the diversity of the observed phenomena, establishing cross-laboratory benchmarking and testing protocols will be key to improving reproducibility and advancing our understanding of spin-enhanced electrocatalysis.

5. Conclusion

Spin-enhanced OER catalysis represents a rapidly evolving yet complex field in the pursuit of sustainable energy conversion technologies. A multitude of intertwined factors influence the interpretation of both experimental and theoretical results, making it challenging to disentangle the contributions of the underlying mechanisms. As outlined in this perspective, meaningful progress in the field will require systematic, interdisciplinary, and in-depth research efforts grounded in a deeper mechanistic understanding of the key principles. To this end, we highlight four key avenues for advancing spin-enhanced OER catalysis:

1) **Improved theoretical methods with stronger links between experiment and theory**. Theoretical methods must be refined to capture the complex interplay between electronic structure, spin structures, and electrochemical environments, and to more effectively align with experimental studies. The DFT+DMFT approach provides improved treatment of spin states and orbital interactions, particularly in the description of magnetic and strongly correlated catalyst materials and their periodic 2D surfaces. However, its applicability to phenomena relevant to electrocatalysis remains to be clearly demonstrated. Important advancement in this direction has been already obtained with multiconfigurational quantum chemistry methods, which, among others, can rigorously

capture QSEI and QEXI effects. Modeling extended surfaces with these methods becomes feasible when combined with DFT in embedded frameworks such as ECW. These embedded frameworks thus provide a powerful, albeit computationally demanding, route to modeling such phenomena in heterogeneous catalytic environments. Microkinetic and multiphysics models offer valuable tools for investigating the influence of spin on the OER across different length scales via continuum modeling. Although still scarce, such efforts are crucial for simulating how fundamental spin phenomena affect electrochemical observables. In parallel, machine learning provides a powerful framework for integrating diverse theoretical approaches across scales, including the treatment of spin-spin interactions and micromagnetic effects. Both approaches can help bridging fundamental spin interactions with measurable catalytic performance, enabling more direct comparisons between theoretical predictions and experimental data. Moreover, incorporating machine learning offers a powerful route to reduce the computational burden of embedded methods and for modeling the emerging topics like polaron-mediated catalysis, help to select catalysts, and create data that is not obtainable experimentally.

These advances in multiscale modeling and machine learning are also highly relevant to the emerging field of chiral catalysis, where theoretical models are progressing despite the absence of a fully established computational framework for the CISS effect. Continued progress will require deeper interdisciplinary collaboration across chemistry, physics, and materials science. Nevertheless, integrating models describing spin-polarized currents within chiral materials adapted from studies on chiral ORR electrocatalysts may already provide valuable insight into spin-related resistance effects that could enhance OER performance.

To further bridge the gap between theory and experiment, the use of well-defined model systems, such as single crystals or epitaxially grown layers, is promising. These systems more closely resemble the periodic representations commonly used in theoretical models due to their well-defined surfaces, lower defect densities, fewer impurities, and simpler geometries. As a result, they enhance the reliability of comparisons between computational predictions and experimental observations.

2) **Improved experimental methods and progress toward operando characterization**. Experimentally distinguishing the key spin-related principles remains one of the greatest challenges in the field. In this roadmap, we have outlined the most promising methods, including electrochemical techniques, scanning probe microscopy (SPM), magnetic characterization, and chiral property measurements, that hold potential for disentangling these complex effects. The integration of operando and in situ measurements of magnetic and chiral properties is essential to capture the true spin characteristics of dynamically evolving catalyst surfaces under reaction conditions. This is a necessary step toward establishing predictive spin-activity relationships. Moreover, performing electrochemical characterization (including product analysis and intermediate detection) simultaneously with measurements of the physical properties of the catalyst can help establish direct links between spin properties and key catalytic parameters, such as electron transfer energetics, activation barriers, intermediate binding energies, and reaction selectivity.

   In parallel, the careful design of catalyst electrodes offers a promising path forward. Model systems that allow precise tuning of long-range spin order and spin polarization of the active site provide the opportunity to directly connect these properties to OER enhancements. Additionally, we highlight the use of materials whose spin states can be modulated externally, via chemical, optical, electronic, or magnetic stimuli. The use of such materials facilitates in situ or operando modulation of spin order, providing a powerful platform to correlate changes in electrochemical behavior with alterations in spin structure. This approach opens the door to more dynamic, responsive catalyst systems where spin effects can be probed and optimized in real time.

3) **Combining chiral and magnetic materials for spin-enhanced OER**. Despite differences in theoretical and experimental approaches, studies on chiral and magnetic catalysts for OER address fundamentally similar questions. Employing materials that exhibit both magnetic and chiral properties, or constructing heterostructures that combine them, may lead to higher spin-enhancement values. Furthermore, comparing these hybrid systems with purely magnetic or purely chiral counterparts could yield deeper insights into the underlying mechanisms, as chiral materials primarily influence spin-polarized electron transfer, whereas magnetic materials encompass a broader range of spin-related phenomena. Lastly, combining these approaches could enable novel experimental designs by integrating techniques from both areas, while broadening the range of available catalyst materials.

4) **Standardization, model systems, and collaboration in spin catalysis research**. Challenges in reproducing experimental results and inconsistencies in quantifying the enhancement effects across different research groups remain major obstacles to advancing our understanding of spin-related phenomena in catalysis. To address this, it is essential to establish standardized experimental procedures and agree on commonly used measurables that enable consistent comparisons and improve reproducibility. Additionally, when applying magnetic fields in electrochemical systems, careful consideration must be given to minimizing non-spin-related effects, such as those arising in the electrolyte or at the counter and reference electrodes. The use of well-defined model systems is also highly beneficial, as they facilitate more controlled studies by removing the uncertainties like exposed facets, particle shape and size, surface area, and the magnetic anisotropy orientation. Finally, fostering cross-laboratory collaborations and community-driven efforts would greatly benefit the field by enabling direct comparison of data across similar materials and setups, helping to pinpoint the sources of discrepancies and accelerate progress.

Finally, realizing the full potential of spin-polarized catalysis requires addressing practical challenges related to long-term operational stability and scalability. Future work should include developing robust, cost-effective electrode architectures that integrate chiral or magnetic elements or a combination of the two, enabling their translation from lab-scale studies to industrial water-splitting systems.

Acknowledgements

The idea for this roadmap was conceived during the Spin matters! workshop held at the Lorentz centre in the Netherlands in 2023. The authors wish to thank all participants who were involved in the Lorentz workshop and kindly acknowledge the important contributions which the Lorentz Center, and its dedicated staff, made to this roadmap. This publication is part of the project MagCats (VR, CB) with file number OCENW.M.21.104 of the research programme ENW-M which is financed by the Dutch Research Council (NWO). E.M. acknowledges the support from the University of Twente in the framework of the tenure track start-up package. P.V. acknowledges financial support from Lingenfelder's Lab. S.H. sincerely thanks Dr. Sachin Kinge of Toyota Motor Europe for his insightful discussions and technical guidance throughout the preparation of this paper. This work was funded by Toyota Motor Europe, whose financial support is gratefully acknowledged. S.H. also acknowledges funding from the Ministry of Economic Affairs through a grant under the Quantum Delta Netherlands Growth Fund program. N.A. acknowledges financial support in France by the National Agency for Research (ANR) through the PRC 20-CE06-0023-01 (SECRETS), the CNRS and the University of Angers. C.F. acknowledges financial support from the Austrian Science Fund (FWF) 10.55776/F8100 project TACO. U.I.K. and L.N. acknowledge financial support by the German research foundation (DFG) for the project CRC 1487, Iron, upgraded! (Grant No. 443703006). S.M. acknowledges support from the European Union's Horizon Europe programme under the Marie Skłodowska-Curie grant agreement n. 101206764 (SPECTRA project). R.P. acknowledges funding by the German Research Foundation within CRC TRR247 (Project No. 388390466, subproject B4). ABH acknowledges financial support from M-ERA.NET project "MuMo4PEC" (project number M-ERA.NET 4089) and COST Action 18234 "CompNanoEnergy" and COST Innovators Grant (CIG) 18234 (NanoCatML) supported by COST (European Cooperation in Science and Technology) www.cost.eu. Y.K. and R.M. acknowledge support from the European Union's Horizon 2020 research and innovation program through the SPINCAT Project (Grant No. 964972). The authors used an AI language model (ChatGPT, OpenAI) to assist in language refinement. The use included improving grammar, clarity and conciseness. No part of the manuscript was generated autonomously by the AI; all scientific content, interpretation, and conclusions were developed and validated by the authors to ensure accuracy and intellectual integrity.

Conflict of Interest

The authors declare no conflict of interest.

Author Contributions

E.M., P.V., V.R., N.A., A.B.H., and C.B. conceptualized the aim and content of the roadmap, based on contributions from all authors during the Spin Matters! conference held at the Lorentz Center, Netherlands, in 2023. E.M., P.V., V.R., S.H., and C.B. identified the key principles, gathered input from the authors, rewrote and integrated the various sections into a coherent manuscript, summarized the content in tables and figures, and drew conclusions to highlight the most promising pathways. The first draft of the results and methodology was written by SH, JF, and E.P. for the theory sections, and by E.M., P.V., V.R., D.W., M.L., Y.K., Y.L., R.M., and N.A. for the experimental sections. The initial draft outlining the key principles, open questions, and challenges was prepared by E.M., P.V., V.R., and C.B. The first draft of the perspective was contributed by E.P. (DFT + DMFT), R.P. and S.H. (DFT+U for OER), S.H. (MCSCF), E.M. (MHD), A.B.H. (multiscale modeling and EIS), J.F. (CISS theory), C.F. and S.H. (machine learning), Z.X. and A.Y. (electrochemical aspects), G.K. (Raman, IR, and UV–vis spectroscopy), M.L., M.V., and P.V. (scanning probe microscopies), S.D. (LEEM/PEEM), F.Go. and J.M. (MOKE), Q.L. (TEM), P.T. and S.M. (XAS), J.B. (EPR/FMR), U.K. and L.N. (Mössbauer spectroscopy), V.R. (VSM/SQUID), P.V., D.W., M.L., and N.A. (CISS experiments and CISS/magnetic combination), V.R. and F.Gu. (materials and model systems), and C.B. (community approach). All authors contributed to the discussions, reviewed and edited the manuscript, and approved the final version.

Keywords

chiral catalysts, CISS, experimental methodology, magnetic catalysts, polaron mediated OER, spin-enhanced OER, theoretical frameworks

Received: June 27, 2025
Revised: September 1, 2025
Published online: October 10, 2025

[1] International Energy Agency, The future of hydrogen, https://www.iea.org/reports/the-future-of-hydrogen, **2019**, Licence: CC BY 4.0. (accessed: April 2025).
[2] N. Mac Dowell, N. Sunny, N. Brandon, H. Herzog, A. Y. Ku, W. Maas, A. Ramirez, D. M. Reiner, G. N. Sant, N. Shah, *Joule* **2021**, *5*, 2524.
[3] J. Liu, H. Liu, H. Chen, X. Du, B. Zhang, Z. Hong, S. Sun, W. Wang, *Adv. Sci.* **2019**, *7*.
[4] T. Wu, Z. J. Xu, *Curr. Opin. Electrochem.* **2021**, *30*, 100804.
[5] W. Mtangi, V. Kiran, C. Fontanesi, R. Naaman, *J. Phys. Chem. Lett.* **2015**, *6*, 4916.
[6] S. Chrétien, H. Metiu, *J. Chem. Phys.* **2008**, *129*, 7.
[7] Y. Jiao, R. Sharpe, T. Lim, J. H. Niemantsverdriet, J. Gracia, *J. Am. Chem. Soc.* **2017**, *139*, 16604.
[8] C. Biz, M. Fianchini, J. Gracia, *ACS Catal.* **2021**, *11*, 14249.
[9] J. Gracia, C. Biz, M. Fianchini, *Phys. Chem. Chem. Phys.* **2024**, *26*, 22620.
[10] R. Naaman, Y. Paltiel, D. H. Waldeck, *Acc. Chem. Res.* **2020**, *53*, 2659.
[11] A. Yu, Y. Zhang, S. Zhu, T. Wu, Z. J. Xu, *Nat. Energy* **2025**, *10*, 435.
[12] F. A. Garcés-Pineda, M. Blasco-Ahicart, D. Nieto-Castro, N. López, J. R. Galán-Mascarós, *Nat. Energy* **2019**, *4*, 519.
[13] Z. Chen, X. Li, H. Ma, Y. Zhang, J. Peng, T. Ma, Z. Cheng, J. Gracia, Y. Sun, Z. J. Xu, *Natl. Sci. Rev.* **2024**, *11*, nwae314.
[14] Y. Liang, M. Lihter, M. Lingenfelder, *Isr. J. Chem.* **2022**, *62*, 11.
[15] Y. Sun, H. Lv, H. Yao, Y. Gao, C. Zhang, *Carbon Energy* **2024**, *6*, 10.
[16] S. Ma, Q. Fu, J. Han, T. Yao, X. Wang, Z. Zhang, P. Xu, B. Song, *Adv. Funct. Mater.* **2024**, *34*, 26.
[17] J. Gracia, *Phys. Chem. Chem. Phys.* **2017**, *19*, 20451.
[18] J. Gracia, R. Sharpe, J. Munarriz, *J. Catal.* **2018**, *361*, 331.
[19] J. Gracia, *J. Phys. Chem. C* **2019**, *123*, 9967.
[20] S. Lehtola, C. Steigemann, M. J. Oliveira, M. A. Marques, *SoftwareX* **2018**, *7*, 1.
[21] X. Liao, R. Lu, L. Xia, Q. Liu, H. Wang, K. Zhao, Z. Wang, Y. Zhao, *Energy Environ. Mater.* **2021**, *5*, 157.
[22] A. J. Cohen, P. Mori-Sánchez, W. Yang, *Chem. Rev.* **2011**, *112*, 289.
[23] J. Rossmeisl, A. Logadottir, J. K. Nørskov, *Chem. Phys.* **2005**, *319*, 178.
[24] J. Rossmeisl, Z.-W. Qu, H. Zhu, G.-J. Kroes, J. K. Nørskov, *J. Electroanal. Chem.* **2007**, *607*, 83.
[25] X. Zhang, C. Cao, A. Bieberle-Hütter, *J. Phys. Chem. C* **2016**, *120*, 28694.
[26] A. Füngerlings, M. Wohlgemuth, D. Antipin, E. van der Minne, E. M. Kiens, J. Villalobos, M. Risch, F. Gunkel, R. Pentcheva, C. Baeumer, *Nat. Commun.* **2023**, *14*, 8284.
[27] J. K. Nørskov, J. Rossmeisl, A. Logadottir, L. Lindqvist, J. R. Kitchin, T. Bligaard, H. Jonsson, *J. Phys. Chem. B* **2004**, *108*, 17886.
[28] S. M. Stratton, S. Zhang, M. M. Montemore, *Surf. Sci. Rep.* **2023**, *78*, 100597.
[29] J. Li, *Nano-Micro Lett.* **2022**, *14*, 112.

[30] Q. Liang, A. Bieberle-Hütter, G. Brocks, *J. Phys. Chem. C* **2022**, *126*, 1337.
[31] A. G. Hufnagel, H. Hajiyani, S. Zhang, T. Li, O. Kasian, B. Gault, B. Breitbach, T. Bein, D. Fattakhova-Rohlfing, C. Scheu, R. Pentcheva, *Adv. Funct. Mater.* **2018**, *28*, 52.
[32] H. Hajiyani, R. Pentcheva, *J. Chem. Phys.* **2020**, *152*, 12.
[33] Y. Peng, H. Hajiyani, R. Pentcheva, *ACS Catal.* **2021**, *11*, 5601.
[34] Z. Liu, H. M. Amin, Y. Peng, M. Corva, R. Pentcheva, K. Tschulik, *Adv. Funct. Mater.* **2023**, *33*, 2210945.
[35] H. Hajiyani, R. Pentcheva, *ACS Catal.* **2018**, *8*, 11773.
[36] F. Li, H. Ai, D. Liu, K. H. Lo, H. Pan, *J. Mater. Chem. A* **2021**, *9*, 17749.
[37] A. Füngerlings, A. Koul, M. Dreyer, A. Rabe, D. M. Morales, W. Schuhmann, M. Behrens, R. Pentcheva, *Chem. - Eur. J.* **2021**, *27*, 17145.
[38] M. Yu, A. Li, E. Kan, C. Zhan, *ACS Catal.* **2024**, *14*, 6816.
[39] J. Gracia, M. Fianchini, C. Biz, V. Polo, R. Gomez, *Curr. Opin. Electrochem.* **2021**, *30*, 100798.
[40] Y. Sun, S. Sun, H. Yang, S. Xi, J. Gracia, Z. J. Xu, *Adv. Mater.* **2020**, *32*, 2003297.
[41] C. Biz, M. Fianchini, J. Gracia, *ACS Appl. Nano Mater.* **2020**, *3*, 506.
[42] C. Franchini, M. Reticcioli, M. Setvin, U. Diebold, *Nat. Rev. Mater.* **2021**, *6*, 560.
[43] P. Gono, J. Wiktor, F. Ambrosio, A. Pasquarello, *ACS Catal.* **2018**, *8*, 5847.
[44] H. Pada Sarker, F. Abild-Pedersen, M. Bajdich, *ChemPhysChem* **2024**, *25*, 11.
[45] R. Sharpe, J. Munarriz, T. Lim, Y. Jiao, J. Niemantsverdriet, V. Polo, J. Gracia, *Top. Catal.* **2018**, *61*, 267.
[46] R. Sharpe, T. Lim, Y. Jiao, J. Niemantsverdriet, J. Gracia, *ChemCatChem* **2016**, *8*, 3762.
[47] F. Evers, A. Aharony, N. Bar-Gill, O. Entin-Wohlman, P. Hedegård, O. Hod, P. Jelinek, G. Kamieniarz, M. Lemeshko, K. Michaeli, V. Mujica, R. Naaman, Y. Paltiel, S. Refaely-Abramson, O. Tal, J. Thijssen, M. Thoss, J. M. van Ruitenbeek, L. Venkataraman, D. Waldeck, B. Yan, L. Kronik, *Adv. Mater.* **2022**, *34*, 2106629.
[48] S. Yeganeh, M. A. Ratner, E. Medina, V. Mujica, *J. Chem. Phys.* **2009**, *131*.
[49] E. Medina, F. López, M. A. Ratner, V. Mujica, *Europhys. Lett.* **2012**, *99*, 17006.
[50] J. Gersten, K. Kaasbjerg, A. Nitzan, *J. Chem. Phys.* **2013**, *139*, 11.
[51] K. Michaeli, R. Naaman, *J. Phys. Chem. C* **2019**, *123*, 17043.
[52] M. Geyer, R. Gutierrez, V. Mujica, G. Cuniberti, *J. Phys. Chem. C* **2019**, *123*, 27230.
[53] A.-M. Guo, Q.-f. Sun, *Phys. Rev. Lett.* **2012**, *108*, 218102.
[54] Y. Utsumi, O. Entin-Wohlman, A. Aharony, *Phys. Rev. B* **2020**, *102*, 035445.
[55] J. Fransson, *Isr. J. Chem.* **2022**, *62*, 202200046.
[56] J. Fransson, *J. Phys. Chem. Lett.* **2019**, *10*, 7126.
[57] K. H. Huisman, J.-B. M.-Y. Heinisch, J. M. Thijssen, *J. Phys. Chem. C* **2023**, *127*, 6900.
[58] A. Chiesa, E. Garlatti, M. Mezzadri, L. Celada, R. Sessoli, M. R. Wasielewski, R. Bittl, P. Santini, S. Carretta, *Nano Lett.* **2024**, *24*, 12133.
[59] G.-F. Du, H.-H. Fu, R. Wu, *Phys. Rev. B* **2020**, *102*, 035431.
[60] L. Zhang, Y. Hao, W. Qin, S. Xie, F. Qu, *Phys. Rev. B* **2020**, *102*, 214303.
[61] J. Fransson, *Phys. Rev. B* **2020**, *102*, 235416.
[62] J. Fransson, R. Naaman, *J. Phys. Chem. Lett.* **2025**, *16*, 1629.
[63] Y. Sang, F. Tassinari, K. Santra, W. Zhang, C. Fontanesi, B. P. Bloom, D. H. Waldeck, J. Fransson, R. Naaman, *Proc. Natl. Acad. Sci. USA* **2022**, *119*, e2202650119.
[64] S. Naskar, V. Mujica, C. Herrmann, *J. Phys. Chem. Lett.* **2023**, *14*, 694.
[65] J. Fransson, L. Turin, *J. Phys. Chem. Lett.* **2024**, *15*, 6370.
[66] J. Fransson, *J. Phys. Chem. Lett.* **2025**, *16*, 4346.
[67] P. Vensaus, Y. Liang, J.-P. Ansermet, J. Fransson, M. Lingenfelder, *ChemRxiv* **2025**.
[68] J. Ge, X. Ren, R. R. Chen, Y. Sun, T. Wu, S. J. H. Ong, Z. J. Xu, *Angew. Chem., Int. Ed.* **2023**, *62*, 26.
[69] P. Guo, Y. Zhang, F. Han, Y. Du, B. Song, W. Wang, X. Wang, Y. Zhou, P. Xu, *J. Phys. Chem. Lett.* **2022**, *13*, 7476.
[70] C.-Y. Huang, H.-A. Chen, W.-X. Lin, K.-H. Chen, Y.-C. Lin, T.-S. Wu, C.-C. Chang, C.-W. Pao, W.-T. Chuang, J.-C. Jan, Y.-C. Shao, N. Hiraoka, J.-W. Chiou, P.-C. Kuo, J. Shiue, D. Vishnu S. K, R. Sankar, Z.-W. Cyue, W.-F. Pong, C.-W. Chen, *J. Am. Chem. Soc.* **2025**, *147*, 13286.
[71] Y. Wang, P. Meng, Z. Yang, M. Jiang, J. Yang, H. Li, J. Zhang, B. Sun, C. Fu, *Angew. Chem., Int. Ed.* **2023**, *62*, 28.
[72] E. van der Minne, L. Korol, L. M. A. Krakers, M. Verhage, C. M. M. Rosário, T. J. Roskamp, R. J. Spiteri, C. Biz, M. Fianchini, B. A. Boukamp, G. Rijnders, K. Flipse, J. Gracia, G. Mul, H. Hilgenkamp, R. J. Green, G. Koster, C. Baeumer, *Appl. Phys. Rev.* **2024**,*11*, 011420.
[73] A. Vadakkayil, C. Clever, K. N. Kunzler, S. Tan, B. P. Bloom, D. H. Waldeck, *Nat. Commun.* **2023**, *14*, 1067.
[74] Y. Liang, K. Banjac, K. Martin, N. Zigon, S. Lee, N. Vanthuyne, F. A. Garcés-Pineda, J. R. Galán-Mascarós, X. Hu, N. Avarvari, M. Lingenfelder, *Nat. Commun.* **2022**, *13*, 3356.
[75] P. Vensaus, Y. Liang, J.-P. Ansermet, G. J. A. A. Soler-Illia, M. Lingenfelder, *Nat. Commun.* **2024**, *15*, 2867.
[76] *Impedance Spectroscopy: Theory, Experiment, and Applications*, (Eds: E. Barsoukov, J. R. Macdonald), John Wiley & Sons, Inc., Hoboken, NJ **2005**.
[77] A. C. Lazanas, M. I. Prodromidis, *ACS Measure. Sci. Au* **2023**, *3*, 162.
[78] H. Xu, J. Qi, Y. Zhang, H. Liu, L. Hu, M. Feng, W. Lü, *ACS Appl. Mater. Interfaces* **2023**, *15*, 32320.
[79] C. A. Mesa, F. A. Garcés-Pineda, M. García-Tecedor, J. Yu, B. Khezri, S. Plana-Ruiz, B. López, R. Iturbe, N. López, S. Gimenez, J. R. Galan-Mascaros, *APL Energy* **2024**, *2*, 016106.
[80] Z. Xiong, C. Hu, X. Luo, W. Zhou, Z. Jiang, Y. Yang, T. Yu, W. Lei, C. Yuan, *Nano Lett.* **2021**, *21*, 10486.
[81] C. Zhong, W. Zhou, X. Luo, T. Li, F. Huang, J. Hu, Z. Jiang, C. Hu, W. Lei, C. Yuan, *Nano Lett.* **2025**, *25*, 1550.
[82] Y. Jin, J. Liu, W. Zhou, C. Hu, Z. Jiang, H. Zhou, C. Zou, Y. Yang, T. Yu, X. Luo, W. Lei, C. Yuan, *Appl. Phys. Lett.* **2025**, *126*, 5.
[83] N. Karki, F. L. Mufoyongo, A. J. Wilson, *Inorg. Chem. Front.* **2024**, *11*, 5414.
[84] W. Zhao, J. Yang, F. Xu, B. Weng, *Small* **2024**, *20*, 34.
[85] F. Xie, Y. Du, M. Lu, S. Yan, Z. Zou, *Energy Environ. Sci.* **2025**, *18*, 1972.
[86] S. Ghosh, B. P. Bloom, Y. Lu, D. Lamont, D. H. Waldeck, *J. Phys. Chem. C* **2020**, *124*, 22610.
[87] B. Adelizzi, A. T. Rösch, D. J. van Rijen, R. S. Martire, S. Esiner, M. Lutz, A. R. A. Palmans, E. W. Meijer, *Helv. Chim. Acta* **2019**, *102*, 5.
[88] P. Vensaus, Y. Liang, N. Zigon, N. Avarvari, V. Mujica, G. J. A. A. Soler-Illia, M. Lingenfelder, *J. Chem. Phys.* **2024**, *160*, 11.
[89] O. van der Heijden, S. Park, R. E. Vos, J. J. J. Eggebeen, M. T. M. Koper, *ACS Energy Lett.* **2024**, *9*, 1871.
[90] J. Chen, J. Ying, Y. Tian, Y. Xiao, X. Yang, *Adv. Funct. Mater.* **2024**, *35*, 8.
[91] Q. Huang, H. Sheng, *Chem. - Eur. J.* **2024**, *30*, 28.
[92] Z. Feng, C. Dai, H. Wang, R. Guo, J. You, X. Liu, *ChemCatChem* **2023**, *15*, 18.
[93] X. Ren, T. Wu, Z. Gong, L. Pan, J. Meng, H. Yang, F. B. Dagbjartsdottir, A. Fisher, H.-J. Gao, Z. J. Xu, *Nat. Commun.* **2023**, *14*, 2482.
[94] Y. Li, Y. Wang, A. F. May, M. Fianchini, C. Biz, S. Oh, Y. Zhu, H. Y. Jeong, J. Yang, J. Gracia, M. Chhowalla, *Mater. Sci. Eng. R.* **2024**, *161*, 100856.

[95] L. Li, J. Zhou, X. Wang, J. Gracia, M. Valvidares, J. Ke, M. Fang, C. Shen, J. Chen, Y. Chang, C. Pao, S. Hsu, J. Lee, A. Ruotolo, Y. Chin, Z. Hu, X. Huang, Q. Shao, *Adv. Mater.* **2023**, *35*, 35.
[96] Y. Cao, L. Gao, Z. Lai, C. Wang, Y. Yao, X. Zhu, Z. Zou, *Appl. Phys. Lett.* **2021**, *119*, 16.
[97] J. Zhang, Y. Zhao, W. Zhao, J. Wang, Y. Hu, C. Huang, X. Zou, Y. Liu, D. Zhang, X. Lu, H. Fan, Y. Hou, *Angew. Chem., Int. Ed.* **2023**, *62*, 52.
[98] X. Lyu, Y. Zhang, Z. Du, H. Chen, S. Li, A. I. Rykov, C. Cheng, W. Zhang, L. Chang, W. Kai, J. Wang, L. Zhang, Q. Wang, C. Huang, E. Kan, *Small* **2022**, *18*, 42.
[99] Y. Zhang, P. Guo, S. Li, J. Sun, W. Wang, B. Song, X. Yang, X. Wang, Z. Jiang, G. Wu, P. Xu, *J. Mater. Chem. A* **2022**, *10*, 1760.
[100] J. Qian, H. Zhang, G. Li, L. Jia, X. Peng, C. Zhong, F. Li, D. Chao, D. Gao, *Adv. Funct. Mater.* **2023**, *34*, 5.
[101] A. Radford, D. Szalay, Q. Chen, M. Ying, M. Luo, X. Pan, M. Stamatakis, Y. Li, C. Wu, S. C. E. Tsang, *Small* **2025**, 2412852.
[102] T. Sun, Z. Tang, W. Zang, Z. Li, J. Li, Z. Li, L. Cao, J. S. Dominic Rodriguez, C. O. M. Mariano, H. Xu, P. Lyu, X. Hai, H. Lin, X. Sheng, J. Shi, Y. Zheng, Y.-R. Lu, Q. He, J. Chen, K. S. Novoselov, C.-H. Chuang, S. Xi, X. Luo, J. Lu, *Nat. Nanotechnol.* **2023**, *18*, 763.
[103] X. Ren, T. Wu, Y. Sun, Y. Li, G. Xian, X. Liu, C. Shen, J. Gracia, H.-J. Gao, H. Yang, Z. J. Xu, *Nat. Commun.* **2021**, *12*, 2506.
[104] J. Ge, R. R. Chen, X. Ren, J. Liu, S. J. H. Ong, Z. J. Xu, *Adv. Mater.* **2021**, *33*, 42.
[105] H. Li, Q. Quan, H. Dong, Y. Zhang, P. Xie, D. Chen, D. Yin, C. Wong, J. C. Ho, *Adv. Funct. Mater.* **2025**, *35*, 2420810.
[106] K. L. Knoche Gupta, H. C. Lee, J. Leddy, *ACS Phys. Chem. Au* **2024**, *4*, 148.
[107] T. Wu, X. Ren, Y. Sun, S. Sun, G. Xian, G. G. Scherer, A. C. Fisher, D. Mandler, J. W. Ager, A. Grimaud, J. Wang, C. Shen, H. Yang, J. Gracia, H.-J. Gao, Z. J. Xu, *Nat. Commun.* **2021**, *12*, 3634.
[108] T. Wu, J. Ge, Q. Wu, X. Ren, F. Meng, J. Wang, S. Xi, X. Wang, K. Elouarzaki, A. Fisher, Z. J. Xu, *Proc. Natl. Acad. Sci. USA* **2024**, *121*, 19.
[109] Z. Zhang, P. Ma, L. Luo, X. Ding, S. Zhou, J. Zeng, *Angew. Chem., Int. Ed.* **2023**, *62*, 15.
[110] P. Huang, M. Meng, G. Zhou, P. Wang, W. Wei, H. Li, R. Huang, F. Liu, L. Liu, *Proc. Natl. Acad. Sci. USA* **2023**, *120*, 21.
[111] Y.-N. Zhou, F.-G. Wang, Y.-N. Zhen, J. Nan, B. Dong, Y.-M. Chai, *Sci. China Mater.* **2022**, *65*, 2665.
[112] Y. Tong, Y. Guo, P. Chen, H. Liu, M. Zhang, L. Zhang, W. Yan, W. Chu, C. Wu, Y. Xie, *Chem* **2017**, *3*, 812.
[113] S. Zhou, X. Miao, X. Zhao, C. Ma, Y. Qiu, Z. Hu, J. Zhao, L. Shi, J. Zeng, *Nat. Commun.* **2016**, *7*, 11510.
[114] Y. Sun, X. Ren, S. Sun, Z. Liu, S. Xi, Z. J. Xu, *Angew. Chem., Int. Ed.* **2021**, *60*, 14536.
[115] L. Lin, R. Xin, M. Yuan, T. Wang, J. Li, Y. Xu, X. Xu, M. Li, Y. Du, J. Wang, S. Wang, F. Jiang, W. Wu, C. Lu, B. Huang, Z. Sun, J. Liu, J. He, G. Sun, *ACS Catal.* **2023**, *13*, 1431.
[116] Y. Ma, T. Wang, X. Sun, Y. Yao, H. Chen, G. Wu, C. Zhang, Y. Qin, *ACS Appl. Mater. Interfaces* **2023**, *15*, 7978.
[117] G. Song, M. Wei, J. Zhou, L. Mu, S. Song, *ACS Catal.* **2024**, *14*, 846.
[118] R. R. Chen, Y. Sun, S. J. H. Ong, S. Xi, Y. Du, C. Liu, O. Lev, Z. J. Xu, *Adv. Mater.* **2020**, *32*, 10.
[119] X. Guan, M. Wang, Z. Chen, C. Cao, Z. Li, R. Xue, Y. Fu, B. Johannessen, A. Tadich, J. Yi, H. Fan, N. Wang, B. Jia, X. Li, T. Ma, *Angew. Chem., Int. Ed.* **2024**, *64*, 3.
[120] X. Xu, J. Guan, *Chem. Sci.* **2024**, *15*, 14585.
[121] C. Hao, Y. Wu, X. Zheng, Y. Du, Y. Fan, W. Pang, A. Tadich, S. Zhang, T. Frauenheim, T. Ma, X. Li, Z. Cheng, *Adv. Sci.* **2024**, *12*, 3.
[122] R. Naaman, Y. Paltiel, D. H. Waldeck, *Nat. Rev. Chem.* **2019**, *3*, 250.
[123] L. Pan, M. Ai, C. Huang, L. Yin, X. Liu, R. Zhang, S. Wang, Z. Jiang, X. Zhang, J.-J. Zou, W. Mi, *Nat. Commun.* **2020**, *11*, 1.
[124] H. Gajapathy, S. Bandaranayake, E. Hruska, A. Vadakkayil, B. P. Bloom, S. Londo, J. McClellan, J. Guo, D. Russell, F. M. F. de Groot, F. Yang, D. H. Waldeck, M. Schultze, L. R. Baker, *Chem. Sci.* **2024**, *15*, 3300.
[125] B. Fang, Z. Xing, W. Kong, Z. Li, W. Zhou, *Nano Energy* **2022**, *101*, 107616.
[126] A. Vadakkayil, W. A. Dunlap-Shohl, M. Joy, B. P. Bloom, D. H. Waldeck, *ACS Catal.* **2024**, *14*, 17303.
[127] F. Tassinari, K. Banerjee-Ghosh, F. Parenti, V. Kiran, A. Mucci, R. Naaman, *J. Phys. Chem. C* **2017**, *121*, 15777.
[128] Y. S. Park, J. Lee, H. Lee, J. B. Park, J. Yun, C. U. Lee, S. Moon, S. Lee, S. Kim, J. H. Kim, D. Kim, J. Han, D.-W. Kim, J. Moon, *ACS Appl. Mater. Interfaces* **2025**, *17*, 18228.
[129] Z. Wang, J. Wan, X. Sun, L. Sun, S. Chen, Q. Zhang, *J. Am. Chem. Soc.* **2025**, *147*, 15767.
[130] H. Al-Bustami, S. Khaldi, O. Shoseyov, S. Yochelis, K. Killi, I. Berg, E. Gross, Y. Paltiel, R. Yerushalmi, *Nano Lett.* **2022**, *22*, 5022.
[131] M. Joy, B. Bloom, K. Govindaraj, J. A. Albro, A. Vadakkayil, D. Waldeck, *J. Mater. Chem. A* **2025**.
[132] B. P. Bloom, Y. Paltiel, R. Naaman, D. H. Waldeck, *Chem. Rev.* **2024**, *124*, 1950.
[133] F. A. Garcés-Pineda, J. Yu, C. A. Mesa, S. Plana-Ruiz, D. Ruano, Y. Liang, M. Lingenfelder, S. Giménez, J. Galán-Mascarós, *Chem. Sci.* **2025**, *16*, 5475.
[134] M. Gazzotti, A. Stefani, M. Bonechi, W. Giurlani, M. Innocenti, C. Fontanesi, *Molecules* **2020**, *25*, 3988.
[135] W. Zhang, C. Jiang, H. Guan, Y. Wang, Y. Hu, W. Wang, W. Tian, L. Hao, *Mater. Adv.* **2024**, *5*, 1340.
[136] W. Zhang, K. Banerjee-Ghosh, F. Tassinari, R. Naaman, *ACS Energy Lett.* **2018**, *3*, 2308.
[137] A. N. Nair, S. Fernandez, M. Marcos-Hernández, D. R. Romo, S. R. Singamaneni, D. Villagran, S. T. Sreenivasan, *Nano Lett.* **2023**, *23*, 9042.
[138] Z. Sun, L. Lin, J. He, D. Ding, T. Wang, J. Li, M. Li, Y. Liu, Y. Li, M. Yuan, B. Huang, H. Li, G. Sun, *J. Am. Chem. Soc.* **2022**, *144*, 8204.
[139] H. Dong, L. Luo, S. Zhou, L. Chen, X. Wu, Y. Yang, Z. Liao, L. Fu, M. Chen, Y. Zhu, P. Su, H. Jiang, Z. Sun, L. Lin, Q. Hua, *Adv. Sci.* **2025**, *12*, 10.
[140] W. H. Lee, M. H. Han, Y.-J. Ko, B. K. Min, K. H. Chae, H.-S. Oh, *Nat. Commun.* **2022**, *13*, 605.
[141] L. M. Monzon, J. Coey, *Electrochem. Commun.* **2014**, *42*, 38.
[142] K. Mitra, A. Adalder, S. Mandal, U. K. Ghorai, *Small Methods* **2024**, *8*, 7.
[143] M. S. Kodaimati, R. Gao, S. E. Root, G. M. Whitesides, *Chem. Catal.* **2022**, *2*, 797.
[144] S. Luo, K. Elouarzaki, Z. J. Xu, *Angew. Chem.* **2022**, *134*, 27.
[145] S.-Y. Lin, J. Fu, *Renewables* **2024**, *2*, 264.
[146] Á. Romero-Calvo, Ö. Akay, H. Schaub, K. Brinkert, *npj Microgravity* **2022**, *8*, 32.
[147] K. Wang, C. Liao, W. Wang, Y. Xiao, X. Liu, Y. Zuo, *ACS Appl. Energy Mater.* **2020**, *3*, 6752.
[148] H. Matsushima, T. Iida, Y. Fukunaka, *Electrochim. Acta* **2013**, *100*, 261.
[149] H.-b. Zheng, Y.-l. Wang, P. Zhang, F. Ma, P.-z. Gao, W.-m. Guo, H. Qin, X.-p. Liu, H.-n. Xiao, *Chem. Eng. J.* **2021**, *426*, 130785.
[150] C. Wei, Z. J. Xu, *Chinese J. Catal.* **2022**, *43*, 148.
[151] D. Sen, K. Isaac, N. Leventis, I. Fritsch, *Int. J. Heat Mass Transfer* **2011**, *54*, 5368.
[152] K. M. Isaac, C. Gonzales, D. Sen, *Microfluidics Nanofluidics* **2014**, *17*, 943.
[153] R. Rousseau, V.-A. Glezakou, A. Selloni, *Nat. Rev. Mater.* **2020**, *5*, 460.
[154] Y. Li, Y. Wang, A. F. May, M. Fianchini, C. Biz, S. Oh, Y. Zhu, H. Y. Jeong, J. Yang, J. Gracia, et al., *Mater. Sci. Eng. R.* **2024**, *161*, 100856.

[155] L. Si, P. Liu, C. Franchini, *Phys. Rev. Mater.* **2025**, *9*, 015001.
[156] L. Zhao, M. von Hopffgarten, D. M. Andrada, G. Frenking, *Wiley Interdiscip. Rev.: Comput. Mol. Sci.* **2018**, *8*, e1345.
[157] L. Li, Y. Wang, R. R. Nazmutdinov, R. R. Zairov, Q. Shao, J. Lu, *Nano Lett.* **2024**, *24*, 6148.
[158] Z. Ergönenc, B. Kim, P. Liu, G. Kresse, C. Franchini, *Phys. Rev. Mater.* **2018**, *2*, 2.
[159] V. Begum, M. E. Gruner, R. Pentcheva, *Phys. Rev. Mater.* **2019**, *3*, 6.
[160] S. Rafiezadeh, V. Begum-Hudde, R. Pentcheva, *Phys. Rev. B* **2024**, *109*, 19.
[161] E. Pavarini, *La Rivista del Nuovo Cimento* **2021**, *44*, 597.
[162] B. Geisler, R. Pentcheva, *Phys. Rev. B* **2020**, *101*, 16.
[163] G. Zhang, E. Gorelov, E. Koch, E. Pavarini, *Phys. Rev. B* **2012**, *86*, 18.
[164] X. Wen, J.-N. Boyn, J. M. P. Martirez, Q. Zhao, E. A. Carter, *J. Chem. Theory Comput.* **2024**, *20*, 6037.
[165] F. Libisch, C. Huang, E. A. Carter, *Acc. Chem. Res.* **2014**, *47*, 2768.
[166] F. Fasulo, A. Mitra, A. B. Muñoz-García, M. Pavone, L. Gagliardi, *J. Phys. Chem. C* **2024**, *128*, 7343.
[167] J. G. Vitillo, C. J. Cramer, L. Gagliardi, *Isr. J. Chem.* **2022**, *62*, 202100136.
[168] Q. Zhao, J. M. P. Martirez, E. A. Carter, *J. Phys. Chem. Lett.* **2022**, *13*, 10282.
[169] S. Hariharan, S. Kinge, L. Visscher, *J. Chem. Inf. Model.* **2024**.
[170] M. Gouy, *J. Phys. Théor. Appl.* **1910**, *9*, 457.
[171] O. Stern, *Zeitschrift für Elektrochem. Angew. Physikalische Chemie* **1924**, *30*, 508.
[172] D. L. Chapman, *The London, Edinburgh, and Dublin Philosophical Magazine J. Sci.* **1913**, *25*, 475.
[173] H. Helmholtz, *Ann. Phys.* **1879**, *243*, 337.
[174] T. A. Butcher, J. M. D. Coey, *J. Phys.: Condens. Matter* **2022**, *35*, 053002.
[175] M. Zec Dr.-Ing., Ph.D. thesis, Technical university of Ilmenau, **2013**.
[176] J. Fidler, T. Schrefl, *J. Phys. D: Appl. Phys.* **2000**, *33*, R135.
[177] H. A. Kamal, M. Y. Salloom, in *International Conference on Robotics, Automation and Intelligent Systems (ICRAINS 21)*, vol. *2670*, AIP Publishing, New York **2022**, 060021.
[178] Z. Szczepanik, Z. Rucki, Z. Moron, *IEEE Trans. Instrum. Meas.* **2003**, *52*, 1648.
[179] H.-b. Liu, H. Xu, L.-m. Pan, D.-h. Zhong, Y. Liu, *Int. J. Hydrogen Energy* **2019**, *44*, 22780.
[180] X. Zhang, A. Bieberle-Hütter, *ChemSusChem* **2016**, *9*, 1223.
[181] B. Samanta, Á. Morales-García, F. Illas, N. Goga, J. A. Anta, S. Calero, A. Bieberle-Hütter, F. Libisch, A. B. Muñoz-García, M. Pavone, M. Toroker, *Chem. Soc. Rev.* **2022**, *51*, 3794.
[182] T. A. Pham, Y. Ping, G. Galli, *Nat. Mater.* **2017**, *16*, 401.
[183] Y. Ping, R. Sundararaman, W. A. Goddard III, *Phys. Chem. Chem. Phys.* **2015**, *17*, 30499.
[184] J. A. Gauthier, S. Ringe, C. F. Dickens, A. J. Garza, A. T. Bell, M. Head-Gordon, J. K. Nørskov, K. Chan, *ACS Catal.* **2018**, *9*, 920.
[185] H. A. Hansen, V. Viswanathan, J. K. Nørskov, *J. Phys. Chem. C* **2014**, *118*, 6706.
[186] K. George, M. Van Berkel, X. Zhang, R. Sinha, A. Bieberle-Hütter, *J. Phys. Chem. C* **2019**, *123*, 9981.
[187] K. George, T. Khachatrjan, M. van Berkel, V. Sinha, A. Bieberle-Hutter, *ACS Catal.* **2020**, *10*, 14649.
[188] C. F. Dickens, C. Kirk, J. K. Nørskov, *J. Phys. Chem. C* **2019**, *123*, 18960.
[189] A. G. Rajan, E. A. Carter, *Energy Environ. Sci.* **2020**, *13*, 4962.
[190] S. Haussener, C. Xiang, J. M. Spurgeon, S. Ardo, N. S. Lewis, A. Z. Weber, *Energy Environ. Sci.* **2012**, *5*, 9922.
[191] M. R. Singh, S. Haussener, A. Z. Weber, *Continuum-Scale Modeling of Solar Water-Splitting Devices*, The Royal Society of Chemistry, London, UK **2018**.
[192] F. E. Bedoya-Lora, I. Holmes-Gentle, S. Haussener, *Electrochim. Acta* **2023**, *462*, 142703.
[193] P. Cendula, S. D. Tilley, S. Gimenez, J. Bisquert, M. Schmid, M. Grätzel, J. O. Schumacher, *J. Phys. Chem. C* **2014**, *118*, 29599.
[194] A. Mitterdorfer, *Solid State Ionics* **1999**, *117*, 203.
[195] A. Mitterdorfer, *Solid State Ionics* **1999**, *117*, 187.
[196] A. Bieberle, *Solid State Ionics* **2002**, *146*, 23.
[197] K. George, M. van Berkel, X. Zhang, R. Sinha, A. Bieberle-Hütter, *J. Phys. Chem. C* **2019**, *123*, 9981.
[198] B., F. H. van den Boorn, F. Vandeputte, M. van Berkel, C. Mempin, D. Sarkar, J. Lataire, G. Vandersteen, A. Bieberle-Hütter, ChemRxiv preprint ChemRxiv: 10.26434/chemrxiv-2025-6g2l2, **2025**.
[199] J. S. Yoo, X. Rong, Y. Liu, A. M. Kolpak, *ACS Catal.* **2018**, *8*, 4628.
[200] S.-J. Shin, D. H. Kim, G. Bae, S. Ringe, H. Choi, H.-K. Lim, C. H. Choi, H. Kim, *Nat. Commun.* **2022**, *13*, 174.
[201] B. F. H. van den Boorn, M. van Berkel, A. Bieberle-Hütter, *Adv. Theory Simul.* **2022**, *6*, 10.
[202] J. Liu, W. Luo, L. Wang, J. Zhang, X.-Z. Fu, J.-L. Luo, *Adv. Funct. Mater.* **2022**, *32*, 2110748.
[203] R. Ding, J. Chen, Y. Chen, J. Liu, Y. Bando, X. Wang, *Chem. Soc. Rev.* **2024**.
[204] T. Wang, Q. Wu, Y. Han, Z. Guo, J. Chen, C. Liu, *Appl. Phys. Rev.* **2025**, *12*, 011316.
[205] Á. B. Höskuldsson, *Curr. Opin. Electrochem.* **2025**, *50*, 101649.
[206] W. Park, J. Noh, G. H. Gu, G. Nam, S. M. Jung, Y. T. Kim, Y. Jung, *Innov. Mater.* **2024**, *2*, 100072.
[207] H. Chun, J. R. Lunger, J. K. Kang, R. Gómez-Bombarelli, B. Han, *npj Comput. Mater.* **2024**, *10*, 246.
[208] D. Wang, S. Wei, A. Yuan, F. Tian, K. Cao, Q. Zhao, Y. Zhang, C. Zhou, X. Song, D. Xue, S. Yang, *Adv. Sci.* **2020**, *7*, 2000566.
[209] C. M. Acosta, E. Ogoshi, J. A. Souza, G. M. Dalpian, *ACS Appl. Mater. Interfaces* **2022**, *14*, 9418.
[210] H. A. Merker, H. Heiberger, L. Nguyen, T. Liu, Z. Chen, N. Andrejevic, N. C. Drucker, R. Okabe, S. E. Kim, Y. Wang, T. Smidt, M. Li, *Iscience* **2022**, *25*, 10.
[211] M. Eckhoff, K. N. Lausch, P. E. Blöchl, J. Behler, *J. Chem. Phys.* **2020**, *153*, 16.
[212] M. Eckhoff, J. Behler, *npj Comput. Mater.* **2021**, *7*, 170.
[213] N. Gerrits, E. W. Smeets, S. Vuckovic, A. D. Powell, K. Doblhoff-Dier, G.-J. Kroes, *J. Phys. Chem. Lett.* **2020**, *11*, 10552.
[214] V. C. Birschitzky, F. Ellinger, U. Diebold, M. Reticcioli, C. Franchini, *npj Comput. Mater.* **2022**, *8*, 125.
[215] V. C. Birschitzky, I. Sokolović, M. Prezzi, K. Palotás, M. Setvín, U. Diebold, M. Reticcioli, C. Franchini, *npj Comput. Mater.* **2024**, *10*, 89.
[216] V. C. Birschitzky, L. Leoni, M. Reticcioli, C. Franchini, *Phys. Rev. Lett.* **2025**, *134*, 216301.
[217] S. S. Dahia, C. Szabo, in *Proceedings of the 38th ACM SIGSIM Conference on Principles of Advanced Discrete Simulation*, SIGSIM-PADS'24. ACM, New York **2024**, pp. 81–87.
[218] C. K. Joshi, X. Fu, Y.-L. Liao, V. Gharakhanyan, B. K. Miller, A. Sriram, Z. W. Ulissi, *arXiv preprint arXiv:2503.03965* **2025**.
[219] Machine Learning of Defects in Crystals — nature.com, https://www.nature.com/collections/ddgajgbfic (accessed: April 2025).
[220] A. Hellman, *Curr. Opin. Electrochem.* **2024**, *49*, 101629.
[221] Y. Wu, J. E. Subotnik, *Nat. Commun.* **2021**, *12*, 700.
[222] Z. Tao, T. Qiu, J. E. Subotnik, *J. Phys. Chem. Lett.* **2023**, *14*, 770.
[223] J. Chen, J. Subotnik, *J. Phys. Chem. Lett.* **2023**, *14*, 5665.
[224] H.-H. Teh, W. Dou, J. E. Subotnik, *Phys. Rev. B* **2021**, *104*, 20.
[225] A. Gupta, Y. Sang, C. Fontanesi, L. Turin, R. Naaman, *J. Phys. Chem. Lett.* **2023**, *14*, 1756.
[226] A. Gupta, A. Kumar, D. K. Bhowmick, C. Fontanesi, Y. Paltiel, J. Fransson, R. Naaman, *J. Phys. Chem. Lett.* **2023**, *14*, 9377.
[227] C. Wei, R. R. Rao, J. Peng, B. Huang, I. E. L. Stephens, M. Risch, Z. J. Xu, Y. Shao-Horn, *Adv. Mater.* **2019**, *31*, 31.
[228] Y. Xia, W. Chen, P. Vensaus, Y. Liang, M. Lingenfelder, W. Ju, *ChemRxiv* **2024**.

[229] H. Schichlein, A. Müller, M. Voigts, A. Krügel, E. Ivers-Tiffée, *J. Appl. Electrochem.* **2002**, *32*, 875.
[230] B. A. Boukamp, *J. Phys.: Energy* **2020**, *2*, 042001.
[231] S. Park, L. Liu, u. Demirkır, O. van der Heijden, D. Lohse, D. Krug, M. T. M. Koper, *Nat. Chem.* **2023**, *15*, 1532.
[232] A. Prajapati, C. Hahn, I. M. Weidinger, Y. Shi, Y. Lee, A. N. Alexandrova, D. Thompson, S. R. Bare, S. Chen, S. Yan, et al., *Nat. Commun.* **2025**, *16*, 2593.
[233] P. Zhao, H. Sun, F. Gao, L. Yu, K. Shang, M. Fang, B. Ma, X. Tan, S. Wang, X. Wang, *Adv. Funct. Mater.* **2024**, *35*, 4.
[234] S. Scaramuzza, S. Polizzi, V. Amendola, *Nanoscale Adv.* **2019**, *1*, 2681.
[235] Y. AlSalka, S. Schwabe, J. Geweke, G. Ctistis, H. Wackerbarth, *Energy Technol.* **2023**, *11*, 3.
[236] A. Bieberle-Hütter, A. Bronneberg, K. George, M. Van De Sanden, *J. Phys. D: Appl. Phys.* **2021**, *54*, 133001.
[237] G. Katsoukis, H. Heida, M. Gutgesell, G. Mul, *ACS Catal.* **2024**, *14*, 13867.
[238] L. Francàs, S. Corby, S. Selim, D. Lee, C. A. Mesa, R. Godin, E. Pastor, I. E. Stephens, K.-S. Choi, J. R. Durrant, *Nat. Commun.* **2019**, *10*, 5208.
[239] C. A. Mesa, E. Pastor, L. Francàs, *Curr. Opin. Electrochem.* **2022**, *35*, 101098.
[240] K. J. Lee, N. Elgrishi, B. Kandemir, J. L. Dempsey, *Nat. Rev. Chem.* **2017**, *1*, 0039.
[241] S. Czioska, K. Ehelebe, J. Geppert, D. Escalera-López, A. Boubnov, E. Saraçi, B. Mayerhöfer, U. Krewer, S. Cherevko, J. Grunwaldt, *ChemElectroChem* **2022**, *9*, 19.
[242] W. Zhang, M. Liu, X. Gu, Y. Shi, Z. Deng, N. Cai, *Chem. Rev.* **2023**, *123*, 7119.
[243] H. N. Dhandapani, M. Ramasubramanian, P. Laxminarayanan, S. Singha Roy, A. De, B. R. Babu, S. Kundu, *J. Mater. Chem. A* **2025**, *13*, 3506.
[244] S. D. Ebbesen, S. H. Jensen, A. Hauch, M. B. Mogensen, *Chem. Rev.* **2014**, *114*, 10697.
[245] L. Li, Y. Wang, R. R. Nazmutdinov, R. R. Zairov, Q. Shao, J. Lu, *Nano Lett.* **2024**, *24*, 6148.
[246] L. Li, J. Zhou, X. Wang, J. Gracia, M. Valvidares, J. Ke, M. Fang, C. Shen, J. Chen, Y. Chang, C. Pao, S. Hsu, J. Lee, A. Ruotolo, Y. Chin, Z. Hu, X. Huang, Q. Shao, *Adv. Mater.* **2023**, *35*, 35.
[247] K. Chae, H. Lee, W. Huang, J. Son, B. Pavageau, T. Kim, S. Lee, J. Kim, J. Moon, R. Liu, J. Bang, D. H. Kim, *Adv. Mater.* **2025**, 2507658.
[248] Q. Huang, S. Xie, J. Hao, Z. Ding, C. Zhang, H. Sheng, J. Zhao, *Angew. Chem., Int. Ed.* **2023**, *62*, 20.
[249] F. Wang, P. Zou, Y. Zhang, W. Pan, Y. Li, L. Liang, C. Chen, H. Liu, S. Zheng, *Nat. Commun.* **2023**, *14*, 1.
[250] P. K. Bhartiya, M. Srivastava, D. Mishra, *Int. J. Hydrogen Energy* **2022**, *47*, 42160.
[251] M. Risch, F. Ringleb, M. Kohlhoff, P. Bogdanoff, P. Chernev, I. Zaharieva, H. Dau, *Energy Environ. Sci.* **2015**, *8*, 661.
[252] J. Du, J. Morales-Santelices, O. Y. Bisen, D. Antipin, D. M. Morales, M. Risch, *Electrochim. Acta* **2025**, *512*, 145489.
[253] J. Scholz, M. Risch, K. A. Stoerzinger, G. Wartner, Y. Shao-Horn, C. Jooss, *J. Phys. Chem. C* **2016**, *120*, 27746.
[254] R. T. Vang, J. V. Lauritsen, E. Lægsgaard, F. Besenbacher, *Chem. Soc. Rev.* **2008**, *37*, 2191.
[255] E. Altman, R. Tanner, *Catal. Today* **2003**, *85*, 101.
[256] B.-C. Huang, C.-C. Hsu, Y.-H. Chu, Y.-P. Chiu, *Prog. Surf. Sci.* **2022**, *97*, 100662.
[257] M. Ercelik, A. P. Solé, L. Zhang, P. Kot, J. Kim, J. Chae, L. E. Spree, H. Guo, A. J. Heinrich, Y. Bae, D. Borodin, *J. Phys. Chem. C* **2024**, *129*, 1110.
[258] R. Gutzler, S. Stepanow, D. Grumelli, M. Lingenfelder, K. Kern, *Acc. Chem. Res.* **2015**, *48*, 2132.
[259] M. Setvín, U. Aschauer, P. Scheiber, Y.-F. Li, W. Hou, M. Schmid, A. Selloni, U. Diebold, *Science* **2013**, *341*, 988.
[260] J. Fester, A. Walton, Z. Li, J. V. Lauritsen, *Phys. Chem. Chem. Phys.* **2017**, *19*, 2425.
[261] Z. Sun, J. Rodríguez-Fernández, J. V. Lauritsen, *J. Phys.: Condens. Matter* **2022**, *34*, 164004.
[262] M. Salmeron, B. Eren, *Chem. Rev.* **2020**, *121*, 962.
[263] M. Verhage, K. Flipse, *arXiv:2410.06598* **2024**.
[264] M. Verhage, S. J. v. d. Broek, C. Weijtens, C. F. J. Flipse, *ACS Appl. Mater. Interfaces* **2025**, *17*, 23237.
[265] A. Biswas, S. Elizabeth, A. K. Raychaudhuri, H. L. Bhat, *Phys. Rev. B* **1999**, *59*, 5368.
[266] R. Wiesendanger, *Rev. Mod. Phys.* **2009**, *81*, 1495.
[267] K. von Bergmann, M. Bode, A. Kubetzka, M. Heide, S. Blügel, R. Wiesendanger, *Phys. Rev. Lett.* **2004**, *92*, 4.
[268] M. R. Safari, F. Matthes, V. Caciuc, N. Atodiresei, C. M. Schneider, K. Ernst, D. E. Bürgler, *Adv. Mater.* **2024**, *36*, 14.
[269] T. N. H. Nguyen, G. Salvan, O. Hellwig, Y. Paltiel, L. T. Baczewski, C. Tegenkamp, *Chem. Sci.* **2024**, *15*, 14905.
[270] M. Lunardon, T. Kosmala, C. Durante, S. Agnoli, G. Granozzi, *Joule* **2022**, *6*, 617.
[271] K. Itaya, E. Tomita, *Surf. Sci.* **1988**, *201*, L507.
[272] Y. Sun, C.-R. Wu, F. Wang, R.-H. Bi, Y.-B. Zhuang, S. Liu, M.-S. Chen, K. H.-L. Zhang, J.-W. Yan, B.-W. Mao, Z.-Q. Tian, J. Cheng, *Chem. Sci.* **2024**, *15*, 12264.
[273] T. H. Phan, K. Banjac, F. P. Cometto, F. Dattila, R. García-Muelas, S. J. Raaijman, C. Ye, M. T. M. Koper, N. López, M. Lingenfelder, *Nano Lett.* **2021**, *21*, 2059.
[274] Y.-Q. Wang, D. Wang, *Curr. Opin. Electrochem.* **2024**, *46*, 101512.
[275] J. H. K. Pfisterer, Y. Liang, O. Schneider, A. S. Bandarenka, *Nature* **2017**, *549*, 74.
[276] Y. Liang, J. H. K. Pfisterer, D. McLaughlin, C. Csoklich, L. Seidl, A. S. Bandarenka, O. Schneider, *Small Methods* **2018**, *3*, 8.
[277] T. O. Schmidt, R. W. Haid, E. L. Gubanova, R. M. Kluge, A. S. Bandarenka, *Top. Catal.* **2023**, *66*, 1270.
[278] Y. Liang, S. O. Parreiras, S. Lee, K. Banjac, V. Boureau, J. M. Gallego, X. Hu, D. Écija, M. Lingenfelder, *Angew. Chem.* **2025**, *137*, 10.
[279] I. Sokolović, M. Reticcioli, M. Čalkovský, M. Wagner, M. Schmid, C. Franchini, U. Diebold, M. Setvín, *Proc. Natl. Acad. Sci. USA* **2020**, *117*, 14827.
[280] J. Redondo, M. Reticcioli, V. Gabriel, D. Wrana, F. Ellinger, M. Riva, G. Franceschi, E. Rheinfrank, I. Sokolović, Z. Jakub, F. Kraushofer, A. Alexander, E. Belas, L. L. Patera, J. Repp, M. Schmid, U. Diebold, G. S. Parkinson, C. Franchini, P. Kocan, M. Setvin, *Sci. Adv.* **2024**, *10*, 44.
[281] S. Su, I. Siretanu, D. van den Ende, B. Mei, G. Mul, F. Mugele, *Adv. Mater.* **2021**, *33*, 52.
[282] L. K. S. Bonagiri, K. S. Panse, S. Zhou, H. Wu, N. R. Aluru, Y. Zhang, *ACS Nano* **2022**, *16*, 19594.
[283] W.-W. Wang, H. Yan, Y. Gu, J. Yan, B.-W. Mao, *Annu. Rev. Anal. Chem.* **2024**, *17*, 103.
[284] M. R. Nellist, F. A. L. Laskowski, J. Qiu, H. Hajibabaei, K. Sivula, T. W. Hamann, S. W. Boettcher, *Nat. Energy* **2017**, *3*, 46.
[285] A. Ziv, A. Saha, H. Alpern, N. Sukenik, L. T. Baczewski, S. Yochelis, M. Reches, Y. Paltiel, *Adv. Mater.* **2019**, *31*, 40.
[286] Q. Liang, G. Brocks, A. Bieberle-Hütter, *ChemPhysChem* **2022**, *24*, 5.
[287] S. Ghosh, S. Mishra, E. Avigad, B. P. Bloom, L. T. Baczewski, S. Yochelis, Y. Paltiel, R. Naaman, D. H. Waldeck, *J. Phys. Chem. Lett.* **2020**, *11*, 1550.
[288] P. M. Theiler, C. Ritz, R. Hofmann, A. Stemmer, *Nano Lett.* **2023**, *23*, 8280.
[289] T. Hackl, G. Schitter, P. Mesquida, *ACS Nano* **2022**, *16*, 17982.

[290] C. Santana Santos, B. N. Jaato, I. Sanjuán, W. Schuhmann, C. Andronescu, *Chem. Rev.* **2023**, *123*, 4972.
[291] A. J. Bard, M. V. Mirkin, *Scanning Electrochemical Microscopy*, CRC Press, Florida **2022**.
[292] T. Kai, C. G. Zoski, A. J. Bard, *Chem. Commun.* **2018**, *54*, 1934.
[293] C. L. Bentley, M. Kang, P. R. Unwin, *J. Am. Chem. Soc.* **2018**, *141*, 2179.
[294] G. Arruda de Oliveira, M. Kim, C. S. Santos, N. Limani, T. D. Chung, E. B. Tetteh, W. Schuhmann, *Chem. Sci.* **2024**, *15*, 16331.
[295] S. Baumann, W. Paul, T. Choi, C. P. Lutz, A. Ardavan, A. J. Heinrich, *Science* **2015**, *350*, 417.
[296] J. Stöhr, *NEXAFS Spectroscopy*, Springer, Berlin Heidelberg **1992**.
[297] J. Stöhr, *J. Magn. Magn. Mater.* **1999**, *200*, 470.
[298] E. Arenholz, G. van der Laan, R. V. Chopdekar, Y. Suzuki, *Phys. Rev. B* **2006**, *74*, 9.
[299] S. Mauri, R. Calligaro, C. F. Pauletti, M. F. Camellone, M. Boaro, L. Braglia, S. Fabris, S. Piccinin, P. Torelli, A. Trovarelli, *Small* **2024**, *20*, 2403028.
[300] J.-J. Velasco-Vélez, L. J. Falling, D. Bernsmeier, M. J. Sear, P. C. J. Clark, T.-S. Chan, E. Stotz, M. Hävecker, R. Kraehnert, A. Knop-Gericke, C.-H. Chuang, D. E. Starr, M. Favaro, R. V. Mom, *J. Phys. D: Appl. Phys.* **2021**, *54*, 124003.
[301] A. I. Frenkel, J. A. Rodriguez, J. G. Chen, *ACS Catal.* **2012**, *2*, 2269.
[302] J. Zhou, L. Zhang, Y.-C. Huang, C.-L. Dong, H.-J. Lin, C.-T. Chen, L. H. Tjeng, Z. Hu, *Nat. Commun.* **2020**, *11*, 1984.
[303] S. K. Beaumont, *Phys. Chem. Chem. Phys.* **2020**, *22*, 18747.
[304] B. Yu, G. Yu, J. Walter, V. Chaturvedi, J. Gotchnik, S. Hameed, J. W. Freeland, C. Leighton, M. Greven, *Appl. Phys. Lett.* **2020**, *116*, 20.
[305] C. Castán-Guerrero, D. Krizmancic, V. Bonanni, R. Edla, A. Deluisa, F. Salvador, G. Rossi, G. Panaccione, P. Torelli, *Rev. Sci. Instrum.* **2018**, *89*, 5.
[306] J. Chapman, E. Waddell, P. Batson, R. Ferrier, *Ultramicroscopy* **1979**, *4*, 283.
[307] A. Tonomura, *Electron Holography*, Springer, Berlin Heidelberg **1999**.
[308] Q. Lan, C. Wang, L. Jin, M. Schnedler, L. Freter, K. Fischer, J. Caron, X.-K. Wei, T. Denneulin, A. Kovács, P. Ebert, X. Zhong, R. E. Dunin-Borkowski, *Phys. Rev. Lett.* **2022**, *129*, 057201.
[309] Q. Lan, M. Schnedler, L. Freter, C. Wang, K. Fischer, P. Ebert, R. E. Dunin-Borkowski, *Phys. Rev. B* **2023**, *108*, 18.
[310] J. Caron, *Modellbasierte Rekonstruktion von Magnetisierungsverteilungen in Nanostrukturen aus elektronenoptischen Phasenbildern*, RWTH Aachen University, Aachen **2018**.
[311] Z. Wang, A. H. Tavabi, L. Jin, J. Rusz, D. Tyutyunnikov, H. Jiang, Y. Moritomo, J. Mayer, R. E. Dunin-Borkowski, R. Yu, J. Zhu, X. Zhong, *Nat. Mater.* **2018**, *17*, 221.
[312] H. Ali, J. Rusz, D. E. Bürgler, J. V. Vas, L. Jin, R. Adam, C. M. Schneider, R. E. Dunin-Borkowski, *Nat. Mater.* **2025**, *24*, 1215.
[313] D. del Pozo-Bueno, M. Varela, M. Estrader, A. López-Ortega, A. G. Roca, J. Nogués, F. Peiró, S. Estradé, *Nano Lett.* **2021**, *21*, 6923.
[314] S. Tao, M. Li, M. Lyu, L. Ran, R. Wepf, I. Gentle, R. Knibbe, *Nano Energy* **2022**, *96*, 107083.
[315] J. Ærøe Hyllested, M. Beleggia, *Ultramicroscopy* **2021**, *221*, 113178.
[316] C. Meng, R. Li, Y. Ning, A. Pavlovska, E. Bauer, Q. Fu, X. Bao, *ChemCatChem* **2020**, *12*, 1036.
[317] G. Sun, F.-D. Yu, M. Lu, Q. Zhu, Y. Jiang, Y. Mao, J. A. McLeod, J. Maley, J. Wang, J. Zhou, Z. Wang, *Nat. Commun.* **2022**, *13*, 1.
[318] C. Baeumer, C. Schmitz, A. Marchewka, D. N. Mueller, R. Valenta, J. Hackl, N. Raab, S. P. Rogers, M. I. Khan, S. Nemsak, M. Shim, S. Menzel, C. M. Schneider, R. Waser, R. Dittmann, *Nat. Commun.* **2016**, *7*, 1.
[319] R. Li, X. Xu, B. Zhu, X.-Y. Li, Y. Ning, R. Mu, P. Du, M. Li, H. Wang, J. Liang, Y. Chen, Y. Gao, B. Yang, Q. Fu, X. Bao, *Nat. Commun.* **2021**, *12*, 1406.
[320] J. Zeininger, P. Winkler, M. Raab, Y. Suchorski, M. J. Prieto, L. C. Tănase, L. de Souza Caldas, A. Tiwari, T. Schmidt, M. Stöger-Pollach, A. Steiger-Thirsfeld, B. Roldan Cuenya, G. Rupprechter, *ACS Catal.* **2022**, *12*, 11974.
[321] G. Mattoni, P. Zubko, F. Maccherozzi, A. van der Torren, D. B. Boltje, M. Hadjimichael, N. Manca, S. Catalano, M. Gibert, Y. Liu, J. Aarts, J.-M. Triscone, S. S. Dhesi, A. D. Caviglia, *Nat. Commun.* **2016**, *7*, 13141.
[322] Y. Ning, Q. Fu, Y. Li, S. Zhao, C. Wang, M. Breitschaft, S. Hagen, O. Schaff, X. Bao, *Ultramicroscopy* **2019**, *200*, 105.
[323] A. Kolmakov, D. A. Dikin, L. J. Cote, J. Huang, M. K. Abyaneh, M. Amati, L. Gregoratti, S. Günther, M. Kiskinova, *Nat. Nanotechnol.* **2011**, *6*, 651.
[324] S. Nemšák, E. Strelcov, T. Duchoň, H. Guo, J. Hackl, A. Yulaev, I. Vlassiouk, D. N. Mueller, C. M. Schneider, A. Kolmakov, *J. Am. Chem. Soc.* **2017**, *139*, 18138.
[325] J. McCord, *J. Phys. D: Appl. Phys.* **2015**, *48*, 333001.
[326] J. Zehner, R. Huhnstock, S. Oswald, U. Wolff, I. Soldatov, A. Ehresmann, K. Nielsch, D. Holzinger, K. Leistner, *Adv. Electron. Mater.* **2019**, *5*, 6.
[327] W. Schindler, J. Kirschner, *Rev. Sci. Instrum.* **1996**, *67*, 3578.
[328] J. A. Weil, J. R. Bolton, *Electron Paramagnetic Resonance: Elementary Theory and Practical Applications*, Wiley, New Jersey **2006**.
[329] S. A. Bonke, T. Risse, A. Schnegg, A. Brückner, *Nat. Rev. Methods Primers* **2021**, *1*, 33.
[330] A. Gonchar, T. Risse, H. Freund, L. Giordano, C. Di Valentin, G. Pacchioni, *Angew. Chem., Int. Ed.* **2011**, *50*, 2635.
[331] F. H. L. Koppens, C. Buizert, K. J. Tielrooij, I. T. Vink, K. C. Nowack, T. Meunier, L. P. Kouwenhoven, L. M. K. Vandersypen, *Nature* **2006**, *442*, 766.
[332] F. Blumenschein, M. Tamski, C. Roussel, E. Z. B. Smolinsky, F. Tassinari, R. Naaman, J.-P. Ansermet, *Phys. Chem. Chem. Phys.* **2020**, *22*, 997.
[333] M. Farle, *Rep. Prog. Phys.* **1998**, *61*, 755.
[334] L. Ni, C. Gallenkamp, S. Paul, M. Kübler, P. Theis, S. Chabbra, K. Hofmann, E. Bill, A. Schnegg, B. Albert, V. Krewald, U. I. Kramm, *Adv. Energy Sustain. Res.* **2021**, *2*, 2.
[335] J. Li, M. T. Sougrati, A. Zitolo, J. M. Ablett, I. C. Oğuz, T. Mineva, I. Matanovic, P. Atanassov, Y. Huang, I. Zenyuk, A. Di Cicco, K. Kumar, L. Dubau, F. Maillard, G. Dražić, F. Jaouen, *Nat. Catal.* **2020**, *4*, 10.
[336] L. Ni, E. S. Davydova, R. K. Singh, L. Kolik-Shmuel, D. R. Dekel, U. I. Kramm, *J. Phys.: Energy* **2023**, *5*, 034009.
[337] D. A. Corrigan, R. S. Conell, C. A. Fierro, D. A. Scherson, *J. Phys. Chem.* **1987**, *91*, 5009.
[338] J. Y. C. Chen, L. Dang, H. Liang, W. Bi, J. B. Gerken, S. Jin, E. E. Alp, S. S. Stahl, *J. Am. Chem. Soc.* **2015**, *137*, 15090.
[339] Z. Kuang, S. Liu, X. Li, M. Wang, X. Ren, J. Ding, R. Ge, W. Zhou, A. I. Rykov, M. T. Sougrati, P.-E. Lippens, Y. Huang, J. Wang, *J. Energy Chem.* **2021**, *57*, 212.
[340] L. Ni, C. Gallenkamp, S. Wagner, E. Bill, V. Krewald, U. I. Kramm, *J. Am. Chem. Soc.* **2022**, *144*, 16827.
[341] L. Ni, P. Theis, S. Paul, R. W. Stark, U. I. Kramm, *Electrochim. Acta* **2021**, *395*, 139200.
[342] N. Heppe, C. Gallenkamp, R. Z. Snitkoff-Sol, S. D. Paul, N. Segura-Salas, H. Haak, D. C. Moritz, B. Kaiser, W. Jaegermann, V. Potapkin, A. Jafari, V. Schünemann, O. Leupold, L. Elbaz, V. Krewald, U. I. Kramm, *J. Am. Chem. Soc.* **2024**, *146*, 12496.
[343] Deutsches Elektronen-Synchrotron (DESY), P01 high resolution dynamics beamline, https://photon-science.desy.de/facilities/petra_iii/beamlines/p01_dynamics/index_eng.html, **2025** (accessed: May 2025).
[344] European Synchrotron Radiation Facility (ESRF), Id18, https://www.esrf.fr/home/UsersAndScience/Experiments/MEx/beamline-snapshots/content/content-list/id18.html, **2025** (accessed: May 2025).

[345] SPring-8, Bl11xu hutch 1 (synchrotron radiation mössbauer spectroscopy station), http://www.spring8.or.jp/wkg/BL11XU/instrument/lang-en/INS-0000001402/instrument_view, **2025** (accessed: May 2025).
[346] B. Huemer, A. Jodlbauer, M. Wilkening, H. Krenn, P. Knoll, R. Würschum, I. Hanzu, S. Topolovec, *J. Mater. Chem. A* **2025**, *13*, 2934.
[347] S. Mandal, D. Biswakarma, A. J. Bhattacharyya, *Phys. Chem. Chem. Phys.* **2024**, *26*, 27131.
[348] B. P. Bloom, B. M. Graff, S. Ghosh, D. N. Beratan, D. H. Waldeck, *J. Am. Chem. Soc.* **2017**, *139*, 9038.
[349] C. Kulkarni, A. K. Mondal, T. K. Das, G. Grinbom, F. Tassinari, M. F. J. Mabesoone, E. W. Meijer, R. Naaman, *Adv. Mater.* **2020**, *32*, 7.
[350] D. Amsallem, A. Kumar, R. Naaman, O. Gidron, *Chirality* **2023**, *35*, 562.
[351] C. Clever, E. Wierzbinski, B. P. Bloom, Y. Lu, H. M. Grimm, S. R. Rao, W. S. Horne, D. H. Waldeck, *Isr. J. Chem.* **2022**, *62*, 11.
[352] S. Mishra, A. K. Mondal, S. Pal, T. K. Das, E. Z. B. Smolinsky, G. Siligardi, R. Naaman, *J. Phys. Chem. C* **2020**, *124*, 10776.
[353] A. Kumar, E. Capua, K. Vankayala, C. Fontanesi, R. Naaman, *Angew. Chem., Int. Ed.* **2017**, *56*, 14587.
[354] R. Sun, Z. Wang, B. P. Bloom, A. H. Comstock, C. Yang, A. McConnell, C. Clever, M. Molitoris, D. Lamont, Z.-H. Cheng, Z. Yuan, W. Zhang, A. Hoffmann, J. Liu, D. H. Waldeck, D. Sun, *Sci. Adv.* **2024**, *10*, 18.
[355] W. Shen, Y. Ye, Q. Xia, P. Xi, *EES Catal.* **2025**, *3*, 10.
[356] A. Manchon, H. C. Koo, J. Nitta, S. M. Frolov, R. A. Duine, *Nat. Mater.* **2015**, *14*, 871.
[357] S. Kaneta-Takada, M. Kitamura, S. Arai, T. Arai, R. Okano, L. D. Anh, T. Endo, K. Horiba, H. Kumigashira, M. Kobayashi, M. Seki, H. Tabata, M. Tanaka, S. Ohya, *Nat. Commun.* **2022**, *13*, 5631.
[358] L. Cheng, L. Wei, H. Liang, Y. Yan, G. Cheng, M. Lv, T. Lin, T. Kang, G. Yu, J. Chu, Z. Zhang, C. Zeng, *Nano Lett.* **2017**, *17*, 6534.
[359] S. Varotto, A. Johansson, B. Göbel, L. M. Vicente-Arche, S. Mallik, J. Bréhin, R. Salazar, F. Bertran, P. L. Fèvre, N. Bergeal, J. Rault, I. Mertig, M. Bibes, *Nat. Commun.* **2022**, *13*, 6165.
[360] W. Jiang, J. Li, C. Zhao, W. Cheng, J. Liu, Y. Chen, *Int. J. Hydrogen Energy* **2024**, *51*, 1486.
[361] W. E. Pickett, J. S. Moodera, *Phys. Today* **2001**, *54*, 39.
[362] Q. Yang, Y. Zhang, Y. Sun, C. Felser, G. Li, *The Innov. Mater.* **2023**, *1*, 100013.
[363] D. W. Boukhvalov, C.-N. Kuo, S. Nappini, A. Marchionni, G. D'Olimpio, J. Filippi, S. Mauri, P. Torelli, C. S. Lue, F. Vizza, A. Politano, *ACS Catal.* **2021**, *11*, 7311.
[364] Y. Kang, Y. He, D. Pohl, B. Rellinghaus, D. Chen, M. Schmidt, V. Süß, Q. Mu, F. Li, Q. Yang, H. Chen, Y. Ma, G. Auffermann, G. Li, C. Felser, *ACS Appl. Mater. Interfaces* **2022**, *14*, 19324.
[365] G. Li, Q. Xu, W. Shi, C. Fu, L. Jiao, M. E. Kamminga, M. Yu, H. Tüysüz, N. Kumar, V. Süß, R. Saha, A. K. Srivastava, S. Wirth, G. Auffermann, J. Gooth, S. Parkin, Y. Sun, E. Liu, C. Felser, *Sci. Adv.* **2019**, *5*, 8.
[366] X. Wu, X. Wang, C. Felser, *La Rivista del Nuovo Cimento* **2025**.
[367] X. Wang, Q. Yang, S. Singh, H. Borrmann, V. Hasse, C. Yi, Y. Li, M. Schmidt, X. Li, G. H. Fecher, D. Zhou, B. Yan, C. Felser, *Nat. Energy* **2024**, *10*, 101.
[368] N. F. Chilton, *Annu. Rev. Mater. Res.* **2022**, *52*, 79.
[369] J. M. Manriquez, G. T. Yee, R. S. McLean, A. J. Epstein, J. S. Miller, *Science* **1991**, *252*, 1415.
[370] E. Beaurepaire, J.-C. Merle, A. Daunois, J.-Y. Bigot, *Phys. Rev. Lett.* **1996**, *76*, 4250.
[371] T. Satoh, R. Iida, T. Higuchi, Y. Fujii, A. Koreeda, H. Ueda, T. Shimura, K. Kuroda, V. I. Butrim, B. A. Ivanov, *Nat. Commun.* **2017**, *8*, 638.
[372] G. Ju, L. Chen, A. V. Nurmikko, R. F. C. Farrow, R. F. Marks, M. J. Carey, B. A. Gurney, *Phys. Rev. B* **2000**, *62*, 1171.
[373] A. Kirilyuk, A. V. Kimel, T. Rasing, *Rev. Mod. Phys.* **2010**, *82*, 2731.
[374] G. Ju, J. Hohlfeld, B. Bergman, R. J. M. van de Veerdonk, O. N. Mryasov, J.-Y. Kim, X. Wu, D. Weller, B. Koopmans, *Phys. Rev. Lett.* **2004**, *93*, 19.
[375] G. V. Astakhov, A. V. Kimel, G. M. Schott, A. A. Tsvetkov, A. Kirilyuk, D. R. Yakovlev, G. Karczewski, W. Ossau, G. Schmidt, L. W. Molenkamp, T. Rasing, *Appl. Phys. Lett.* **2005**, *86*, 15.
[376] U. Huizi-Rayo, J. Gutierrez, J. M. Seco, V. Mujica, I. Diez-Perez, J. M. Ugalde, A. Tercjak, J. Cepeda, E. San Sebastian, *Nano Lett.* **2020**, *20*, 8476.
[377] X. Han, C. Jiang, B. Hou, Y. Liu, Y. Cui, *J. Am. Chem. Soc.* **2024**, *146*, 6733.
[378] C. Wang, Q. Zhang, B. Yan, B. You, J. Zheng, L. Feng, C. Zhang, S. Jiang, W. Chen, S. He, *Nano-Micro Lett.* **2023**, *15*, 1.
[379] T. Wu, M. L. Stone, M. J. Shearer, M. J. Stolt, I. A. Guzei, R. J. Hamers, R. Lu, K. Deng, S. Jin, J. R. Schmidt, *ACS Catal.* **2018**, *8*, 1143.
[380] M. L. Weber, F. Gunkel, *J. Phys.: Energy* **2019**, *1*, 031001.
[381] L. Liu, C. Zhen, J. Feng, X. Wang, L. Ma, G. Li, D. Zhao, D. Hou, *Phys. Rev. B* **2024**, *110*, 22.
[382] L. Heymann, I. C. G. van den Bosch, D. H. Wielens, O. Kurbjeweit, E. van der Minne, E. M. Kiens, A. Kaus, D. Schön, S. Menzel, B. Boukamp, F. Gunkel, C. Baeumer, *ACS Appl. Mater. Interfaces* **2025**, *17*, 21110.
[383] J. Shan, C. Ye, Y. Jiang, M. Jaroniec, Y. Zheng, S.-Z. Qiao, *Sci. Adv.* **2022**, *8*, 17.
[384] L. Heymann, A. Schreiber, C. Pithan, C. Baeumer, F. Gunkel, *ChemRxiv* **2024**.
[385] Z. Wang, M. F. Navarro Poupard, R. R. Mohan, L. Boddapati, J. Zhang, S. Kamali, C. Biz, M. Fianchini, F. L. Deepak, J. Gracia, L. M. Salonen, Y. V. Kolen'ko, *ACS Nano* **2025**, *19*, 29195.
[386] S. Sun, Y. Sun, Y. Zhou, J. Shen, D. Mandler, R. Neumann, Z. J. Xu, *Chem. Mater.* **2019**, *31*, 8106.
[387] K. B. Ghosh, W. Zhang, F. Tassinari, Y. Mastai, O. Lidor-Shalev, R. Naaman, P. Möllers, D. Nürenberg, H. Zacharias, J. Wei, E. Wierzbinski, D. H. Waldeck, *J. Phys. Chem. C* **2019**, *123*, 3024.
[388] Z. Bian, K. Kato, T. Ogoshi, Z. Cui, B. Sa, Y. Tsutsui, S. Seki, M. Suda, *Adv. Sci.* **2022**, *9*, 17.
[389] C. J. Mingoes, B. C. Schroeder, A. B. Jorge Sobrido, *ACS Mater. Au* **2023**, *4*, 204.
[390] D. K. Bhowmick, N. Yuran, M. Fadeev, S. Yochelis, Y. Paltiel, R. Naaman, *Energy Fuels* **2024**, *39*, 764.
[391] T. Feng, W. Chen, J. Xue, F. Cao, Z. Chen, J. Ye, C. Xiao, H. Lu, *Adv. Funct. Mater.* **2023**, *33*, 27.
[392] W. Mtangi, F. Tassinari, K. Vankayala, A. Vargas Jentzsch, B. Adelizzi, A. R. A. Palmans, C. Fontanesi, E. W. Meijer, R. Naaman, *J. Am. Chem. Soc.* **2017**, *139*, 2794.
[393] O. Kazakova, R. Puttock, C. Barton, H. Corte-León, M. Jaafar, V. Neu, A. Asenjo, *J. Appl. Phys.* **2019**, *125*, 6.
[394] B. Ding, J. Liu, H. Li, J. Liang, J. Chen, Z. Li, X. Li, X. Xi, Z. Cheng, J. Wang, Y. Yao, W. Wang, *Adv. Funct. Mater.* **2022**, *32*, 19.
[395] C. Phatak, A. Petford-Long, M. De Graef, *Curr. Opin. Solid State Mater. Sci.* **2016**, *20*, 107.
[396] R. E. Dunin-Borkowski, T. Kasama, M. Beleggia, G. Pozzi, *Handbook of Nanoscopy*, Wiley, New Jersey **2012**.
[397] K. Yamamoto, S. Anada, T. Sato, N. Yoshimoto, T. Hirayama, *Microscopy* **2020**, *70*, 24.
[398] T. Tanigaki, T. Akashi, T. Yoshida, K. Harada, K. Ishizuka, M. Ichimura, K. Mitsuishi, Y. Tomioka, X. Yu, D. Shindo, Y. Tokura, Y. Murakami, H. Shinada, *Nature* **2024**, *631*, 521.

Emma van der Minne is currently a Ph.D. candidate at the MESA+ Institute for Nanotechnology at the University of Twente. She earned a double M.Sc. degree in Chemical Science and Engineering and Applied Physics from the University of Twente in 2021 and was recognized as an excellent graduate by the VNCI Topsector Chemistry scholarship program. Her research focuses on gaining a fundamental understanding of how finely tuned properties of model electrocatalysts influence the oxygen evolution reaction (OER), with a particular emphasis on magnetic interactions and operando characterization techniques.

Priscila Vensaus is a chemist graduated from the University of Buenos Aires. She earned her Ph.D. in 2024 from the National University of General San Martín, under the supervision of Dr. Galo J.A.A. Soler-Illia (UNSAM) and Dr. Magalí Lingenfelder (EPFL). Her thesis, which explored the enhancement of the oxygen evolution reaction through nanostructuration, sunlight, and magnetic fields, was financed by CONICET and the Swiss Government Excellence Scholarship, and was awarded the Hans J. Schumacher Prize for the best doctoral thesis in physical chemistry conducted in Argentina. Currently, she is a postdoctoral researcher at the Laboratory of Nanoscience for Energy Technologies (LNET) at EPFL, where she aims to integrate nanophotonics and CISS for advanced energy conversion applications.

Vadim Ratovskii is currently a Ph.D. candidate at the MESA+ Institute for Nanotechnology, University of Twente. He obtained his M.Sc. degree in Materials science from Lomonosov Moscow State University in 2023, studying the room-temperature multiferroic materials, based on epitaxial films multilayers approach. His Ph.D. research focuses on correlating magnetic properties of iron-based spinel electrocatalysts with their oxygen evolution reaction (OER) performance. Using epitaxial model systems of such materials allows him for precise modulation of their properties and unique operando characterization approaches.

Seenivasan Hariharan obtained his Ph.D. in 2016 from Indian Institute of Science Education and Research (IISER) Kolkata, India, specializing in the energetics and dynamics of chemical reactions at surfaces. Following several postdoctoral positions focusing on modeling high-temperature reaction dynamics, diffusion, and energy dissipation (to phonons) in surface reactions, he is currently based at the Institute of Physics, University of Amsterdam, and QuSoft, CWI, The Netherlands. His research lies at the intersection of quantum chemistry, heterogeneous catalysis, and quantum computing, with a focus on developing and applying quantum algorithms to real-world problems pertaining to heterogeneous catalysis.

Christoph Baeumer is an adjunct professor at the University of Twente and guest scientist at Forschungszentrum Jülich. He obtained his MSc in Materials Science from the University of Illinois, his PhD in Physics from RWTH Aachen University and Forschungszentrum Jülich in 2016 and he was a Marie Skłodowska Curie Fellow at Stanford University (2018-2020). His Electrochemical Thin Films and Interfaces group focuses on operando characterization and fundamental structure-function relations in model electrocatalysts. He received several awards and personal grants, including the Helmholtz Doctoral Prize (2017) and the ERC Starting Grant (2022). He is the scientific leader of the NWO-funded project "MagCats", aiming at a fundamental understanding of the role of magnetism in OER using epitaxial thin-film model systems.